CPG-CARRIER SIZE AND DENSITY AFFECTS DENDRITIC CELL SIGNALING, SUBSET-TROPISM AND SYSTEMIC IMMUNE POLARIZATION

A Dissertation
Presented to
The Academic Faculty

by

Jardin A. Leleux

In Partial Fulfillment
of the Requirements for the Degree
Doctor of Philosophy in the
Department of Biomedical Engineering

Georgia Institute of Technology
December 2015

CPG-CARRIER SIZE AND DENSITY AFFECTS DENDRITIC CELL SIGNALING, SUBSET-TROPISM AND SYSTEMIC IMMUNE POLARIZATION

Approved by:

Dr. Krishnendu Roy, Advisor
Department of Biomedical Engineering
Georgia Institute of Technology & Emory University

Dr. Ravi Bellamkonda
Department of Biomedical Engineering
Georgia Institute of Technology & Emory University

Dr. M.G. Finn
Department of Chemistry and Biochemistry
Georgia Institute of Technology

Dr. Susan Thomas
Department of Mechanical Engineering
Georgia Institute of Technology

Dr. Phil Santangelo
Department of Biomedical Engineering
Georgia Institute of Technology & Emory University

Date Approved: August 10, 2015

To my family and friends who supported me throughout graduate school.

ACKNOWLEDGEMENTS

They say there is no "i" in team. It turns out, there is no "i" in graduate school either. My success in graduate school was completely dependent on the unwavering support of my family, friends and mentors. First, I'd like to thank my adviser, Dr. Krishnendu Roy, who gave me the opportunity to work in his lab and has provided endless encouragement and advice over the years. You know your adviser is pretty good when you move across the country with them! I would also like to thank all of my committee members: Dr. Ravi Bellamkonda, Dr Susan Thomas, Dr. M.G. Finn and Dr. Phil Santangelo for their insightful suggestions and expertise and for not being impossible to schedule meetings with! I'm also grateful to the Boes lab in Utrecht, Netherlands for allowing me to work alongside them for a summer. Through that experience, I not only gained exposure to new techniques that helped me with my own project, but also changed my perspective on immunotherapies and how they are helping real people.

Next, I would like to express my appreciation for all of the core and animal facility staff that I've worked with over the years. The staff at both the ARC at UT Austin and PRL at Georgia Tech have been incredibly helpful and friendly, even when we're giving mice tumors the size of their heads. Steve Woodard, Nadia Boguslavsky and Andrew Shaw all provided expert advice and help with flow cytometry and microscopy studies. The core would never function without you. Finally, the staff at both the Yerkes Pathology Center and the Winship Cancer Center Histology Core at Emory University provided me with pristine histological samples, giving me one less thing to worry about in my last few months of experiments.

To the members of the UT Austin "Klub Krish" (Eileen, Prinda, Asha, Michelle, Krista, Lonnissa, Tracy, Rachit, Pallab and Irina): Thank you all for being a source of inspiration, constructive criticism and laughs. You all helped me in some invaluable way over the years and my memories of all of you are very fond. I especially will never forget our Roy lab road trip and New Orleans adventure, when I learned more than I probably ever needed to know about many of you, but enjoyed your friendship just the same. To Eileen: Thanks for being my partner in the struggle for cooperative DCs and for reminding me that there is always light at the end of the tunnel. To Rachit: You were the best office mate I could ask for, even if you did make me feel like a slacker through most of graduate school. I'm glad you decided to follow us to Georgia; you've kept me in shape (sort of) and kept Gracie happy when I'm out of town. To Pallab: You and I have stuck it out the longest together and I will forever pray to ALL of the gods before doing anything as massive as our animal experiments. To Tracy: I'm not sure what I would have done if you hadn't decided to move to Atlanta. You made the experience much more fun and managed to keep me sane through my toughest times in grad school.

To the current members of Klub Krish (Kyung-Ho, Randy, Ranjna, Michael, Kirsten, Ingrid, Joscelyn, Alex, Adriana and Ni): Thanks for putting up with my lab cleanup fairy emails and for listening to all of my crazy theories about experiments. You guys have inspired me to be a better scientist and I am very happy to pass down the torch to you guys after I leave. I am thoroughly convinced that Klub Krish is in good hands.

To all of my friends in Austin and Atlanta, especially Alex: Thanks for being there with me through good times and bad. We all know how much of a roller coaster grad school can be, but you all were there for me regardless of where on the roller coaster you were at

the time. Even after I moved away, every visit to Austin felt like no time had passed. All of you will always hold one of the most special places in my heart.

Finally, I would like to express my deepest thanks and appreciation to my family, who have been a constant source of support throughout my entire life, graduate school being no different. I would never have gotten where I am today without all of you and your individual contributions to my life.

TABLE OF CONTENTS

LIST OF TABLES

LIST OF FIGURES

CHAPTER 2

CHAPTER 3

CHAPTER 4

CHAPTER 5

APPENDIX

LIST OF SYMBOLS AND ABBREVIATIONS

APC	Antigen presenting cell
DC	Dendritic cell
MHC I	Major histocompatibility complex I
MHC II	Major histocompatibility complex II
HLA	Human Leukocyte Antigen
IL12	Interleukin 12
IL10	Interleukin 10
IL6	Interleukin 6
IFNγ	Interferon gamma
Th1	Type 1 helper T cell
Th2	Type 2 helper T cell
CTL	Cytotoxic T cell
Treg	Pathogen associated molecular pattern
pDC	Pathogen recognition receptor
LC	Toll-like receptor
cDC	Nuclear factor κ-light-chain-enhancer of activated B cells
LEC	Pathogen-like particle
PAMP	Draining lymph node
PRR	Pathogen recognition receptor
TLR	Toll-like receptor
RLR	RIG-I like receptor
CLR	C-type lectin receptor

NLR	NOD-like receptor
NFκB	Nuclear factor kappa B
PLP	Pathogen-like particle
dLN	Draining lymph node
PLGA	Poly (lactide-co-glycolide) acid
MP	Microparticle
NP	Nanoparticle
GMCSF	Granulocyte-macrophage colony stimulating factor
IL4	Interleukin 4
PDL2	Programmed Death Ligand 2
IFNα/β/γ	Interferon alpha/beta/gamma
Flt3L	Fms-related Tyrosine Kinase 3 ligand
ODN	Oligodeoxynucleotide
PVA	Poly vinyl alcohol
DCM	Dichloromethane
Micro-PLP	Micro-pathogen-like particle
Nano-PLP	Nano-pathogen-like particle
PEI	Polyethylenimine
OVA	Ovalbumin
SEM	Scanning electron microscopy
SIM	Structured illumination microscopy
FACS	Fluorescence-activated cell sorting
MACS	Magnetic-activated cell sorting

BMDC	Bone marrow derived cells
ELISA	Enzyme-linked immunosorbent asaay
iPDL2	Induced programmed death ligand 2
MFI	Mean fluorescence intensity
iDC	Inflammatory dendritic cell
NK	Natural killer cell
NKT	Natural killer- T cell
GC	Germinal center
TLR9	Toll-like receptor 9
IRAK	Interleukin-1 receptor-associated kinase
IRF	Interferon regulatory factor
PLA	Proximity ligation assay
Phosphor-STAT3	Phosphorylated STAT3
SEAP	Secreted embryonic alkaline phosphate

SUMMARY

Microbial pathogens range in size, shape, as well as biochemical and molecular properties. This has led to the evolution of a variety of pathogen recognition receptors (PRRs) in mammalian immune cells that are responsible for sensing pathogen-associated molecular patterns (PAMPs) and initiating specific types of immune responses. However, the breadth of the PRR responses, especially how dendritic cells sense pathogen physical properties in conjunction with specific molecular patterns and translate that into unique immune responses, remains unknown. Here, we have developed pathogen-like particles (PLPs) that mimic physical properties of large viruses or bacteria to demonstrate that CpG-mediated dendritic cell signaling can be precisely modulated by varying PLP parameters, specifically size and adjuvant density. We demonstrate controlled tunability of DC programming, allowing directed maturation of distinct T cell phenotypes, antibody class switching and in vivo immune-polarization. Furthermore, we show, for the first time, that the surface-density of CpG on PLPs can finely control DC signaling by regulating the kinetics of NFκB transcription and STAT3 phosphorylation. These findings suggest that DCs sense physical aspects of pathogen-like materials, broadening the tools that can be used to modulate immunity, better understand innate immune response mechanisms, and develop new and improved vaccines.

CHAPTER 1 OVERVIEW, HYPOTHESIS AND SPECIFIC AIMS

1.1 OVERVIEW

The implementation of vaccines has been one of the most successful global health initiatives to date, but there are still a significant number of disease states (i.e. infectious, cancerous, autoimmune) that are treatable via an immunotherapy. Therefore, vaccine design must become more advanced in order to tackle these evasive diseases. Vaccines that will prove effective must target immune cells of interest so not to induce an undesired systemic response, provide potent and persistent modulatory signals and direct immune cell programming to the most effective mode of therapeutic action. Particulate vaccines offer a tunable platform that can be targeted (chemically or otherwise), can carry multiple antigens and adjuvants to ensure potent (sometimes synergistic) signaling and there is building evidence that they can be used to specifically direct immune cell activity. This evidence motivates the investigation of more efficacious vaccine designs that are specific to each disease, as they will each require a unique therapeutic approach.

Furthermore, dendritic cells have been identified as the conductors of the adaptive immune response, as they give the primary signals to T cells, which drive the attack on infection. Therefore, it is essential that we gain understanding of how these cells function and how that function can be successfully modulated.

Recent literature has established that there are multiple subsets of DCs in peripheral tissues that have the ability to direct the body's immune response[1]. Biomaterials-based delivery systems have been shown to increase vaccine efficacy and targeting molecules have been added to these systems to preferentially direct vaccines to DCs[2]. However, it has not yet been explored whether physical parameters, such as size, can be used to direct delivery to specific DC subsets. In this work, we have demonstrated that relevant tissue-resident DC subsets can be targeted by particle size, resulting in a distinct immunological

response. Furthermore, we describe a mechanism by which particles direct functional programming of DCs.

1.2 HYPOTHESIS

Our **primary hypothesis** was that particle parameters, specifically size and ligand density significantly affect the efficiency of our particles vaccines by modulating DC programming. The **overall objective** was to develop pathogen-like particle (PLP) vaccine delivery systems that will induce a more robust, long-lasting immune response.

1.3 SPECIFIC AIMS

1.3.1 Aim 1: Determine how DCs of two peripheral subsets interact with PLPs in vitro.

In this aim, (a) PLGA nanoparticles (NPs) were fabricated using a method similar to microparticles (MPs) previously used in the lab, including cationic modification using branched polyethylenimine. The NPs were characterized to determine size, zeta potential and loading potential of various vaccine components. (b) Additionally, primary murine bone marrow derived dendritic cells (BMDCs) or spleen-derived DCs were grown in varying culture conditions that result in phenotypes relevant for vaccination. Delivery efficacy of these particles was tested in vitro using DCs studied previously alongside MP equivalents. Maturation markers, secreted cytokines and antigen presentation to CD4+ and CD8+ T cells were studied.

1.3.2 Aim 2: Investigate the efficacy of PLP formulations screened in Aim 1 in vivo.

This aim was split into three goals. We first investigated how PLP vaccination affected migration of skin-resident DC subsets and which subsets were responsible for carrying PLPs to draining lymph nodes. We then characterized the resultant adaptive immune

response to determine whether PLP-size dependent immunomodulation was evident. Finally, we tested whether the PLP-driven immune responses were robust enough to protect mice against a challenge with a lethal dose of melanoma.

1.3.3 Aim 3: Evaluate mechanism that dictates formulation size-dependent DC programming.

In this aim, we deconstructed the primary pro-inflammatory signaling axis to determine where the divergence in signaling between micro- and nano-PLPs occurs. We investigated the well-characterized TLR9-NFκB signaling pathway. Specifically, we focused on uptake, TLR9 activation, NFκB transcription and NFκB inhibition.

1.4 OUTLINE

This work focuses on characterizes the interaction of pathogen-like particles (PLPs) with varying subsets of skin-resident migratory dendritic cells. Specifically, we investigated whether particle size or adjuvant density play a role in influencing dendritic cell programming, which thereby attenuates downstream immune events. CHAPTER 2 provides a short overview of the immune-biology, focusing on dendritic cells (DC) of the innate immune response and their subsequent signals to cells of the adaptive immune response. We further elaborate on DC subset biology and then discuss the state of the field of molecular adjuvant research and how particle carriers can be considered adjuvants. PLP characterization and in vitro dendritic cell culture development are discussed in CHAPTER 3 , along with the demonstration that DC subsets exhibit preferences for different sized carriers and that size plays a critical role in DC programming. 3.4validates this dichotomy in vivo and further demonstrates the immunomodulatory potential of carrier size through their ability to tune T cell mediated systemic immunity. In CHAPTER 5 we have proposed a mechanism by which particle size mediates the observed shift in DC programming. We have demonstrated that nano-PLPs, despite being taken up at a similar rate and magnitude as micro-PLPs, promote delayed signaling through TLR9, leading to inhibition of downstream signaling processes. Furthermore, we observed rapid activation of an inhibitory pathway in cells treated with nano-PLPs. Finally, **CHAPTER 6** discusses implications of these studies and proposes future work.

CHAPTER 2 BACKGROUND AND SIGNIFICANCE[1,2]

Immunotherapy is the use of drugs and/or biological agents to initiate, modulate and control an immune response. There is a wide range of immunotherapeutic strategies that are currently being investigated for both prophylactic and therapeutic purposes. Some of these have been previously reviewed in detail[3]. Prophylactic immunotherapy (i.e. vaccination) refers to the use of specific antigens along with immunomodulators or immunostimulators (often referred to as adjuvants) to generate protective immunity against future infections or antigenic challenge while therapeutic immunotherapies are applied after the onset of a disease. This chapter focuses on polymer-based nano and microparticle carriers for vaccine-related applications, although most of the concepts presented here are broadly applicable for immunotherapies in general.

---

[1] Leleux, J. and Roy, K. (2013), Micro and Nanoparticle-Based Delivery Systems for Vaccine Immunotherapy: An Immunological and Materials Perspective. Advanced Healthcare Materials, 2: 72–94. doi: 10.1002/adhm.201200268 – used with permission from publisher (License #: 369151318056)

[2] Leleux, J., Atalis, A., Roy, K. (2015), Engineering Immunity: Modulating Dendritic Cell Subets and Lymph Node Response to Direct Immune-polarizatoin and Vaccine efficacy. Journal of Controlled Release, *In Review.*

2.1 IMMUNITY: A PRIMER

Before Edward Jenner's discovery of the cross-reactive cowpox vaccine two centuries ago, which eventually eradicated smallpox in humans, the primary disease prevention strategy was to intentionally induce a mild infection using pathogenic serum or lysate. While these techniques often provided protection, there were also many cases of severe, even fatal reactions[4]. As safety concerns have risen and biological technology modernized, scientists have begun to develop vaccines with four crucial criteria in mind: they must be safe, effective, scalable and cheap while at the same time provide a robust, long-term immune response.

2.1.1 Inducing a robust memory response: innate and adaptive immunity

The immune response is separated into innate immunity and adaptive immunity. The main differentiating factors between the two are the response time and the level of specificity. The innate response is initiated almost immediately and involves the migration of phagocytic cells, mainly macrophages and dendritic cells (DCs) to the site of infection[5,6]. While all of these cell types have the ability to present antigen, DCs are considered to be the primary antigen presenting cells (APCs). Immature DCs migrate out of the bone marrow and reside in the bloodstream and peripheral tissue where they encounter pathogens or antigen. Once this interaction occurs and the DC ingests a microbe or other antigen, it undergoes directed activation and maturation. As the name APC implies, the cells digest (process) pathogens and present highly specific peptides on their surface in combination with a major histocompatibility complex (MHC I or MHC II in mice, HLA or Human Leukocyte Antigens in humans) that provide signals through the T cell receptor complex to induce T cell maturation, specificity and subsequent clonal expansion (Figure 1)[7]. Additionally, costimulatory molecules, such as CD40, CD83, and CD86 move to the surface of the APC where they provide critical stimulatory signals in T lymphocyte activation[8,9]. Finally, activated APCs begin to secrete immunomodualtory

cytokines, such as IL12p70, IL10 and IL6. The specific combination of MHC complexes carrying antigen specific peptides, costimulatory molecules expressed on the surface of a DC and immunomodulatory cytokines directs T lymphocyte activation and functionalization[10]. Expression of an MHC class I molecule on the surface of a DC and secretion of IL12p70 will more often result in the differentiation of an immature T lymphocyte to a CD8 expressing cytotoxic T lymphocyte (CTL). MHC class II molecules will induce the maturation of CD4-expressing-helper T cells (Th cells)[11]. CTLs go on to eliminate pathogen-infected cells and are being studied as a potential stategy for cancer eradication[12]. Th cells' have a wide variety of functions that are highly dictated by DC signals (i.e. cytokines) including facilitating B cell activation, which induces the humoral immune response, and promoting maturation of other T cells. In some cases, CD4 is also expressed on the surface of CTLs[13].

After helper T cell differentiation and antigen specification, these cells are able to provide secondary costimulatory signals to B lymphocytes that have been activated by an antigen. This secondary signal is essential for B lymphocyte maturation into a plasma cell. Mature plasma cells produce antigen-specific serum and mucosal antibodies[14]. Antibodies participate in host defense by neutralizing toxins and coating pathogens to aid in phagocyte identification.

Humoral immunity has been targeted for years in order to develop effective vaccines. Significantly increased titers and long residence time of antigen specific antibodies are the hallmarks of an effective inoculation regimen[15,16]. However, with increasing safety restrictions and the need for a robust cellular response to persistent or immune-evading pathogens, the addition of specific adjuvants to vaccines can enhance cell-mediated immunity and provide immunostimulatory enhancement to ensure prolonged memory.

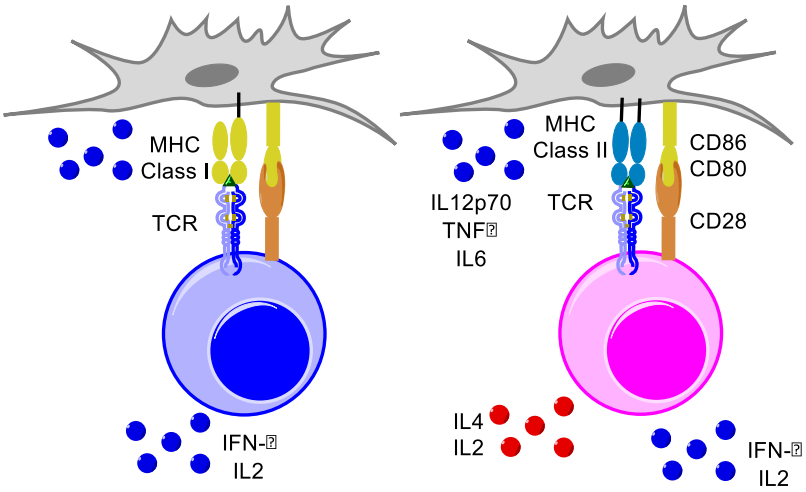

Figure 1: APCs present antigen via MHCI or MHCII molecules to CD8+ or CD4+ T cells, respectively.

2.1.1.1 DC Subsets

It is now recognized that based on primary location, DCs can be sub-categorized into many functionally distinct groups, extending the influence that DCs have on immunity. In addition to DC subsets in the periphery, there are also lymphoid-resident DC subsets that have significant impact on T cell maturation [17–19]. In this section, we will discuss some of the key subsets and their functional differences. Table 1 provides a summary of these DC subsets, along with surface markers used to distinguish and isolate them, the related maturation markers and primary cytokine types that the cells secrete upon activation and maturation. While this table includes human subsets, we will focus on murine DCs in this section. Additionally, Figure 2 delineates the skin, lymphatics, and lymph node biointerface, designating the relevant anatomy, various DC subsets present, and highlighting that peripheral DCs must migrate to the local immune hubs (i.e. draining lymph nodes) in order to initiate a robust adaptive, systemic vaccine response.

Table 1: DC Subsets: Location and Function

DC Subset	Primary Location	Species	Phenotype	Function†	Source
CD8α+	Lymphoid tissue	M	$CD205^{+}$ $CD11b^{lo/-}$ MHC I Clec9A TLR 3	Cross presentation CD8+ T cell priming Maintain self-tolerance	17,18,20,21
CD8α-	Lymphoid tissue	M	$CD205^{lo}$ $CD11b^{+}$ $CD4^{+/-}$ MHC II TLR 7	CD4+ T cell activation	18,21,22
Plasmacytoid	Blood/Lymphoid Tissue/Inflammatory Tissue	M/H	$CD11c^{lo}$ TLR 7 TLR 9	Type I interferon secretion Promote wound repair	23–26
Langherans	Epidermis	M/H	Langerin $^{+}$ $CD205^{+}$ * $CD11b^{+}$ $EpCAM^{+}$ MHC I (M) ** MHC II (M) HLA-DR (H)	CD4+ T cell priming Th2/Th17 induction Treg induction Cross presentation **	27–30
CD103+	Dermis	M	Langerin^{+} $CD11b^{lo/-}$ $CD11c^{+}$ MHC I MHC II Clec9A TLR 3	CD8+ T cell priming Cross presentation Th1/Th17 induction	29,31–33
CD11b+	Dermis	M	Langerin^{-} $CD11b^{+}$ $CD11c^{+}$ MHC II	Treg induction Th induction	31,34,35
CD1a+	Dermis	H	Langerin^{-} $CD205^{+}$ $CD11c^{+}$ $HLA\text{-}DR^{+}$	CD8+ T cell priming CD4+ T cell proliferation	36,37
CD14+	Dermis	H	Langerin^{-} $CD11c^{+}$ $DCSIGN^{+}$ $CD206^{+}$ $HLA\text{-}DR^{+}$	CD4+ T cell activation Th2 induction	38,38,39
CD141+	Blood/Lymphoid Tissue/Dermis	H	$BCDA3^{+}$ $CD11c^{+}$ $CD1a^{-}$ $CD11b^{lo}$ $HLA\text{-}DR^{+}$	Cross presentation	25,40,41
Mo-derived	Blood/Inflammatory Tissue	M/H	$Ly6C^{+}$ $CD11b^{+}$ $CD11c^{+}$ MHC II	Infiltrate inflammatory tissue	25,28

†DC subsets not limited to these functions; those listed are discussed in this review
*Expression of CD205 may be inflammation dependent in humans **Controversial whether mLCs cross present

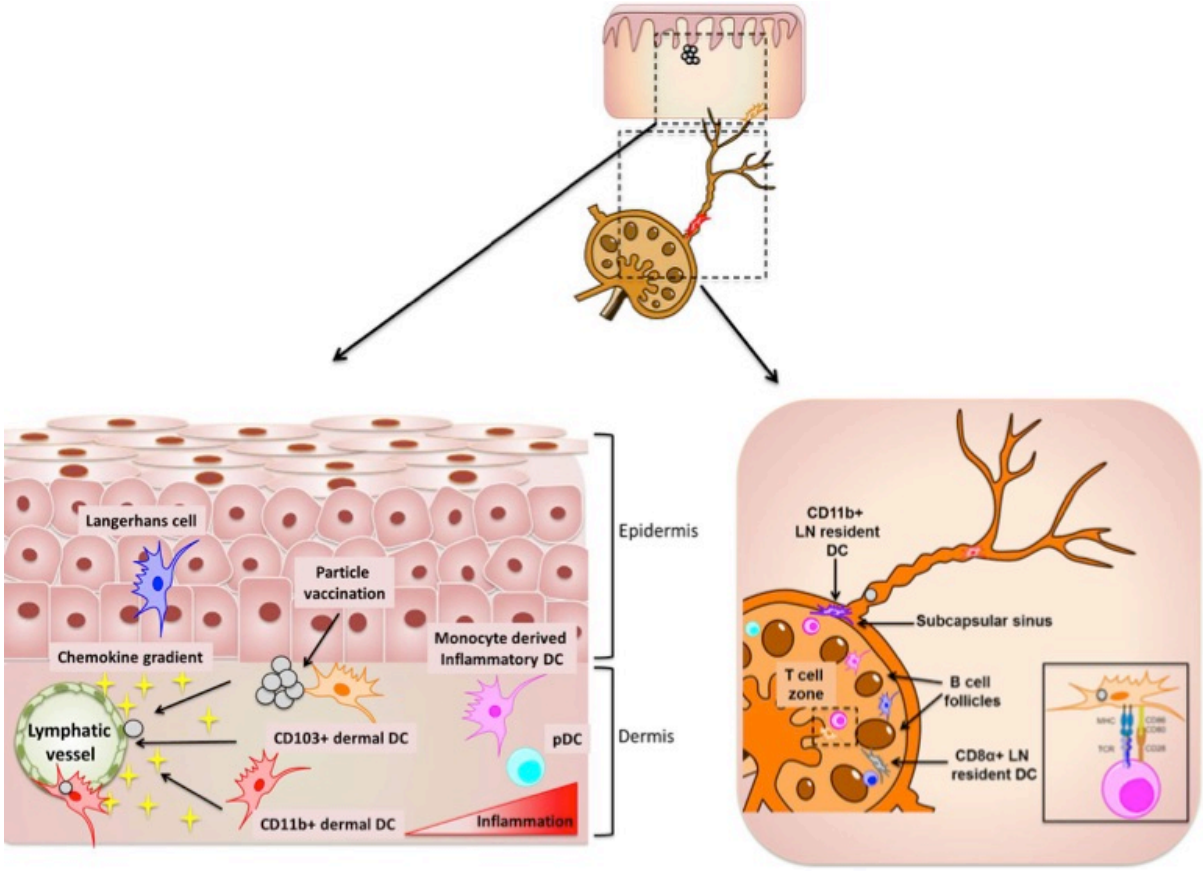

Figure 2: Schematic of skin and lymph node resident DC subsets.

2.1.1.1.1 Secondary Lymphoid Organ Resident Dendritic Cells

Secondary lymphoid organ resident dendritic cells were the first to be classified in the mouse system by Steinman and Cohn over 40 years ago [42]. Since their initial discovery and characterization, our understanding of their complexity has greatly increased, leading to multiple sub-classifications with very different functions. To date, these DCs are placed into two subsets based on their expression of CD8α and CD11b and their corresponding functions to the third subset, which is the plasmacytoid DC.

CD8α+DC

CD8α+DCs, also characterized by their expression of C-type lectin receptor DEC-205 (CD205) but not integrin CD11b, have been the most extensively studied and shown to efficiently cross-present antigen, induce CD8+ T cell activity and cytotoxic behavior [17,18,20]. A functionally homologous cell type was only recently discovered in the human system and is characterized by its expression of BDCA-3 (discussed later in this section)[43,44]. Is has also been shown that CD8α+ DCs have the ability to receive antigen from migratory DCs that arrive from the peripheral tissues for presentation to CD8+ T cells, effectively increasing the range of T cell activation associated with relatively few migratory cells in the LNs [45]. This antigen exchange may not be isolated to proteins, but may also include glycolipid antigens essential for natural killer-T cell activation [46]. Additionally, CD8α+ DCs play a role in maintaining self-tolerance by promoting self-reactive T cell proliferation and subsequent elimination, as well as maturation of Foxp3+ regulatory T (Treg) cells [19,47].

CD8α- (CD11b+) DC

CD11b+ lymphoid DCs do not express CD8α nor high levels of DEC-205, but can express CD4 and interact primarily with CD4+ T cells [18,22]. These cells preferentially activate a type II helper response from CD4+ T cells, likely due to their proficiency in MHC II antigen presentation [48–50]. These cells also exist in a double negative (CD8-CD4-) state and maintain their ability to promote type II polarization of the helper T cell (Th) response. However, CD4+ DCs have also been shown to secrete type I associated cytokines, such as IL-12, when activated by certain toll-like receptor (TLR) agonists, linking these cells to antiviral immunity with the appropriate signals [51]. Lastly, these cells are the predominant scavengers of antigen that circulate through the lymphoid organs, especially lymph nodes, via lymphatic drainage [50].

Plasmacytoid DC

The final subset of lymphoid-resident dendritic cells is plasmacytoid DC (pDC), which has been identified in secondary lymphoid tissues as well as blood and certain peripheral tissues (mostly during inflammatory episodes) [52,53]. pDCs have been shown to differ from conventional DCs in morphology, migration patterns, and primary function [54,55]. Their hallmark is the ability to secrete large amounts of type I interferon after exposure to viral pathogenic patterns, particularly agonists for TLRs 7 and 9 [23,24,56]. These receptors typically recognize pathogenic RNA and DNA, respectively, and have mechanisms by which they differentiate these patterns from autogenic nucleic acid debris [57]. However, there is recent evidence that certain disease states can promote recognition of self-DNA, leading to overproduction of type I interferon and autoimmunity [58–60]. pDCs have also been implicated in Treg priming, plasma cell differentiation and tolerance against allergies [61–65].

2.1.1.1.2 Skin-resident Dendritic Cell Subsets

Though peripheral dendritic cells reside in many organs such as the gut, intestine, and lungs, skin and muscle are the most common sites of vaccination. Because of recently developed devices such as microneedles and needle free injectors, skin-based vaccination is gaining further importance. Furthermore, significant knowledge exists on skin-resident DCs, their various subsets, and related lymphatic transport; which will be the primary focus of this section.

Langerhans cells

Langerhans cells (LCs) are epidermal DCs characterized by their Birbeck granules, formed by the C-type lectin receptor, Langerin [27,66]. They specialize in surveying the epidermis for antigen, extending their dendrites between apical cells [67]. In mice, LCs (mLCs) can promote and regulate multiple T cell-mediated responses [40,68,69]. They

primarily present antigen via MHC II to induce proliferation of Th17 cells, known for mediating immunity against bacteria and fungi, and Th2 cells, required for humoral immunity against large extracellular pathogens [28,29]. However, the ability of mLCs to induce type I helper immunity is controversial. In mice infected with *Candida albicans*, mLCs were unable to induce Th1 responses or cross-present antigens to CD8+ T cells [29]. However, Nizza et al. observed that murine CD11b+ Langerin+ migratory DCs (mainly mLCs) were able to cross-prime naïve CD8+ T cells and imprint them with skin-homing specificity [30]. mLCs can also induce proliferation of Treg cells and restrain self-reactive T cells, suppressing inflammation and autoimmunity [28].

Dermal Dendritic Cells

Within the dermis are conventional DCs (cDCs), distinguishable from their lymphoid-resident counterparts by their intermediate to high levels of CD11c and high levels of MHC II [70,71]. In both homeostatic and inflammatory conditions, they travel from the skin to lymph node guided by the chemokine receptor, CCR7, which will be discussed in greater detail later. At steady state, dermal DCs present self-antigens, aiding in maintenance of peripheral tolerance. However, when they encounter a pathogen, dermal DCs mature similarly to LCs and upregulate costimulatory molecules on their surface in order to activate antigen-specific CD4+ and CD8+ T cells. The two major murine dermal DC subsets are CD103+ and CD11b+ DCs [67,72].

In the dermis, CD103+ DCs express Langerin but not CD11b (although some are $CD11b^{lo}$) [31,67]. These dermal DCs are most known for their superior ability to cross-prime CD8+ T cells [32].. In addition to cross-presentation, CD103+ DCs also drive Th1 and Th17 cell differentiation [29,73].

CD11b+ DCs express DEC-205, but not Langerin [31,67,71]. They are the most abundant type of DC in a healthy dermis and share phenotypical characteristics with monocyte-derived DCs that infiltrate tissue during inflammation [34,74]. They can also be

broken down into further subcategories with varying functions but their predominant role is thought to be MHC II presentation and induction of Treg and Th cells [75,76]. For example, Plantinga et al. observed that migratory CD11b+ cDCs but not CD103+ DCs initiated Th2 cell-mediated immunity against house dust mite allergen in the lymph node[34]. Though they do not directly activate Treg cells, they express the enzyme aldehyde dehydrogenase that metabolizes vitamin A into retinoic acid, which has been implicated in Foxp3+ Treg cell generation in vitro [35,77,78].

2.1.1.1.3 DC Migration

Migratory dendritic cells travel to the lymph node through afferent lymphatic vessels in homeostatic and inflammatory conditions. Tissue-resident dendritic cells are constantly presenting antigens; in the steady state, they present self-antigens via MHC II, resulting in tolerogenic activity. Immature migratory dendritic cells do not express high levels of co-stimulatory molecules such as CD40, CD80, or CD86, which bind to receptors on T cells during activation [79,80]. In the presence of MHC II without engagement of co-stimulatory molecules, T cells either die or become anergic [81]. Immature, migratory DCs can also convert naïve CD4+ T cells into Tregs [82].

It is well known that DCs activated by microbial antigens and inflammatory stimuli upregulate chemokine receptor CCR7, which binds to ligands CCL21/SLC and CCL19/ELC for recruitment to the lymphatic vessels [83–85]. CCL21 is released by lymphatic endothelial cells (LECs) and is highly concentrated around the vessel, since it binds to sulfated proteoglycans (i.e. heparin) [86,87]. On the other hand, CCL19 is more soluble and acts in both autocrine and paracrine fashions, as it is released by both dendritic cells and LECs [87]. While this recruiting mechanism may play a role in steady state maturation and migration, there is still much to learn. Baratin et al. speculates NF-κB signaling is required for maturation and migration and demonstrates IKKβ deletion is sufficient to prevent the steady state accumulation of migratory DCs in the lymph node[88].

2.1.1.2 Adjuvants: Enhancing immunity through pathogenic recognition

While the innate response is not considered specific and will not retain any memory of a previous infection, there are mechanisms at the DC level that can provide the initial direction of the immune response. Adjuvants can be categorized into two groups: immunostimulatory molecules and antigen delivery vehicles[89]. The immunostimulatory molecules that are responsible for guiding specific cytokine production by DCs as well as DC activation are called pattern recognition receptors (PRRs), which are individually stimulated by a class of molecules called pathogen associated molecular patterns (PAMPs). PAMPs are being extensively investigated as adjuvants to activate specific PRRs and thereby control the DC behavior towards a specific type of immune response and thus increase vaccine efficacy[6]. The sections below provide an overview of DC-related PRRs and their associated PAMPs.

2.1.1.2.1 Membrane-spanning PRRs

Toll-like receptors (TLRs) are transmembrane proteins located on the cell and endosomal membranes **(**Figure 3**)**. Their position correlates to the type of adaptive immune response that they induce **(**Table 2**)**[90–93]. Therefore, TLR ligands (PAMPs) can be selected to specifically engineer adjuvants that elicit predictable reactions. The recognition of lipopolysaccharide by TLR4 was the first of the TLR-ligand relationships to be elucidated and has since driven further investigation of how TLRs affect the end point of an immune response[6]. Other TLRs that recognize bacteria-derived ligands are TLR1, 2, 5 and 6, which all reside on the cell membrane[94,95]. Their location allows them to interact with bacteria cell wall constituents, such as lipopolysaccharide, flagellin or lipoproteins. TLRs 3, 7/8, and 9 are recruited to the endosomal membrane upon the uptake of viral components. These TLRs recognize double-stranded RNA (e.g. poly(I:C)), single-stranded RNA and unmethylated CpG motifs in DNA, all of which are not native to

mammalian cells[92]. With the exception of TLR3, all of the TLRs are associated with a MyD88 dependent signaling pathway, which is responsible for the downstream activation of many transcription factors, most significantly NF-κB[96,97]. NF-κB positively regulates the production of cytokines crucial to the adaptive immune response[98,99]. These cytokines play an essential role in determining the direction of the innate response and subsequently, the cellular response[100]. In the case of MyD88 inhibition or damage, TLR3 and 4 can also trigger a MyD88 independent pathway via the adaptor protein TRIF that results in the production of the antiviral cytokine IFN-β[101]. Utilization of specific activation of these receptor-ligand interactions has become of particular interest for chronic infections and cancer therapeutics[102].

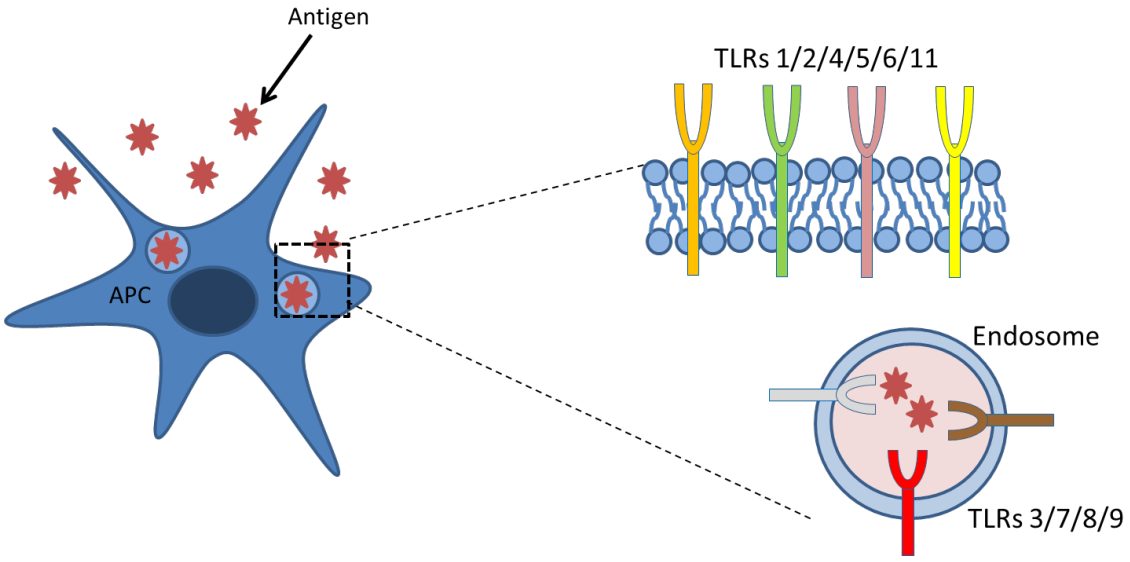

Figure 3: Toll-like receptors on APC cell and endosomal membranes recognie specific patterns associated with pathogenic molecules.

Table 2: Toll-like receptors and their ligands

TLR	Receptor Location	PAMP recognized	Cell Response
TLR 1	cell membrane	bacterial triacyl lipopeptides	Induce production of inflammatory cytokines
TLR 2	cell membrane	- bacterial lipoproteins/lipopeptides and lipopolysaccharides of non-enterobacteria - fungal β-glucan	Induce production of inflammatory cytokines
TLR 3	endosome	viral double stranded RNA/ polyinosinic: polycytidylic acid	Synthesis of type 1 interferons
TLR 4	cell membrane	- lipopolysaccharaide from Gram-negative bacteria - heat shock proteins - domain A of fibronectins, hyaluorinic acid, heparan sulfate and fibrinogen	Synthesis of type 1 interferons
TLR 5	cell membrane	bacterial flagellin	Found in intestinal endothelium and lung epithelium which implicates its importance in mucosal immunity
TLR 6	cell membrane	bacterial diacyl lipopeptides	Induce production of inflammatory cytokines
TLR 7	endosome	Imidazoquinoline/ Single stranded RNA	Anti-viral response
TLR 8	endosome	Imidazoquinoline (in humans)/ Single stranded RNA	Anti-viral response
TLR 9	endosome	Unmethylated CpG motifs	Dependent on type of CpG Type A/D induces IFN-α Type B/K induces IL-12 and TNF-α production
TLR 10	unknown	unknown	unknown
TLR 11	cell membrane	Uropathogenic bacterial components	Prevention of urinary tract infection
TLR 12/13	only in mice -- unknown	unknown	unknown

2.1.1.2.2 Cytoplasmic PRRs

Pathogenic material can also be detected intracellularly by a series of cytoplasmic receptors including RIG-1-like receptors (RLRs), nucleotide-binding domain-like receptors (NLRs) and C-type lectin receptors (CLRs)[103,104]. RLRs recognize viral replication byproducts such as dsRNA in the cytoplasm and subsequently activate NF-κB and type 1 interferon production[103]. While about 30 NLRs have been identified, only the functions of nucleotide-binding domain-1 (NOD-1) and NOD-2 have been elucidated. Peptidoglycan containing components of bacteria are recognized by NOD-1 and NOD-2 which also results in induction of an inflammatory response lead by NF- κB activation[105]. CLRs also identify cell wall components but specifically of mycobacteria. CLR activation is implicated in promoting the generation of type 1 helper T cells[106]. In addition to the use of single PAMPs for APC activation and innate immunity direction, the synergistic effect of combining multiple PAMPs as adjuvants is being thoroughly investigated[107,108].

2.1.1.2.3 Delivery vehicles as adjuvants

Delivery vehicle adjuvants are most often particulate in nature and include polymer particles, emulsions, liposomes, virosomes and others[109]. Their main functions are to stabilize the antigen by protecting it from the surrounding biological conditions, to slow down the clearance of antigens or diffusion of adjuvant from the site of injection and to enhance delivery to antigen presenting cells (APCs)[110].

Antigen delivery systems, while not always being inherently immunostimulatory do promote the necessary interactions for antigens to be efficiently presented to DCs for humoral and cellular memory. There are three important steps that are essential for a

vaccine to be efficacious: targeting, activation and transfection/antigen presentation. While this process has recently been reviewed it is worth being discussed briefly here[111]. Before an antigen is taken up by an APC, it is vulnerable to its surrounding environment, which consists of numerous enzymes that can denature the antigen such that it no longer has immunomodulatory abilities. The first benefit of particulate antigen delivery is the protection it provides the antigen from premature degradation in biological environments[112]. Once the antigen is stable in the body, it is critical that it is found and taken up by an APC, ideally a DC. Another benefit of particle delivery is tighter control on the active and passive targeting to APCs to increase uptake of the antigen[113]. Regardless of route of delivery, soluble antigens and adjuvants rarely reach the appropriate antigen presenting cells; therefore the resulting immune response is not potent enough for long term protection. This is partially because of the rapid rate at which hydrophilic or small molecule adjuvants diffuse into systemic circulation[114,115]. Particles mimic the size and structure of a pathogen, so APCs are more likely to take up particles than soluble antigen. Especially when combined with chemokines and/or APC targeting molecules, particles can simulate a depot for the antigen, increasing the efficiency of delivery of the antigen to APCs. Additionally, controlled release of antigen and other molecules can lead to prolonged presentation to APCs. Particles can also aid in facilitating endosomal release of the antigen post-uptake, which is necessary for antigen cross-presentation within the APC[116,117]. Cross presentation is an important mechanism for the surface expression of MHC I molecules, which is critical for the production of CD8+ cytotoxic T cells (CTLs). Generally antigens that are phagocytosed will be presented by MHC class II molecules, which generate CD 4+ T cells causing antibody

production and other humoral responses. However, in the case of persistent viruses and cancer, this response is not sufficient; a cellular response is also necessary. Therefore, cross-presentation of the antigen to promote expression of a MHC I-antigen complex is essential[118]. In addition to cross presentation, endosomal release allows for DNA vaccines to migrate to the cell nucleus where they can transfect the cell[119].

Lastly, particulate delivery of antigens allows the co-delivery of multiple molecules, i.e., antigen and adjuvants to the same cell and potentially at higher doses than would be possible in soluble conditions. This increases the probability that the intended response will be observed due to discretized heightened response on an individual cell basis. These enhancements would affect both the antibody response produced by B cells as well as the many functions of T cells.

2.2 PARTICLES FOR DELIVERY OF ANTIGEN AND ADJUVANTS: PATHOGEN-LIKE PARTICLES AS VACCINES

Particle-based delivery systems have gained attention due to their potential benefits as drug and vaccine carriers. These carriers should incorporate several design constraints: they must be biocompatible, able to deliver a variety of drugs or vaccines that can be released in a targeted and controlled fashion, must be stable throughout processing and delivery in vivo and should be biodegradable or easy to clear[120]. The following sections will elaborate on various polymer-based particulate delivery systems and will address how they fulfill the above design criteria.

2.2.1 Comparison of particle parameters

Many particulate systems have been effective in eliciting an immune response; however, it is important to understand how the many differences in physical properties can render a particular technique useful for specific applications. Specifically, particle size has been heavily studied in the context of immune cell uptake and some aspects of immunomodulation, but there is still no consensus about how size can be used to specifically direct immunity. Additionally, ligand density is inherently coupled with size and has been relatively unstudied compared to many other parameters. This section will discuss the major claims provided by size and ligand density studies to date.

2.2.1.1 Does Size Matter?

Particle size is a critical factor that can drastically affect interaction of particles with cells as well as their biodistribution. In drug delivery, particles in the nanometer range are considered attractive *in vivo* carriers because they can easily permeate tissue barriers (e.g. vasculatures) and better migrate into target tissues, especially in diseased tissues like tumors[121]. However, size-effects for particles designed to target immune cells and their ultimate influence on the immune response, has not been definitively established. It is

postulated that particles of several microns in size would be phagocytosed readily and thus provide improved delivery of antigens and adjuvants to APCs[122]. However, pathogenic material is often smaller than a micron; viruses can even be tens of nanometers in diameter. Additionally, particles larger than 100 nm have difficulty moving into lymphatic vessels and traveling to the lymph nodes, where they can increase the probability of immune cell interaction[117]. Particle size also influences a cell's mechanism of uptake, some of which are more efficient than others. How a cell takes up a vaccine could eventually determine how it processes the antigen[123].

Although several groups have investigated how size correlates to immunotherapeutic benefits, the inherent complexity of the immune response makes pinpointing an optimal solution difficult. There is some evidence that smaller particles can induce a type 1, antiviral response while immunization with larger particles tends to induce a more significant humoral reponse[124,125]. Additionally, particle size effects could vary with route of administration[126]. For example, while particles 100 nm in diameter are taken up more efficiently in the Peyer's patch after oral immunization, particles this size are not suitable for an intranasal or inhalable vaccination[122,127]. Lastly, as discussed earlier, particle size can dictate whether particles can be transported via interstitial flow to the lymph nodes. Reddy et al. demonstrated that the cutoff for efficient movement of particles through the lymphatic capillaries is about 45 nm[128]. Table 3 provides more examples of studies investigating how particle size has an impact on the resultant immunity.

Table 3: Effect of particle-size on immune response

Type of Particle	Particle Size Range	Application	Results
PLGA[127]	100nm, 500nm, 1µm, 10 µm	*In situ* GI tract tissue uptake in rats	60% increase 100nm uptake in Peyer's patch. Larger particles in epithelium.
PLGA[129]	200 nm and 2 µm	Targeted and nontargeted particles to deliver antigen to human DCs *in vitro*	MPs more nonspecific uptake. Targeting enhanced NP uptake..
PLGA[126]	200 nm, 500 nm, 1 µm	Particle size dependent serum antibody response following immunization IN, OR and SC..	Administration of largest particles (1 µm) elicited highest serum IgG response.
PLA[130]	Between 50-150 µm, 10-70 µm, 2-8 µm, less than 2 µm	Particles loaded with tetanus toxoid for long term anti-TT antibody titer	2-8 µm MPs elicited the most significant antibody response.
Charged fluorescent polystyrene (negative, positive and neutral)[131]	50, 100, 200, 500 nm	Permeation of nanoparticles for transdermal vaccine delivery using pig skin	Negatively charged 50nm and 500nm particles permeated deepest into the skin.
Fluorescent Polystyrene[132]	100 nm, 500 nm, 1 µm, 4.5 µm	Optimal DC uptake to enhance antigen delivery	<500nm NPs taken up best by DCs

Table 3: Effect of particle-size on immune response

Type of Particle	Particle Size Range	Application	Results
Fluorescent Polystyrene[133]	930 nm, 1.87 µm, 2.3 µm, 2.98 µm, 4.3 µm, 5.71 µm, 9 µm	Investigate the dependence of size on phagocytosis	2 µm-3 µm MPs preferentially phagocytosed by alveolar macrophages.
Polystyrene [124]	20 nm, 40 nm, 49 nm, 67 nm, 93 nm, 101 nm, 123 nm	NP uptake by DCs and induction of type 1 or type 2 responses	40-49 nm NPs had highest IFN-γ. 93-123 nm NPs induced IL-4
Pluronic-stabilized polypropylene sulfide[134]	25nm, 100nm	Ultra-small versus small NPs transport to lymph modes via interstitial flow	25 nm NPs 10x more efficient drainage to LNs than 100nm NPs
Various [120]	500 nm - 5 µm	Intranasal or inhaled delivery of vaccines for mucosal immunization	> 5 µm MPs will not reach the deep lung. <500 nm will be immediately exhaled.
Various[122]	1 - 5 µm	Maximum interaction with phagocytic cells	Particles this size will be efficiently taken up.
Various[125]	20 - 200 nm	Maximum receptor mediated endocytosis	Stimulate anti-viral response

2.2.1.2 Does Ligand Density Matter?

Particle surface area to volume ratio varies as a function of size, with smaller particles having a larger ratio. This means that when testing particulate vaccines that it is impossible to keep antigen/adjuvant dose, particle mass and ligand density the same for all formulations. Therefore, it is essential to quantify which of these variables plays the greatest role in immune-modulation. It is now well established that antigen and adjuvant dose play a large role in generating robust immunity[130,135–138]. While some have argued that APCs response directly to material properties[85,139], it is thought that (and we have observed) at the small dose associated with vaccination that APC programming is dominated by other molecular signals. Interestingly, there has been very little attention given to the importance of ligand density. One study examined whether density of targeting ligands (anti-DEC-205) on PLGA carriers would induce variable responses from DCs. They found that production of the regulatory cytokine IL10 was correlated with increased anti-DEC-205 density, which they attributed to cross-linking of DEC-205 receptors at higher densities. This cross-linking event caused DCs to express scavenger receptor CD36, which they found was directly linked to the IL10 response[140]. Clearly this variable needs to be further studied, especially in the context of how antigen and adjuvant density changes immune cell programming.

2.3 FUTURE DIRECTIONS

Over the past several decades, particulate vaccine carriers have been extensively reported on. However, broad success in human immunotherapy has been largely elusive. The benefits of particle based systems including protection of antigens and adjuvants, ability to directly target specific antigen-presenting cells, extended release of vaccine components (depot effect) and ability to deliver vaccine components more efficiently, have been well documented. Yet there remain several grand design challenges. Materials that can act as potent immunostimulators, immunomodulators or both and can be processed into nano or microparticles that can safely deliver antigens and TLR ligands to APCs are still being studied to determine their efficacy in humans. Similarly, particulate systems that are broadly applicable to a variety of diseases and therapeutics and can be delivered through multiple routes need to be developed. It is also critical for the field to study the fundamental mechanism of particulate vaccines, especially how these carriers are internalized and transported in-vivo, which types of immune cells interact with these carriers and where etc. Intravital molecular and cellular imaging should play a key collaborative role in gathering this critical information, which would then allow rational design of carriers. While there are myriads of factors to consider when developing an immunotherapy, there is an almost equally large repertoire of tunable polymers and delivery strategies to meet the needs of any given system. Together with the constantly advancing fields of antigen and adjuvant development, particulate vaccine systems are likely to be at the forefront of immunotherapeutics for bacterial and viral infections alike as well as for cancer prevention and elimination.

2.4 ABBREVIATIONS

APC	Antigen presenting cell
DC	Dendritic cell
MHC I	Major histocompatibility complex I
MHC II	Major histocompatibility complex II
HLA	Human Leukocyte Antigen
IL12	Interleukin 12
IL10	Interleukin 10
IL6	Interleukin 6
IFNγ	Interferon gamma
Th1	Type 1 helper T cell
Th2	Type 2 helper T cell
CTL	Cytotoxic T cell
Treg	Pathogen associated molecular pattern
pDC	Pathogen recognition receptor
LC	Toll-like receptor
cDC	Nuclear factor κ-light-chain-enhancer of activated B cells
LEC	Pathogen-like particle
PAMP	Draining lymph node
PRR	Pathogen recognition receptor
TLR	Toll-like receptor
RLR	RIG-I like receptor
CLR	C-type lectin receptor
NLR	NOD-like receptor

NFκB	Nuclear factor kappa B
PLP	Pathogen-like particle
dLN	Draining lymph node
PLGA	Poly (lactide-co-glycolide) acid
MP	Microparticle
NP	Nanoparticle

CHAPTER 3 AIM 1

FABRICATION AND EVALUATION OF MICRO- AND NANO-PLPS IN IN VITRO MURINE DC CULTURE SYSTEMS

In nature, pathogens come in varying sizes, from small (< 100 nm) and large (200-400 nm) viruses to bacteria and other parasites (~1-2 microns or larger). It is well established that viruses and bacteria elicit different types of host immune responses; the fundamental mechanisms of which are still being elucidated [141–144]. However, most research to date has focused on pathogen associated molecular pattern (PAMP) induced signaling mechanisms, such as TLR activation. Concurrently, biomaterial-based, particulate vaccine formulations designed to mimic pathogens are being widely investigated for delivery of antigens and PAMPs [145–147] to study prophylactic and therapeutic immune responses against infectious diseases, autoimmune disorders, or tumors. These formulations are thought to interact primarily with DCs at the site of administration or within the draining lymph nodes (dLNs). However, few studies have investigated how physical properties of pathogen-like carriers (e.g. size, ligand density, etc.) affect their tropism to various dendritic cell (DC) subsets.

Bone marrow derived dendritic cells have been heavily used in vitro to predict how vaccine formulations will perform in in vivo experiments. However, production of these cells in vitro is not standardized across the field and is, in fact extremely variable from publication to publication. Moreover, it is typical for a study to perform in vitro experiments on cells from only one culture protocol, sometimes without even characterizing the cells on which the experiment is being performed.

Inaba et al. established one of the first protocols for generating over 70% CD11c+ dendritic cells from the bone marrow of mouse leg bones using granulocyte-macrophage colony stimulating factor (GMCSF) to promote the DC phenotype[148]. In addition to GMCSF, other growth factors have been used to induce high yields of immature DCs that are responsive to common pathogenic stimuli. Interleukin 4 (IL4) is frequently added to bone marrow cultures as studies have historically correlated it with maturation and production of Type 1 Helper T cells promoting cytokines[149]. Dendritic cells that are produced using these cultures resemble conventional, migratory DCs that are found in the periphery and have a high capacity for antigen presentation. It has also been shown that the effects on DC phenotype induced by the addition of IL4 to a GMCSF supplemented culture system are temporally dependent[150]. Most recently, it has been determined that IL4 also reduces the growth of macrophage-like cells in bone marrow derived cultures[151]. Recently this notion that IL4 produces the best DC culture system in vitro to test antigen presentation and Th1 polarization has been challenged. Gao et al. discovered a population of DCs that express IRF4, which has been implicated in regulation of many types of immune cells and prevents important inflammatory responses such as skin DC migration to lymph nodes and TLR-induced gene expression in macrophages. They found that expression of PDL2 is also associated with this cell type and that IL4 promoted PDL2 expression. Gao et al. were also able to show that these PDL2+ cells that were regulated by IRF4 did not respond to TLR agonists, likely due to reduced endocytic activity[75].

Another important DC phenotype that has been developed in vitro is the plasmacytoid dendritic cell. Unlike conventional dendritic cells, plasmacytoid DCs are not as efficient at antigen presentation. However, their role in promoting a Th1 response has been realized. They highly express TLR7 and TLR9, making them very sensitive to microbial infection[152]. In response, these cells secrete large amounts of IFN-α, which promotes Th1 cytokine production[153]. These cells can be isolated from mouse spleens in reasonable

quantities and techniques have also been developed to culture them from bone marrow using Fms-like tyrosine kinase 3 ligand (FLT3L)[1,153–155].

In this aim, we strive to fully characterize the culture system in which we test our vaccine formulations as well as elucidate how treatment of cells with different growth factors can affect cell phenotype and ultimately, interaction with particulate vaccines.

At the same time, we have developed particulate formulations to test whether a fundamental particle parameter (i.e. size) can be utilized to passively target specific DC subsets and modulate downstream immune events while all other vaccine properties (antigen/adjuvant dose, particle dose, etc.) were kept constant. Using these two systems together, we were able to determine whether particle size plays a significant role in programming DC phenotype and subsequent T cell maturation in vitro.

3.1 METHODS

3.1.1 Materials

Acid end-capped PLGA RG502H (MW 7,000-17,000) and poly (vinyl alcohol) (PVA, MW 31,000) was purchased from Sigma-Aldrich (St. Louis, MO). Sulfo-NHS and EDC used for conjugation chemistry were from Pierce (Life Technologies, Grand Island, NY). Polyethylenimine (PEI, branched, MW 70,000) was purchased from Polysciences Inc. (Warrington, PA). Unmodified CpG oligiodeoxynucleotide (ODN) 1826 (5'-tccatgacgttcctgacgtt-3') was purchased and characterized by OligoFactory (Holliston, MA) and contained negligible amounts of endotoxin. Fluorescent CpG (Alexafluor 647) was custom-made by Integrated DNA Technologies (Coralville, IA). Endotoxin-free ovalbumin (OVA) was from BioVendor (Ashville, NC). Ribogreen and BCA assays (Life Tech) were used to quantify CpG and OVA, respectively. All antibodies were purchased from either Ebioscience or Biolegend (San Diego, CA). ELISA Ready-Set-Go kits were purchased from Ebioscience.

3.1.2 Mice and primary cell isolation

The use of animals was approved by The Institutional Animal Care and Use Committee (IACUC) at Georgia Institute of Technology (Atlanta, GA). Female (4-5 weeks) C57BL/6 mice were purchased from Jackson Labs. Experiments were conducted when mice were between 5-8 weeks old.

For bone marrow derived cells, mouse long bones (femur and tibia) were collected and cleaned of skin and muscle tissue. Bone marrow was flushed with cold PBS using a 28-gauge needle and syringe. Red blood cells were lysed and remaining cells were cultured in dishes at $5*10^5$ cells/ml of medium. Medium consisted of RPMI 1640 + 10% heat-

inactivated characterized FBS + 1% Penicillin/Streptomycin + 1mM sodium pyruvate, 1% non-essential amino acids and 1x beta-mercaptoethanol. Cell cultures were also supplemented with 20ng/uL of granulocyte-macrophage colony stimulating factor (GMCSF) and 10ng/uL of interleukin 4 (IL4) throughout the course of the culture. Medium was refreshed every other day for 7 days, at which point loosely adherent cells were removed and replated for use in in vitro evaluation of particle formulations. Cells were sometimes sorted using a Pan Dendritic Cell Isolation magnet activated cell sorting (MACS) kit (Miltenyi Biotec, San Diego, CA) to enrich the mature DC population (CD11c+CD11b+). Purity following sorting was above 95%.

Splenic DCs were isolated from whole spleens of C57 black mice. Spleens were cut into pieces and incubated with collagenase D (2mg/ml) for 1 hour. Splenic tissue was then mashed through a cell strainer and lysed of its red blood cells. Plasmacytoid DCs were isolated using a Plasmacytoid Cell Isolation kit MACS kit (Miltenyi). Purity following sorting was above 80%.

3.1.3 Synthesis of micro- and nano- PLGA particles with polyethylenimine conjugation

PLGA microparticles were prepared using a water-oil-water double emulsion (W/O/W), solvent evaporation method as previously published[156–158]. Briefly, 200 mg PLGA (Resomer 502H) was dissolved in 7ml dichloromethane (DCM) and added to 300uL of filtered water. The first emulsion was homogenized at 10,000 RPM for 2 minutes. The first emulsion was then added to 1% polyvinyl alcohol (PVA) and homogenized again for 2 minutes (10000 RPM). DCM was allowed to evaporate from W/O/W emulsion for ~3.5 hours and particles were washed several times with water. PLGA nanoparticles were

fabricated using a similar method with slight modifications. Specifically, PLGA was dissolved in dichloromethane (DCM) at 5% w/v and 1ml of water was added to form the first emulsion. The first emulsion was then sonicated using a probe sonicator (VibraCell, CT) at 85W for 2 minutes at room temperature and added to 16ml of 5% PVA to form the second emulsion. This emulsion was then sonicated at 85W for 5 minutes, followed by constant stirring for ~3 hours to allow for solvent evaporation. Nanoparticles were collected and larger particles were size excluded using centrifugation. The smaller particle population was then collected at 20,000 xg, washed 3 times with deionized water and lyophilized.

Particles were then covalently surface modified with branched PEI using EDC/sulfo-NHS linker chemistry, which has been described previously. Particle size and zeta potential was determined using a Zetasizer Nano ZS (Malvern, MA).

3.1.4 CpG/OVA loading on PEI-PLGA particles

All molecules were loaded onto particles in a DNase/RNase-free sodium phosphate buffer (pH 6). Dried particles were weighed out and resuspended at 1mg/100uL loading buffer. Suspensions were vortexed and sonicated to break up aggregates. For PLPs loaded with only CpG, CpG was diluted to 13ug/900uL loading buffer. The particle suspension was then added, drop-wise, to the CpG solution while vortexing. Loading was allowed to proceed overnight at 4°C. Particles loaded with only OVA were loaded in presence of 50ug/ml ovalbumin overnight at 4°C. Particles that were loaded with OVA+CpG were loaded with OVA first, using the overnight protocol above. CpG was added the following day and left to load on OVA-loaded particles for 4 hours at 4°C. Ribogreen and BCA assays were used to determine loading levels of CpG and OVA, respectively.

3.1.5 Microscopy of PLPs

Particles were characterized using scanning electron microscopy (e.g. size, morphoplogy) and structured illumination microscopy (e.g. dual loading of antigen and adjuvant).

For SEM, particles were suspended in filtered water and pipetted onto carbon paper attached to an SEM stud, where they were allowed to dry overnight. Studs were coated with a 10nm layer of gold to enhance conductance using a spin-coater. Samples were then imaged using InLens imaging.

For SIM microscopy, samples were dual loaded with fluorescent CpG (FITC) and fluorescent OVA (Alexafluor 647) together. Particles were washed and resuspended in PBS then pipetted onto a glass slide. A coverslip was applied over the samples before imaging.

3.1.6 Dendritic cell uptake

After 7 days of culture, loosely adherent BMDCs were sorted, replated and treated with particle formulations. Fluorescent CpG was given at $5ug/10^6$ cells (~385ug PLGA particles) and was kept constant for all delivery formats. Cells were allowed to interact with formulations for 24 hours, after which they were collected. Analysis was performed using an Accuri C6 flow cytometer. Gating was determined using fluorescence readout of untreated cells.

3.1.7 Dendritic cell activation evaluation – flow cytometry

After 7 days of culture, loosely adherent BMDCs were replated and treated with particle formulations. CpG was given at $5ug/10^6$ cells (~385ug PLGA particles) and was kept constant for all delivery formats. Cells were allowed to interact with formulations for 24 hours, after which they were collected. Cells were washed and blocked to prevent non-specific interactions with Fc antibody portions (anti-CD16/CD23, Ebioscience). Cells were then stained using anti-CD11c-APC, anti-CD86-FITC, anti-PDL2-FITC/PE, anti-

PDL1-PE-Cy7 and/or anti-CD40-PerCp-Cy5.5 and analyzed on an Accuri C6 flow cytometer (BD Biosciences). Gating was determined using isotype controls.

3.1.8 Dendritic cell activation evaluation – intracellular staining

After 24 hours of treatment, cells were washed and stained for extracellular markers as described above. Following initial staining, cells were fixed with Cytofix buffer (BD Biosciences) for 10 minutes at RT. Cells were then washed using Perm/Wash Buffer (BD Biosciences) and stained (in Perm/Wash) with anti-IL10-PerCp-Cy5.5 and anti-IL12p70-APC. After suitable incubation, cells were washed with Perm/Wash buffer and resuspended in FACS buffer (0.5% BSA in PBS) and analyzed using an Accuri C6 flow cytometer.

3.1.9 Dendritic cell activation evaluation – ELISA cytokine analysis

After 24 hours of treatment, cells were removed and supernatant collected for analysis using ELISA. These assays were performed to determine IFNγ, and IFNβ protein concentrations in cell supernatant. IFN assays were also performed following 48 hours of particle treatment.

3.1.10 Dendritic cell activation evaluation – Antigen presentation

For studies of antigen presentation, cells were treated with 10ug of soluble OVA in addition to CpG formulations for 24 hours. Antigen presentation was determined in two ways. The first was staining using anti-MHC I-SIINFEKL and was analyzed using an Accuri C6 flow cytometer.

Another method of determining antigen presentation efficiency is a mixed leukocyte reaction. For these experiments, DCs were cultured for 24 hours with OVA alongside CpG formulations then added to a co-culture system with CD4 or CD8 T cells isolated from OVA-specific transgenic mice (OTII and OTI, respectively) and a 1:2 DC:T cell ratio. Supernatant and cells were collected either 24 or 72 hours later. T cells were then

stained for early activation markers (i.e. CD25) or regulatory T cell markers (i.e. Foxp3) and analyzed using flow cytometry. Supernatant was analyzed for cytokine content, specifically IFNγ, IL4 or IL2 (ELISA).

3.1.11 Statistical Analysis

Student's t-test was used to perform statistical analysis between two groups, where $p<0.05$ was considered significant. In vitro experiments were conducted a minimum of three iterations (n=6 for each sample) to ensure reproducibility.

3.2 RESULTS

3.2.1 Characterization of pathogen-like particles (PLPs)

Characterization of PLPs (i.e. size, zeta potential, maximum loading of CpG) is summarized in Table 4. In order to test the influence of formulations size, it must be ensured that the formulations being compared are disparate enough in size. Figure 4 indicates that there is minimal overlap of the two formulations chosen for this study, with average micro-PLP size at ~1.18um and nano-PLPs averaging at ~280nm. This was further validated using scanning electron microscopy (Figure 5). Additionally, PEI conjugation was optimized to ensure that surface charge was similar (~32mV) and provided sufficient cationicity to load a variety of relevant molecules, including larger protein and small oligos (

Figure 6). We were also able to demonstrate dual loading of antigen and adjuvant molecules simultaneously on the same particle (Figure 7).

Table 4: PLP Characterization

	Size	Zeta before loading	Zeta after loading	Max Load
Micro	1.18 +/- 0.28 um	36.7 +/- 3.73 mV	-24.2 +/- 8.7 mV	13ug/mg
Nano	0.278 +/- 0.8 um	29 +/- 7.83 mV	4.65 +/- 4.12mV	50ug/mg

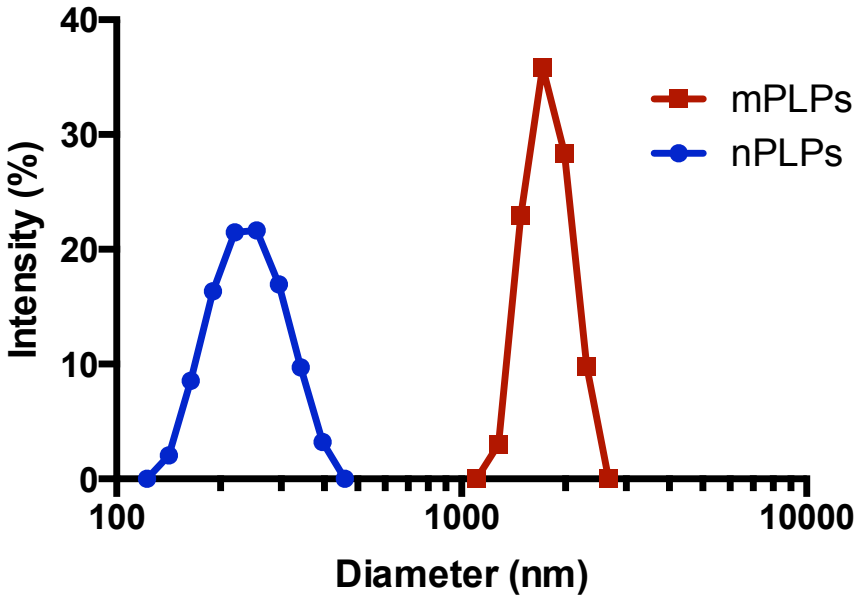

Figure 4: PLP size - Particles were measured using dynamic light scattering. Peaks show that there is minimal overlaps between micro- and nano-formulations

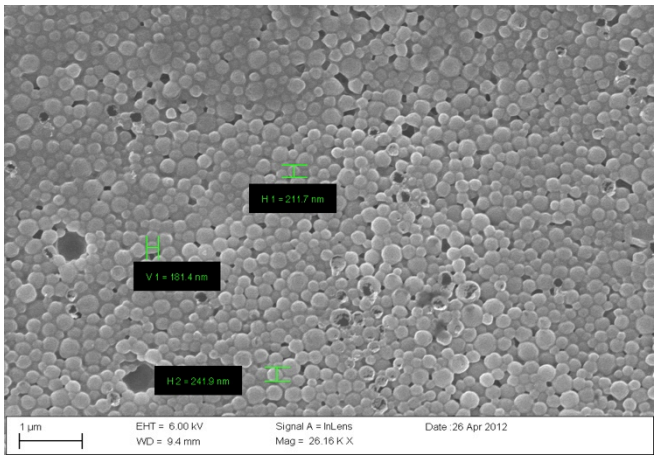

Figure 5: SEM of nano-PLPs - Scanning electron microscopy validates DLS size measurments for nano-PLPs.

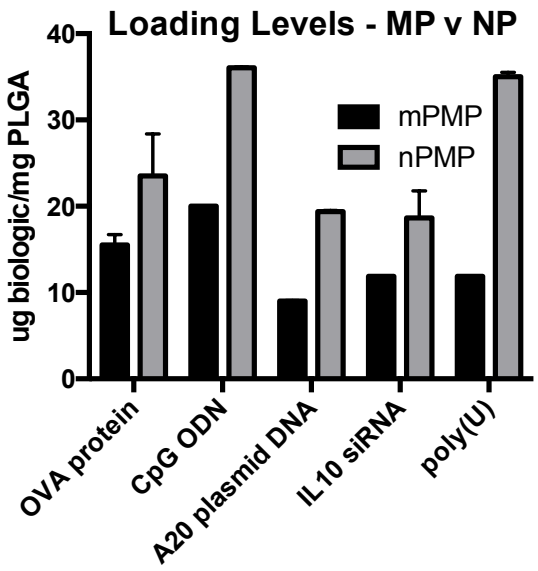

Figure 6: PLP loading capacity - Both micro- and nano-PLPs were capable of loading suitable amounts of relevant biological antigens and adjuvants.

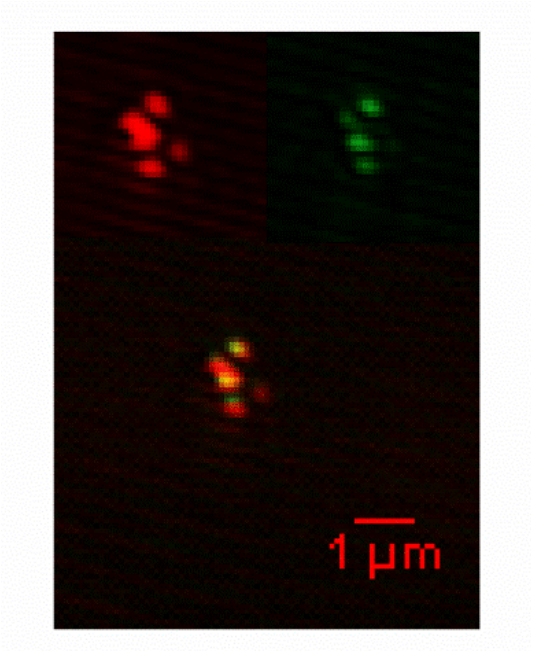

Figure 7: Dual loading of OVA+CpG on nano-PLP - FITC-CpG and AF647-OVA were loaded simultanously on nano-PLPs and images used SIM microscopy.

3.2.2 Development of DC subset cultures

The culture system that has been extensively used in the Roy lab over the last decade involves isolation of bone marrow from naïve, female mouse femurs and tibias. After red blood cell lysis, the remaining cell population is cultured in medium supplemented with 20ng/ml murine GMCSF and 10ng/ml murine IL4. These cytokines were replenished with media changes every other day for the total 6 days of culture. At Day 6, cells were stained for common DC maturation markers including CD11c, PDL2, CD11b, MHCII and CD86. We have used this system to extensively test the effect of various TLR ligands, both soluble and attached to micro- and nano-PLPs. While we have consistently observed size effects, we soon identified the variability of cells within these cultures, making it impossible to correlate effects with a specific cell phenotype (Figure 8). We later also compared our results to a system without IL4 and to the system used by Gao et al. to study PDL2+ cells (GMCSF+IL4 burst) (Figure 9).

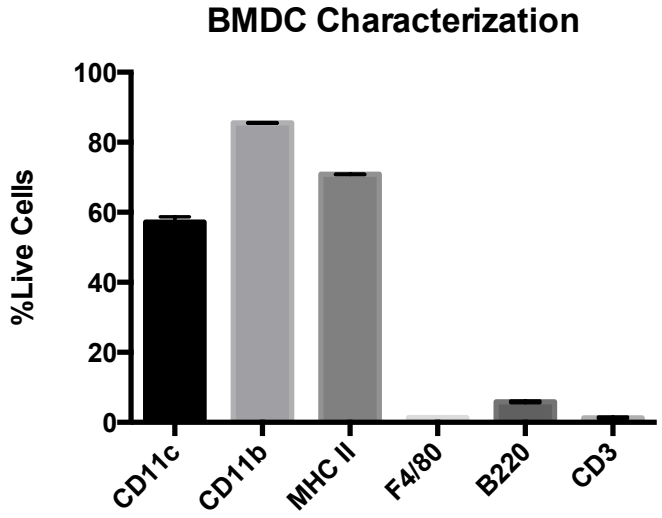

Figure 8: BMDC Characterization of GMCSF+IL4 Culture - We observed that cells originating from isolated bone marrow progenitors were heterogeneous and included a non-negligible percentage of non-CD11c expressing cells.

This allowed us to test the differential expression of maturation markers induced by IL4 given in two temporally different fashions. CD11c, the identification marker for dendritic cells in mice, was highly expressed (between 60-70%) in all culture systems and therefore this population was gated to determine marker expression on CD11c+ cells exclusively. CD11b was also highly expressed (over 85%) in all systems. Interestingly, our system seems to induce more spontaneous maturation (indicated by higher levels of MHCII and CD86) than the Gao method and when cultures were only supplemented with GMCSF (Figure 9). More importantly, it is demonstrated here that the addition of IL4 in both cases significantly increases the expression of PDL2 and presumably the potential for these cells to induce Th2 polarization.

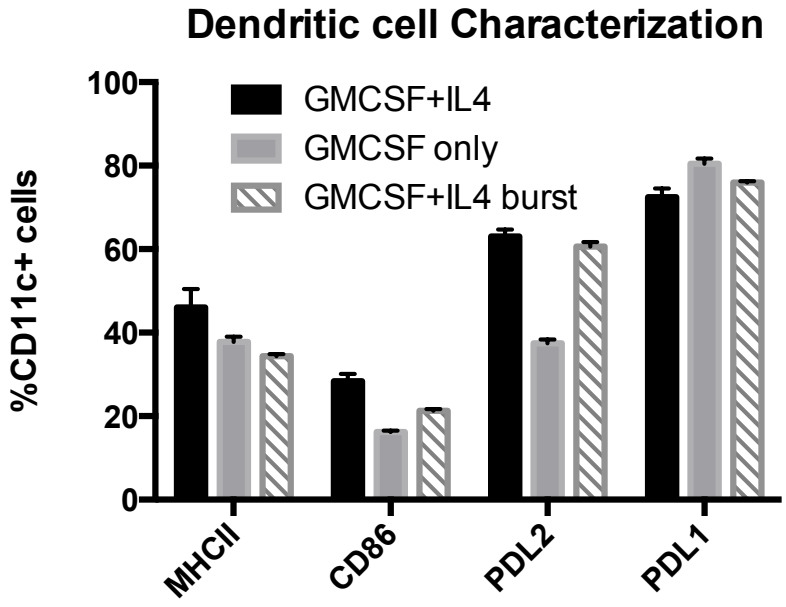

Figure 9: Characterization of DC expression profiles with and without IL4 supplementation. Classic DC markers were analyzed after 6 days of culture with only GMCSF, GMCSF+IL4 and GMCSF with a burst of IL4 only on Day 5. IL4 (both constant and burst) drastically increased the expression of PDL2 and also CD86. This was similar to observations made by Gao et al.

Based on these results, we decided it is important to separate the PDL2+ and PDL2- populations to differentiate their contributions to cytokine secretion and T cell maturation in our system. To do this, we cultured our cells using the aforementioned technique including IL4 and sorted, using fluorescence activated cell sorting (FACS), the PDL2+ from the PDL2- populations (>95% purity). These populations were then used to test how TLR agonist stimulation affects their maturation and cytokine secretion.

We were also interested in investigating the interaction of our vaccine formulations with plasmacytoid DCs. For these studies, we isolated the spleens of naïve, female mice and using the Miltenyi Plasmacytoid Isolation Kit (negative sort), sorted out CD11c+B220+Ly6C+ cells (Figure 10).

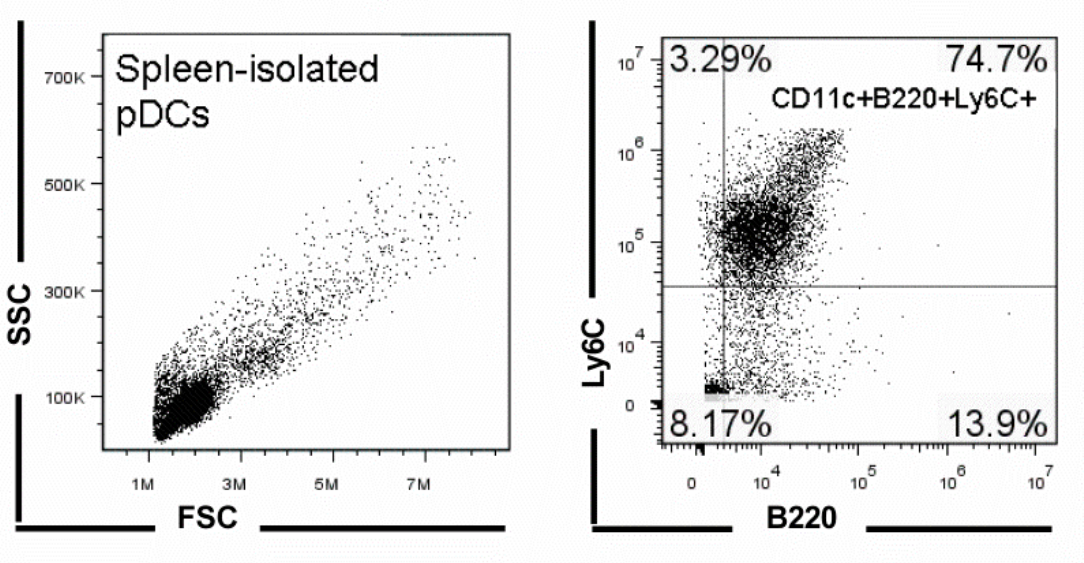

Figure 10. Spleen isolated pDC purity - Plasmacytoid DCs were isolated from spleens of naïve mice by sorting using a Plasmacytoid DC Isolation kit (Miltenyi). Purity of the cell population post-sort was about 75%.

3.2.2.1 PDL2+ DCs – Spontaneous maturation vs induced expression

It has been shown in the literature that mechanical disruption of immature DC clusters formed during differentiation leads to nonspecific maturation that is mediated by the β-catenin pathway rather than the typical TLR-L induced NF-κB pathway. While these cells to have upregulated expression of costimulatory markers on their surface, they do not secrete inflammatory cytokines and therefore promote a immunosuppressive T cell phenotype rather than an effector phenotype[159]. This can be triggered simply by pipetting the cells for replating or by sorting using magnetic columns. For example, in our hands the PDL2+ cell population increases significantly after replating without any other stimulation (Figure 11). This population, going forward, will be referred to as induced PDL2+ DCs (iPDL2).

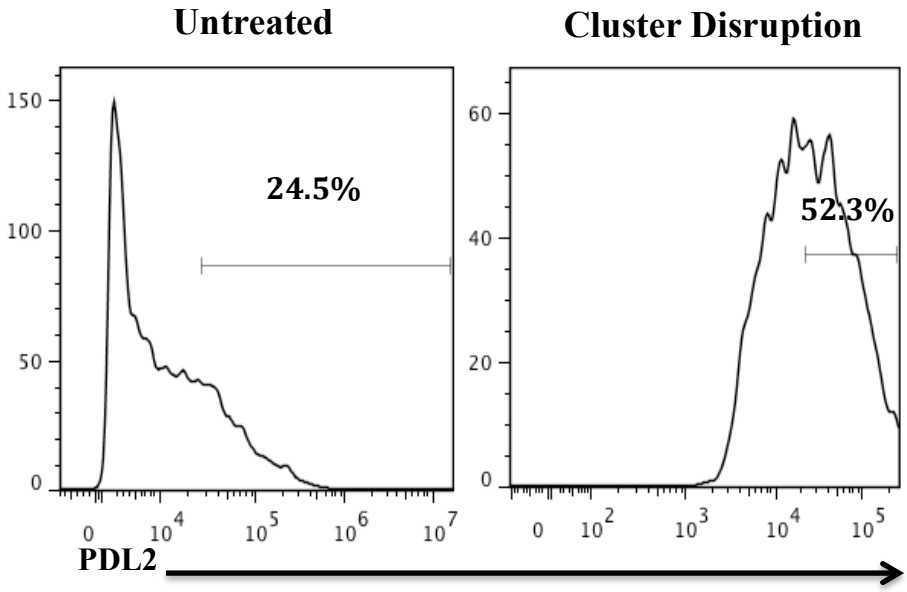

Figure 11: Cluster disruption increases PDL2 expression in BMDCs.

3.2.3 DCs show size preference in vitro

After cultures were appropriately characterized, we began to investigate how each of these DC subsets of interest interacts with our PLP formulations. First, we quantified uptake of PLPs carrying fluorescent CpG. To properly evaluate preference, we cultured mixed populations of PDL2+ and PDL2- cells with soluble fCpG, micro-PLPs or nano-PLPS for 24 hours. Our first observation was that PDL2+ and PDL2- cells showed opposite preference towards PLP formulations. PDL2+ cells took up significantly more micro-PLPs, while PDL2- cells preferred nano-PLPs (Figure 12).

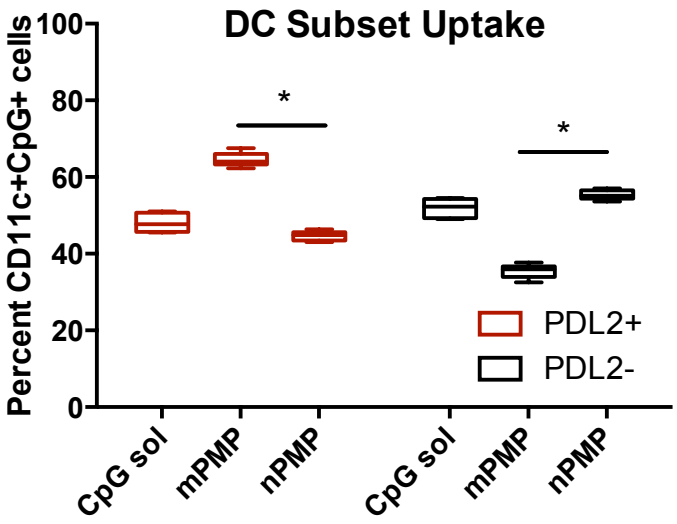

Figure 12: BMDCs exhibit size-dependent preference for PLPs in a PDL2 dependent manner. PDL2+ cells took up significantly more micro-PLPs than either nano-PLPs or soluble formualtions. PDL2- cells, on the other hand, took up nano-PLPs and soluble CpG similarly, but did not efficiently take up micro-PLPs.

Furthermore, we observed that CpG-PLP+ cells took up similar amounts of CpG, regardless of PLP size. Therefore, dose of CpG per cell is largely the same, despite particle number and PLGA dose per cell varying (Figure 13). When we performed similar experiments on plasmacytoid DCs, we validated that this subset also demonstrates a formulation size preference for micro-PLPs (Figure 14).

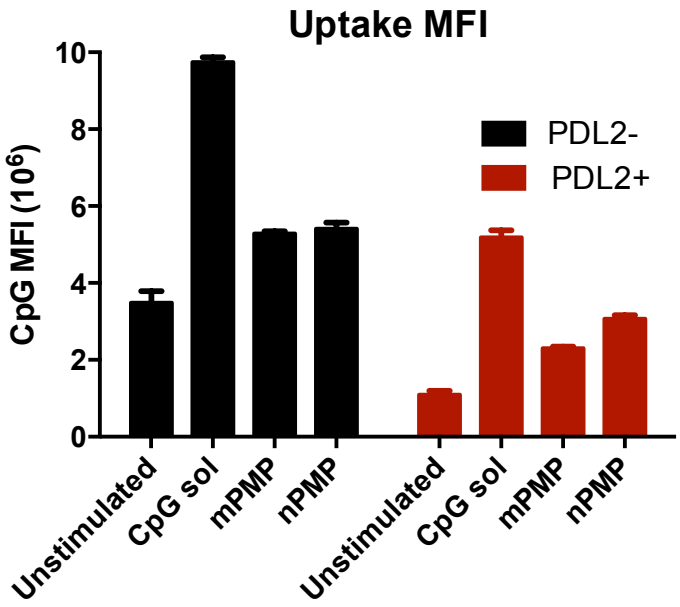

Figure 13: BMDCs take up similar amounts of CpG, regardless of PLP delivery format.

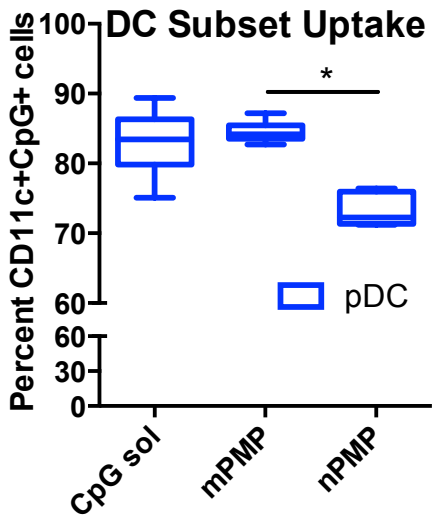

Figure 14: pDCs prefer micro-PLPs over nano-PLPs

Also similar to BMDCs, pDCs also take up a comparable amount of CpG regardless of PLP formulation (Figure 15).

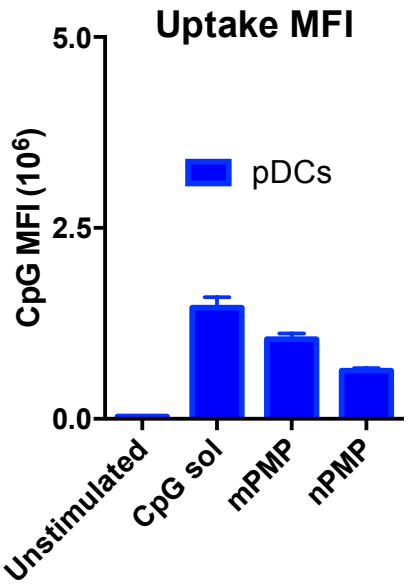

Figure 15: pDCs take up similar amounts of CpG regardless of PLP carrier. It was also observed that pDCs take up significantly less CpG than BMDCs.

3.2.4 DC activation is modulated in a PLP-size dependent manner

DC activation is evaluated based on signals that are required for them to effectively induce T cell maturation. These signals include upregulation of co-stimulatory molecules present on the DC cell membrane, secretion of pro-inflammatory (or anti-inflammatory) cytokines and presentation of peptide-MHC complexes. Here we evaluated each of these to determine whether DC activation signals were affected by PLP size.

3.2.4.1 PLPs promote differntial expression of co-stimulatory molecules

Multiple molecules promote co-stimulation of T cells during antigen presentation. As described previously, these include CD86/CD80, which engage T cell CD28, promoting immune synapse formation. Additionally, CD40 (a TNF receptor) is also expressed following DC maturation. PDL2+/PDL2- DC expression profiles of CD86 followed uptake patterns. PDL2+ cells increased expression of CD86 following treatment with micro-PLPs and this response was abrogated by nano-PLPs treatment. The inverse expression pattern was observed in PDL2- cells (Figure 16, left). CD40 expression did not follow a similar pattern, but instead was expressed similarly regardless of PLP treatment (Figure 16, right). Average expression of CD86 or CD40 per cell (mean fluorescence intensity) did not vary with carrier size (Figure 17).

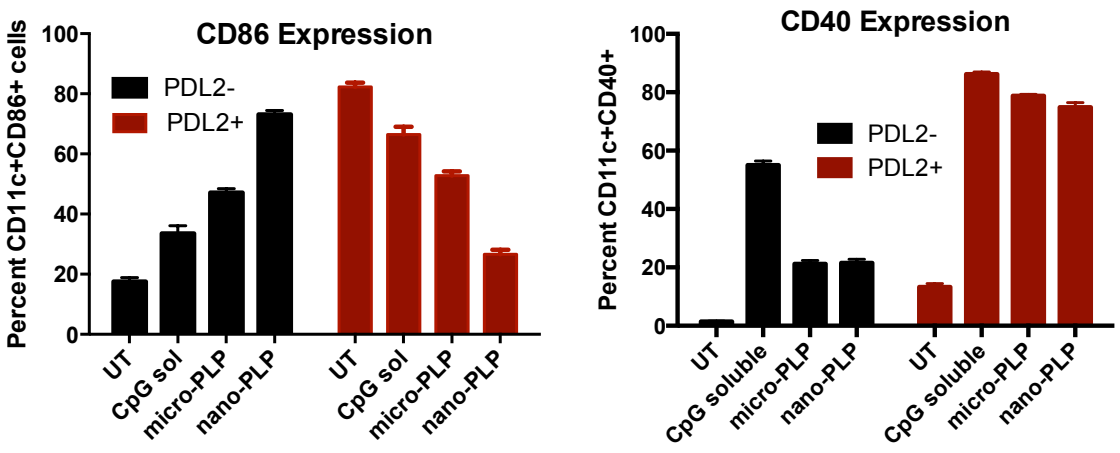

Figure 16: DC co-stimulatory molecule expression varies with PLP size. PDL2+ cells become more activated (based on CD86 expression) after stimulation after treatment with micro-PLPs. PDL2- cells exhibited an opposite expression pattern. CD40 expression did not vary with PLP size.

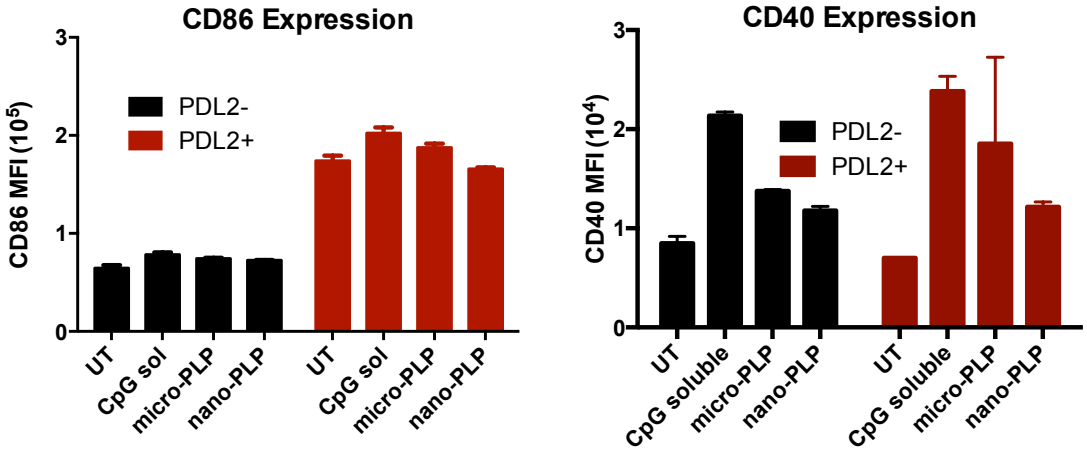

Figure 17: Mean expression of CD86 or CD40 did not vary with PLP size.

Interestingly, despite plasmacytoid DC's preference for micro-PLPs, we observed that they are activated more efficiently (i.e. expression of CD86) by nano-PLP (Figure 18, left). However, the average expression of CD86 per cell did not vary based on PLP treatment (Figure 18, right).

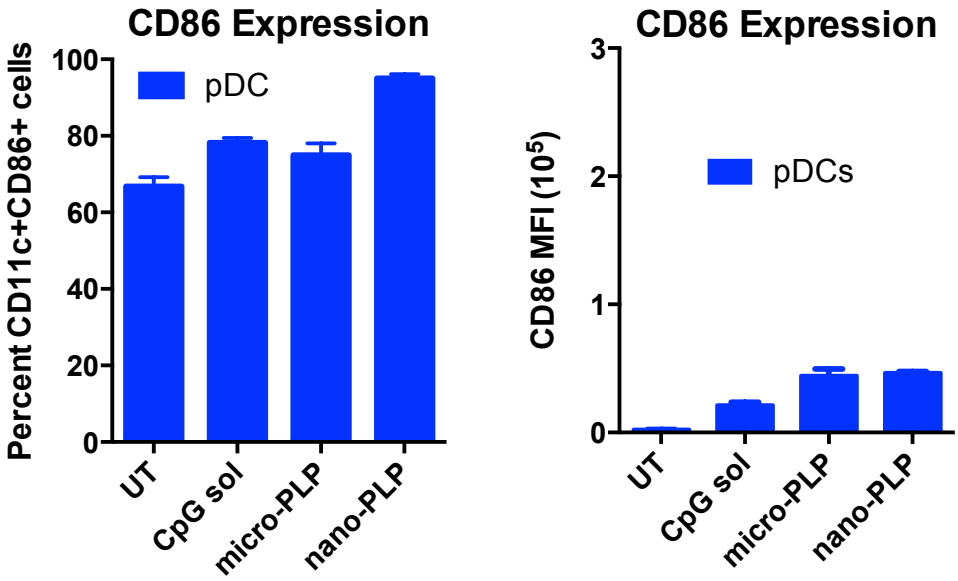

Figure 18: A greater percentage of pDC population expresses CD86 after treatment with nano-PLP. Mean expression does not vary.

3.2.4.2 DC secretome indicates size-dependent programming

The presence of pro-inflammatory cytokines is essential to promote effector T cell function. In the absence of cytokines, T cells receiving antigenic signals from DCs will either become anergic or apoptose. This mechanism regulates self-reactive T cells and promotes tolerance[160]. Additionally, DCs produce anti-inflammatory cytokines as negative feedback for immune response generation to prevent autoimmunity or immune over-activity[161,162]. Therefore, the ratio of pro-inflammatory to anti-inflammatory cytokines present during T cell maturation will critically affect the resultant effector/regulatory response.

IL12p70, one of the main pro-inflammatory DC cytokines, is known to promote effector T cell activity and can be induced by TLR engagement and signaling[163,164]. TLR signaling also promotes production of IL10, a regulatory, anti-inflammatory cytokine[165,166]. Therefore, we analyzed the ratio of these two cytokines to determine the phenotypic state of our DC subsets.

Our first observation was that PDL2- cells do not produce detectable levels of cytokine, making PDL2+ cells the primary cytokine-secreting cells in GMCSF+IL4 culture systems (Figure 19).

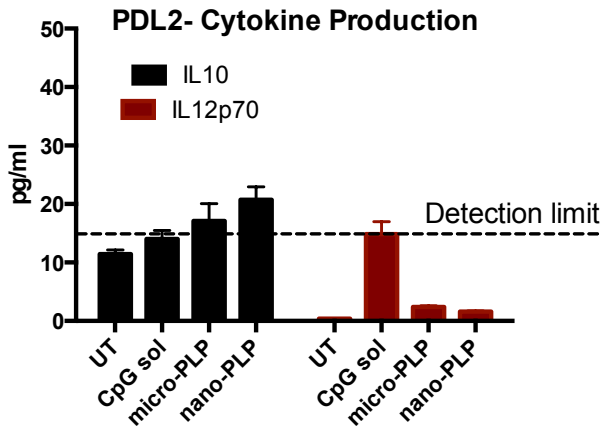

Figure 19: PDL2- cells produce negligible amounts of cytokine

PDL2+ cells were able to produce IL12p70, IL10 upon stimulation. Interestingly, the ratio of IL12p70:IL10 production varies significantly with delivery format. We observed that treatment with micro-PLPs promoted a pro-inflammatory dominated cytokine profile, with IL12p70 being produced in around 4 times more PDL2+ cells. This dominance was less pronounced in cells treated with nano-PLPs and almost completely absent in cells treated with soluble CpG (Figure 20).

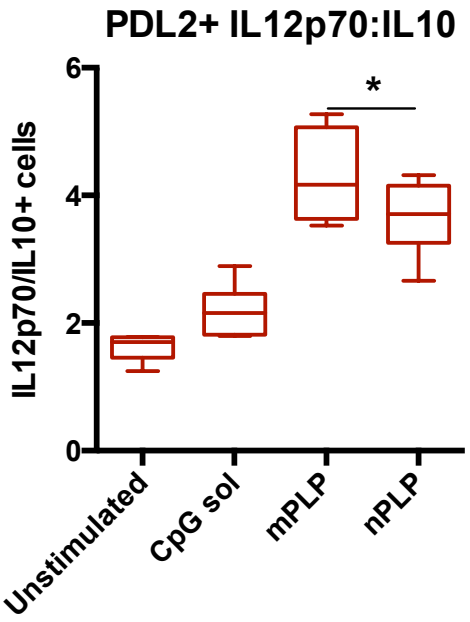

Figure 20: IL12p70:IL10 in PDL2+ cells. PDL2+ cells treated with mPLPs exhibit a pro-inflammatory dominated program. Nano-PLPs induce greater production of anti-inflammatory cytokine IL10.

In addition to these cytokines, CpG is known to also promote interferon (IFN) production in DCs. Type 1 IFN (IFNα/β) are associated with anti-viral immunity and can promote type 1 polarization in both DCs, cytotoxic T cell development and natural killer cell activation[167]. Type 2 IFNs (IFNγ) are known to be very important for type 1 T cell effector function, but have also been shown to promote pro-inflammatory signaling in DCs as well[168]. We therefore also looked at the expression levels of this class of cytokines in PDL2+ DCs.

We found that, while PDL2+ cells do produce a significant amount of IFNγ by 24 hours after CpG dosing, especially when treated with soluble or micro-PLP delivered CpG. However, there is a significant reduction of IFNγ associated with nano-PLP delivered CpG. Interestingly, levels of IFNγ are indistinguishable from untreated samples 48 hours after treatment (Figure 21). This validates that DCs use this cytokine as an autocrine signal, potentially to promote subsequent pro-inflammatory signals. IFNα was undetectable in these cultures, but IFNβ was produced at low levels (Figure 22). It's possible that the kinetics of IFNβ production are much faster and that, at 24 hours, much of it has already been consumed. Overall, this data suggests that PLP-size directs programming and promotes unique functions. Specifically, micro-PLPs induce an effector phenotype in PDL2+ cells, while nano-PLPs promote a more tolerogenic DC program.

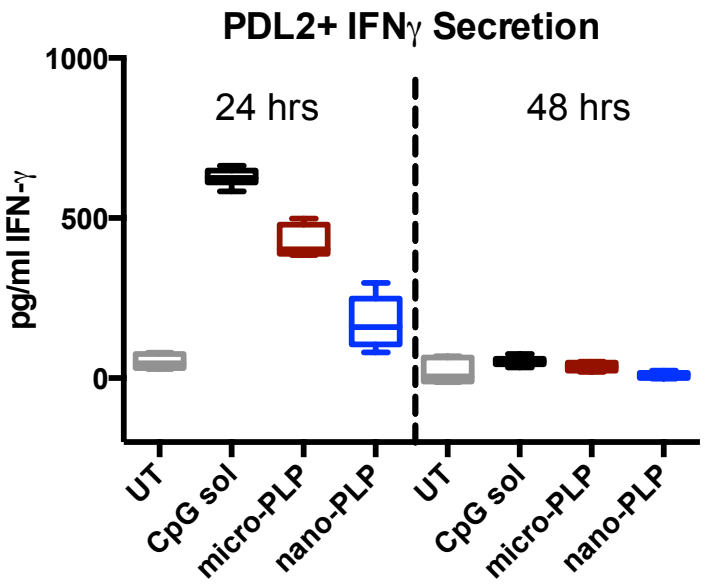

Figure 21: PDL2+ cell production of IFN-gamma. PDL2+ cells produce significant amounts of IFN-gamma, especially when treated with soluble or micro-PLP delivered CpG. However, it is consumed over the next 24 hours, as indicated by the drop to baseline at 48 hours.

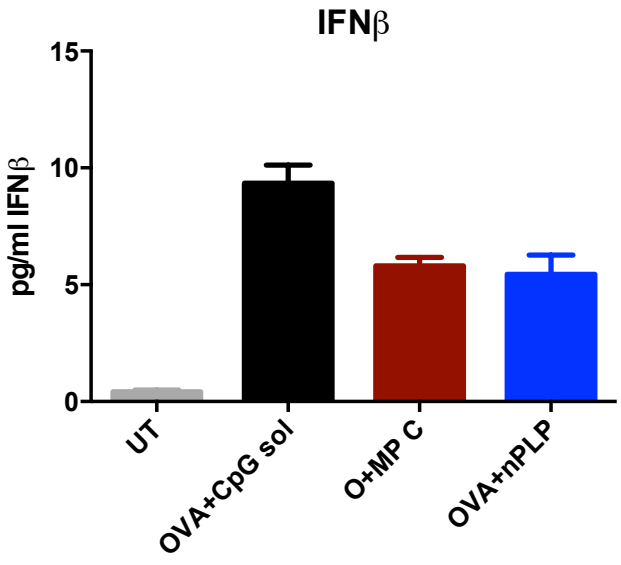

Figure 22: PDL2+ DC IFN-beta production after 24 hours of treatment with CpG.

3.2.5 PLP size-dependent DC programming influences T cell maturation

The primary function of activated DCs is to present antigen to T cells, alongside activation signals, to promote antigen-specific T cell proliferation and effector activity. In order to evaluate the ability of DCs to promote antigen-specific T cell maturation, we employed a mixed leukocyte reaction technique. Antigen-specific T cells were isolated from spleens of transgenic mice whose T cells are engineered to recognize specific OVA epitopes. These cells were cocultured with DC pulsed with whole OVA protein alongside CpG formulations. Our first indication that T cells were receiving sufficient maturation signals from primed DCs was T cell upregulation of an early activation marker, CD25. First, as we suspected, PDL2- cells were not able to induce T cell activation, likely due to the lack of cytokine production observed previously (Figure 23).

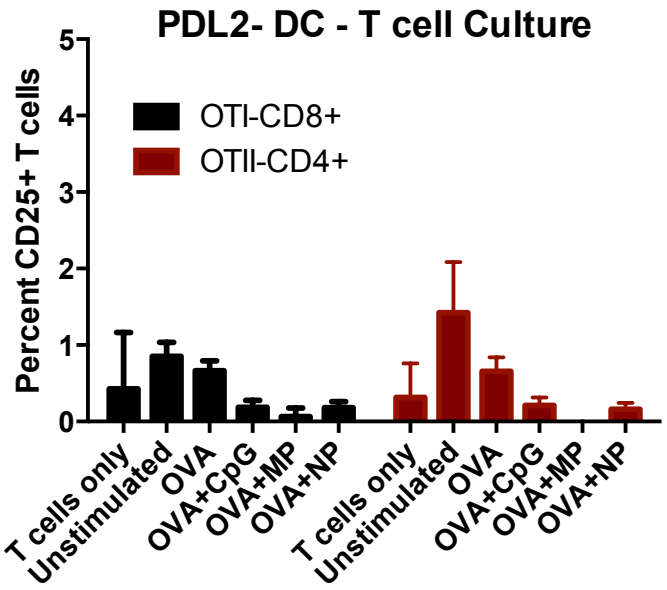

Figure 23: PDL2- cells do not induce T cell activity.

However, PDL2+ DCs were able to promote increased expression of CD25 after one day of coculture with either CD4+ or CD8+ T cells. Micro-PLPs induced the most potent upregulation of CD25 in CD8+ T cells, which was likely due to increase pro-inflammatory signals provided by DCs in this group (Figure 24, left). While soluble CpG induced the most robust activation of CD4+ T cells, micro-PLPs-DCs still outperformed DCs treated with nano-PLPs (Figure 24, right).

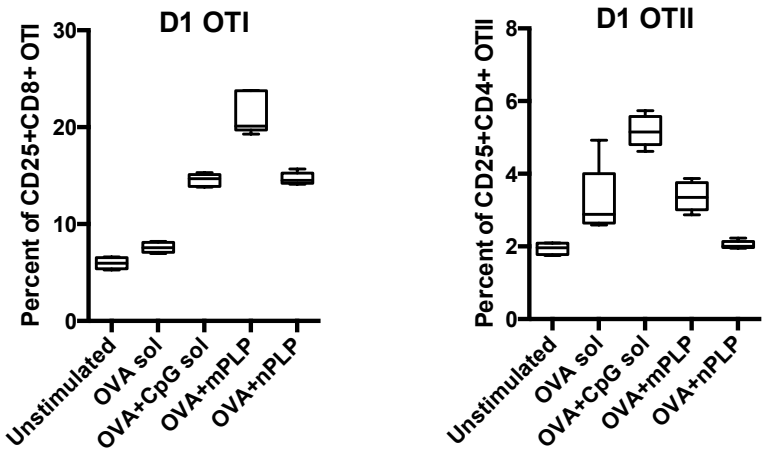

Figure 24: CD8+ (OTI) and CD4+ (OTII) T cells are activated by OVA-pulsed PDL2+ cells

When T cells mature into effector phenotype, they become efficient producers of immunomodulatory cytokines, especially IFNγ, IL4 and IL2. IFNγ is secreted by cells of a type 1 phenotype and promotes the proliferation of CD8+ cytotoxic T cells and antibody class switching to those isotypes with greater antibody dependent cell-mediated cytotoxicity (ADCC) efficiency[169,170]. On the other hand, IL4 is implicated in type 2 T cell effector activity and IgG1 antibody production[171]. IL2 is important for T cell maintenance and persistence of T cell effector function[172].

After 3 days of co-culture with primed PDL2+ DCs, T cell supernatant was removed and analyzed for the cytokines discussed above. Both CD8+ (OTI) and CD4+ (OTII) cells produced significant amounts of IFNγ, especially when cultured with DC primed with either soluble or micro-PLP delivered CpG. Interestingly, DCs treated with nano-PLPs were not able to induce IFNγ production in either type of T cell (Figure 25).

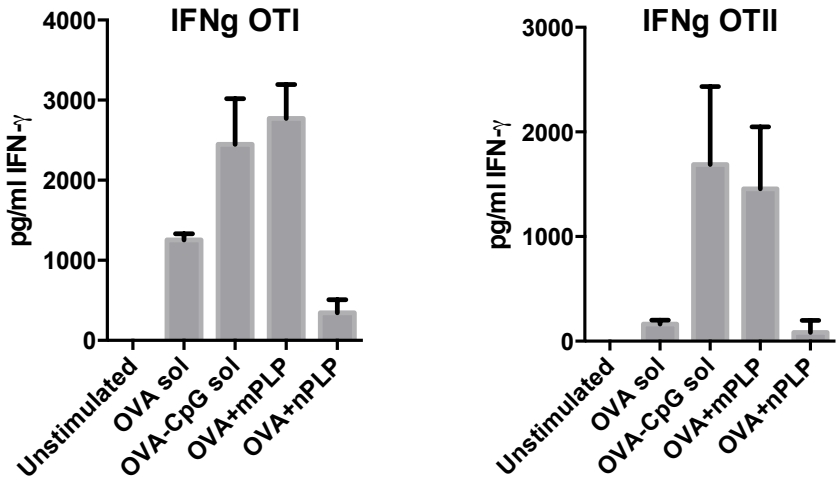

Figure 25: PDL2+ DCs primed with soluble CpG or micro-PLPs induced IFNγ production in CD8+ and CD4+ T cells.

Inversely, T cells that were co-cultured with soluble CpG-DCs did not produce more IL4 than those cultured with untreated DCs. Micro-PLP-DCs promoted a small amount of IL4 production in both CD8+ and CD4+ T cells, but nano-PLP-DCs induced significantly more (Figure 26). This inverse trend mirrors cytokine signals observed in DC themselves and confirms the PLP size-induced polarization of DCs and, subsequently, T cells.

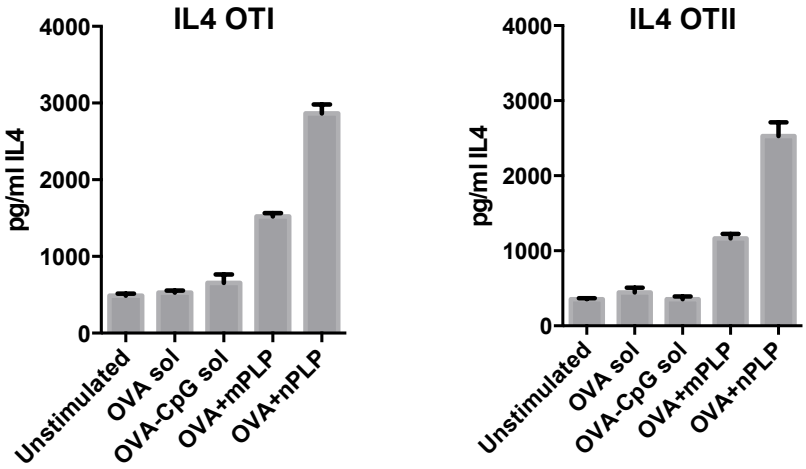

Figure 26: PDL2+ DCs primed with nano-PLPs induced IL4 production most efficiently in CD8+ and CD4+ T cells.

Interestingly, for PDL2+ DC co-cultures, all treatments caused CD8+ T cells to produce IL2 at similar levels and none of the formulations induced IL2 efficiently in CD4+ cells (Figure 27). However, when CD4+ T cells were co-cultured with pre-primed pDCs, only those treated with nano-PLPs promoted any IL2 production (Figure 28). This finding implies that enhanced activation that was associated with nano-PLP delivery of CpG to pDCs does have a significant influence over pDC directed T cell activity.

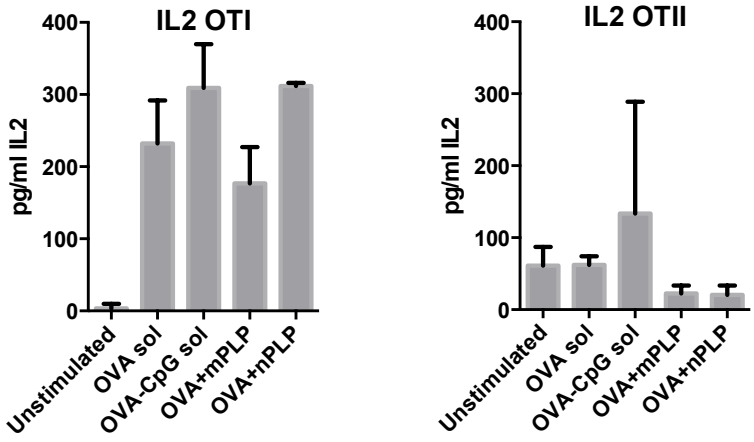

Figure 27: IL2 production is not influenced by formulation used to prime DCs

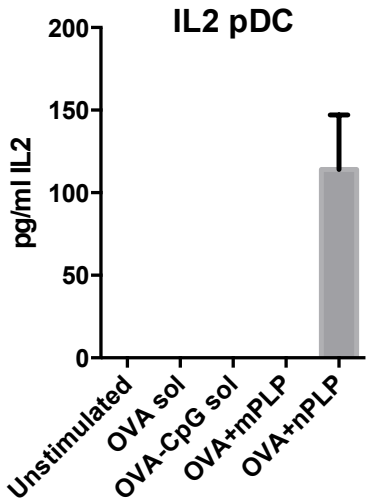

Figure 28: Only pDCs treated with nano-PLPs can induce IL2 production in CD4+ T cells.

Finally, it is known that DCs are able to provide signals to T cells that support differentiation of regulatory T cells, responsible for prohibition of effector T cell function and providing an internal control for the immune response[173]. Consistent with tolerogenic cytokine profiles of PDL2+ DCs treated with nano-PLPs, these DCs also promoted regulatory T cell proliferation within CD4+ T cell cultures (Figure 29).

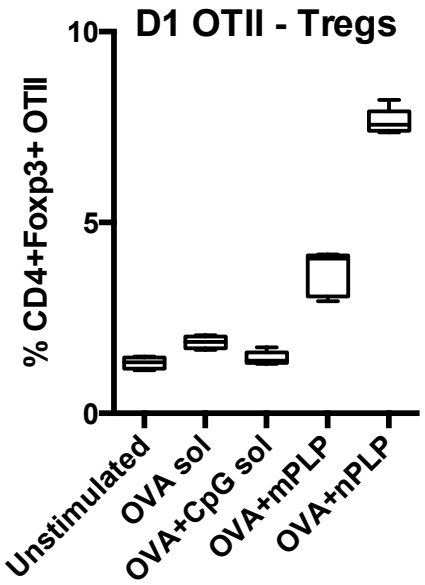

Figure 29: PDL2+ DCs primed with nano-PLPs induce regulatory T cell proliferation

3.3 DISCUSSION

Particle biomaterial-based vaccine formulations are being widely investigated for delivery of antigens and adjuvants. It is our current understanding that tissue–resident antigen presenting cells, most notably dendritic cells (DCs) take up vaccine-carrying particles at the site of injection, become activated then migrate to draining lymph nodes where they modulate the cellular immune response. While it is now well appreciated that many subsets of DCs reside in peripheral tissues and can uniquely direct immunity, little is known about whether particle formulations preferentially target particular DC subsets and/or whether this can be used to specifically modulate the resultant immune response. For this work, we've designed a modular particle platform (pathogen-like particles, PLPs) that can be used to test a large variety of variables. We can easily tune PLP size and charge, as well as load a large variety of antigen and adjuvant molecules both inside (encapsulated) and on the surface of the particles[156,157,174,175]. This tunability provides us with a system that can be used to mimic natural pathogens and study how physical parameters play a role in modulating immunity. Specifically, this works proposes the use of a physical parameter (i.e. size) of particular vaccine carriers as a means of targeting specific peripheral dendritic cell populations.

The immunological significance of particle size has been widely studied and also disputed (recently reviewed by Leleux et al. and Oyewumi et al)[145,176]. While it has been established that particles must be under 10um to allow phagocytosis and preferably under about 5um to be immunogenic, there is still debate over whether nanoparticles (NPs) under 1um or microparticles (MPs) between 1-5um are better for immunotherapy[177]. NPs under 100nm in diameter can travel through the lymphatic vessels to lymph nodes where they can carry out immunomodulatory tasks[128]. However, studies using particles that are intended for DC uptake at the site of injection have shown efficacy across particle sizes. This is likely due to DC ability to take up both viral and bacterial pathogens in the body, which range in size from 10nm to a few microns. While most of these studies concerning

particle size draw conclusions about which generates a more robust immune response, there have been no studies analyzing DC subset preference and the resultant effects on immunity.

Our in vitro data demonstrate that there is a DC-phenotype dependent preference of microparticles or nanoparticles and we have convincingly demonstrated that this preference can affect eventual T cell immune modulation. T cells are essential for both elimination of infected or cancerous cells (CTLs) and induction of B cell maturation and antibody production. Therefore, size-driven effects at the DC level have the potential to alter the overarching immune response towards a particle vaccine, making this finding pivotal to future vaccine design.

3.4 ABBREVIATIONS

PAMPs	Pathogen associated molecular pattern
TLR	Toll-like receptor
dLN	Draining lymph node
DC	Dendritic cell
GMCSF	Granulocyte-macrophage colony stimulating factor
IL4	Interleukin 4
Th1	Type 1 helper T cell
Th2	Type 2 helper T cell
PDL2	Programmed Death Ligand 2
IFNα/β/γ	Interferon alpha/beta/gamma
Flt3L	Fms-related Tyrosine Kinase 3 ligand
pDC	Plasmacytoid Dendritic cell
ODN	Oligodeoxynucleotide
PVA	Poly vinyl alcohol
DCM	Dichloromethane
Micro-PLP	Micro-pathogen-like particle
Nano-PLP	Nano-pathogen-like particle
PEI	Polyethylenimine
OVA	Ovalbumin
SEM	Scanning electron microscopy
SIM	Structured illumination microscopy
FACS	Fluorescence-activated cell sorting

MACS	Magnetic-activated cell sorting
BMDC	Bone marrow derived cells
ELISA	Enzyme-linked immunosorbent asaay
iPDL2	Induced programmed death ligand 2
MFI	Mean fluorescence intensity
Treg	Regulatory T cell

CHAPTER 4 AIM 2

VALIDATE EFFICACY OF PLP FORMULATIONS IN VIVO

Despite success in vitro, translation is the eventual goal of all vaccine delivery platforms, the success rate of which has been grave, especially in clinical trials. The first step to translation is adapting the vitro models used to screen vaccines to small animal in vivo models to determine whether the same effects are observed in live animals. In this aim, we tested vaccine formulations that have been successful in inducing in vitro DC activation and antigen presentation. We have demonstrated that particle parameters such as size significantly influence (a) the ability of APCs to take up particles and travel to draining lymph nodes and (b) the resultant immunomodulation provided by the vaccines.

4.1 METHODS

4.1.1 Materials

The use of animals was approved by The Institutional Animal Care and Use Committee (IACUC) at Georgia Institute of Technology (Atlanta, GA). C57BL/6 mice (female, 4-5 weeks) were purchased from Jackson Laboratories (Bar Harbor, Maine). Antibodies were purchased from Ebioscience or Biolegend (San Diego, CA). Multi-plex mouse cytokine kits (8-plex) were purchased from Bio-rad (Hercules, CA). Cyrosectioning prep materials (OCT medium, cryomolds, glass slides) were purchased from Fisher Scientific (Waltham, MA).

4.1.2 Particle distribution and DC subset analysis of draining lymph nodes

Female C57BL/6 mice (5-6 weeks) were injected subcutaneously with 20ug of either soluble or particle-delivered Alexa-647-CpG. Control mice were given saline injections. Injections were performed either one day, five days or seven days prior to lymph node isolation. Mice that were given injections seven days prior to isolation were also given a booster injection one day prior to isolation to evaluate the effect of boosting.

Inguinal lymph nodes were isolated and processed into a single cell suspension or frozen for cryosectioning. Processed cells were then stained with anti-mouse FITC-Ly6C, anti-mouse FITC-CD86, anti-mouse FITC-CD103, anti-mouse PE-PDL2, anti-mouse PE-Langerin, anti-mouse PE-CCR7 and anti-mouse PE-Cy5 CD11c. Cells were washed, resuspended in FACS buffer and analyzed using a BD Accuri C6 flow cytometer.

Lymph nodes kept for cryosectioning were dried of excess liquid then snap frozen in OCT medium in liquid nitrogen. Cryosectioning was performed by the Yerkes Pathology Lab (Emory University, Atlanta, GA) or the Winship Cancer Institute Pathology Lab (Emory University, Atlanta, GA). Sections were blocked and incubated with primary antibodies (Biotin-CD3 and FITC-B220) overnight at 4°C. After washing, sections were stained with secondary antibodies (streptavidin-eFluor 570) for one hour, washed and

coverslips were mounted. Sections were imaged using a Zeiss LSM 700 Confocal Microscope.

4.1.3 Immunization protocol

Female C57BL/6 mice (5-6 weeks) were injected subcutaneously with either soluble or particle-delivered ovalbumin (10ug) and CpG (25ug). Ovalbumin and CpG were loaded onto the same particle for those groups. Control mice were given saline injections. Mice were given three injections at two week intervals. Lymphoid organs and blood were collected one week following the final injection.

Lymph nodes and spleens were processed into single cell suspensions. Splenocytes were stained with FITC-CD8a, PE-NK1.1, PE-Cy7 CD3, APC-SIINFEKL-Class I tetramer, PE-CD4, PerCP-Cy5.5 Ly6G, PE-Cy7 CD11b, APC CD11c, APC-Cy7 CD25 and/or APC-Foxp3. Lymph node cells were stained with FITC-CD8a, PE-Cy7 CD3, APC-SIINFEKL-Class I tetramer, PE-CD4, PerCP-Cy5.5 Ly6G, PE-Cy7 CD11b, APC CD11c, APC-Cy7 CD25, APC-Foxp3, FITC GL-7, and/or PerCP-Cy5.5 B220.

Splenocytes were also restimulated with ovalbumin to determine cytokine section profiles of splenic antigen-specific T cells. Ovalbumin was given to cells at 200ug/10^6 cells for 72 hours. Supernatant was collected for analysis using Bio-rad Bio-plex for mouse cytokines.

Blood was centrifuged to pellet cells and serum was collected. IgG titers were assayed using ELISA for diluted serum samples.

4.1.4 Immunohistochemistry staining

Lymph nodes were isolated from vaccinated mice, rinsed with PBS and patted dry. They were then embedded within cyromolds filled with OCT freezing medium and snap frozen using liquid nitrogen. Sectioning was performed by the Yerkes Pathology Core (Emory University, Atlanta, GA).

4.1.5 OVA-B16 Melanoma survival study

Mice were inoculated with $5*10^5$ OVA-B16 tumor cells subcutaneously on Day 0. Vaccinations were then given at Day 11, 18 and 25. Lymphoid organs and serum were collected for a percentage of mice on Day 29 for immunological analysis and the remaining mice were sacrificed according to tumor progression. Tumor size threshold was 1.5cm in any direction.

4.1.6 Statistical Analysis

Student's t-test was used to perform statistical analysis between two groups, where $p<0.05$ was considered significant. In vivo experiments were conducted with n=6 to ensure reproducibility.

4.2 RESULTS

4.2.1 Micro-PLPs traffic more efficiently to draining lymph nodes

Lymph nodes are split into functional zones, including a T cell zone where T cells are introduced to antigen and mature, and germinal centers, where T cells interact with B cells and antibody is secreted. Migratory cells must end up in one of these zones in order to modulate adaptive immunity. Alternatively, it has been shown that migratory cells can also hand off antigen to lymphoid resident cells, which reside in high numbers in the periphery, near sinuses[45,46,50]. We therefore first investigated the location within the lymph node of PLPs 24 hours after injection, using immunohistochemistry (**Figure 30**). Micro-PLPs were found in large amounts, both in the periphery of the lymph node and in the T cell zones. It is likely that particles found in T cell zones were brought there by migratory skin DCs. However, it is possible that peripheral particles were able to drain to the lymph node on their own, similar to the observations made by Gerner et al. [50]. Nano-PLPs were found in T cell zones as well, but in significantly fewer numbers than micro-PLPs, indicating their either do not induce DC migration as efficiently and/or cannot drain to the lymph nodes.

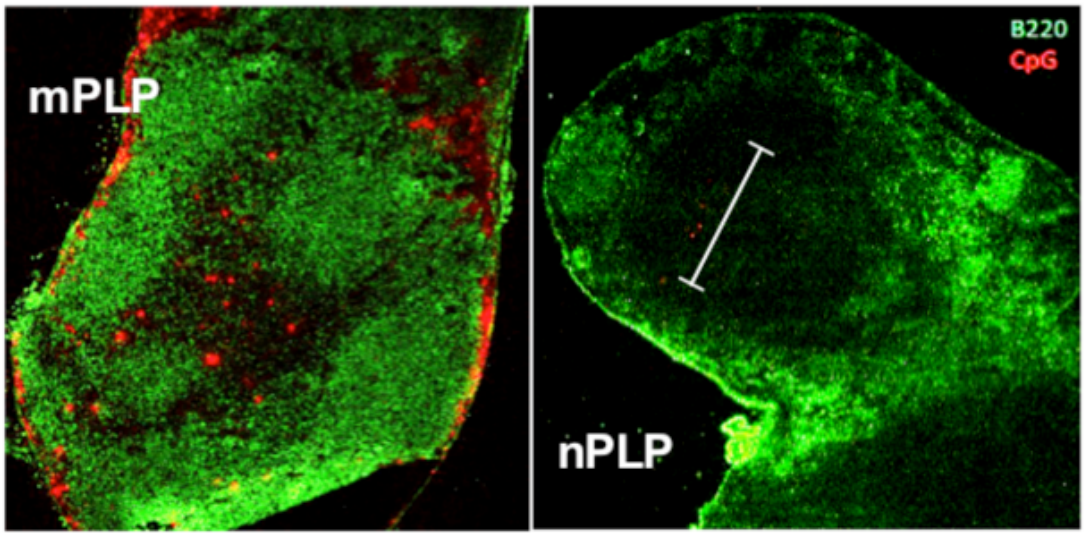

Figure 30: Micro-PLPs traffic to draining lymph nodes more efficiently at 24 hours. (left) Micro-PLPs are found in both the periphery (i.e. sinuses) of the lymph nodes as well as the T cell zones. Nano-PLPs are found in very small amounts and only in T cell zones.

4.2.2 Migratory DCs carry CpG-PLPs to draining lymph nodes from skin

Once we validated that PLPs could be found in the draining lymph node, we wanted to analyze the migratory population responsible for their trafficking with more granularity. To do this, we isolated lymph nodes 24 hours after subcutaneous immunization with PLPs carrying fluorescent CpG (or soluble fCpG) and stained them for multiple DC subsets found in the skin. These included PDL2+ dermal DCs, CD103+ dermal DCs, Langerhans cells, monocyte-derived inflammatory DCs and plasmacytoid DCs[34,55,69,73,75,76,178]. One day following injection, all of these cell types appeared in draining lymph nodes in varying percentages. Additionally, all of these subsets had a percentage of fCpG+ cells, indicating they are all responsible for transporting CpG to a certain degree (Figure 31). Migratory DCs that made up the largest CpG-carrying populations were PDL2+ dermal DCs and monocyte-derived inflammatory DCs. These two populations made up over 80% of cells that were CpG+ in the draining lymph nodes in mice treated with soluble CpG or micro-PLPs. Interestingly, both of these populations were found in significantly fewer numbers in lymph nodes of mice treated with nano-PLPs. This could be related to PDL2+ cells' preference for micro-PLPs (observed in vitro). CD103+Langerin+ cells were found in appreciable amounts as well and also seemed to prefer soluble CpG and micro-PLPs over nano-PLPs. Langerhans cells were found in small amounts at this time point. Finally, while plasmacytoid DCs made up a small portion of the total CpG carriers in the lymph nodes, they were found in significantly higher numbers in mice treated with nano-PLPs. This finding also correlates with in vitro data, indicating that nano-PLPs more efficiently activated pDCs.

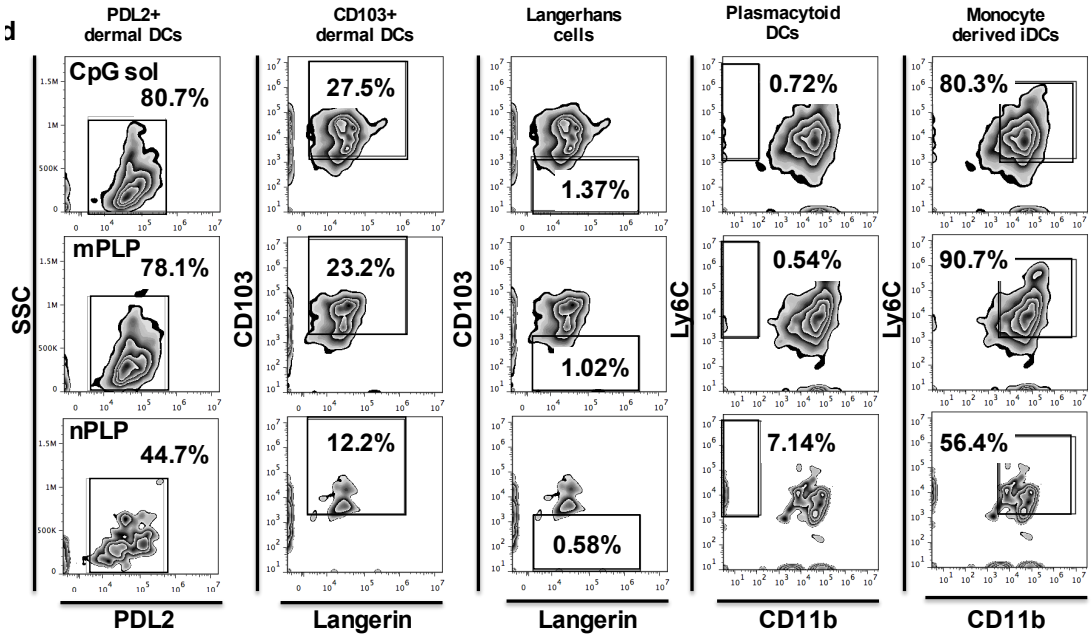

Figure 31: Skin-resident migratory DCs carry CpG-PLPs to draining lymph nodes. PDL2+ dermal DC make up the majority of migratory DCs in the lymph node and therefore, are the primary carriers of CpG (PLPs), especially micro-PLPs. Monocyte-derived inflamatory DCs also make up a large portion of CpG carriers and likely overlap with PDL2 expressing DCs. Interesting nano-PLPs do are carried most efficiently by plasmacytoid DCs when compared to soluble CpG or micro-PLPs.

While these findings were very interesting and are certainly important to early T cell maturation, it is also known that some DC subsets exhibit delayed migration kinetics, including Langerhans cells[179,180]. Therefore, we also isolated lymph nodes 5 days after initial injection, as well as 7 days after initial injection with a booster given on day 6. The three populations that seemed interesting 24 hours after injection (PDL2+ DCs, monocyte derived iDCs and pDCs) all exhibited similar kinetics over the course of the experiment (Figure 32). They all peaked at early time points and fell to what may be the baseline by day 5. Boosting was able to reactivate monocyte derived iDCs and pDCs, promoting a second wave of migration. However, PDL2+ DCs were only able to recover and migrate again after boosting in mice given soluble CpG. This could potentially be due to a persistent availability of CpG only associated with PLP delivery.

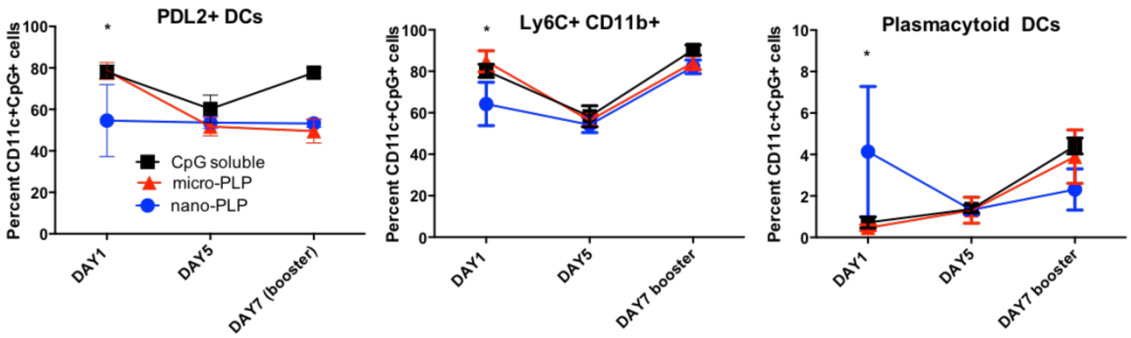

Figure 32: Primary CpG-carrying DC migration kinetics. PDL2+ DC populations peak early then taper off by Day 5. Boosting promotes reinfiltration of PDL2+ cells in mice given soluble CpG only. Monocyte-derived iDCs, however, can be reactivated with boosting. Plasmacytoid DCs migrate more rapidly in groups treated with nano-PLPs, but all groups respond equally well to boosting.

Other skin DC subsets exhibited different migration kinetics. PDL2+ dermal DCs that were described previously in literature also express CD301b. We therefore split this population into CD301b+ and CD301b- subpopulations (Figure 33a-b). Interestingly, CD301b+ populations did make up a larger percentage of the CpG+PDL2+ population but did not vary at all with delivery format. Additionally, none of these formulations were able to restimulate cells to a migratory state with a boost. However, in CD301b- populations showed a distinct preference for soluble CpG and micro-PLPs and also exhibited a lack of restimulation after boosting with micro-PLPs. Langerin+ DC migration was delayed and did not peak until 5 days after injection (Figure 33 c-d). They also were not able to repopulate the lymph nodes after one boosting, but could possibility at a later time point. While there seemed to be a slight preference for micro-PLPs in Langerhans cells at Day 5, these differences were not as defined as in other subsets.

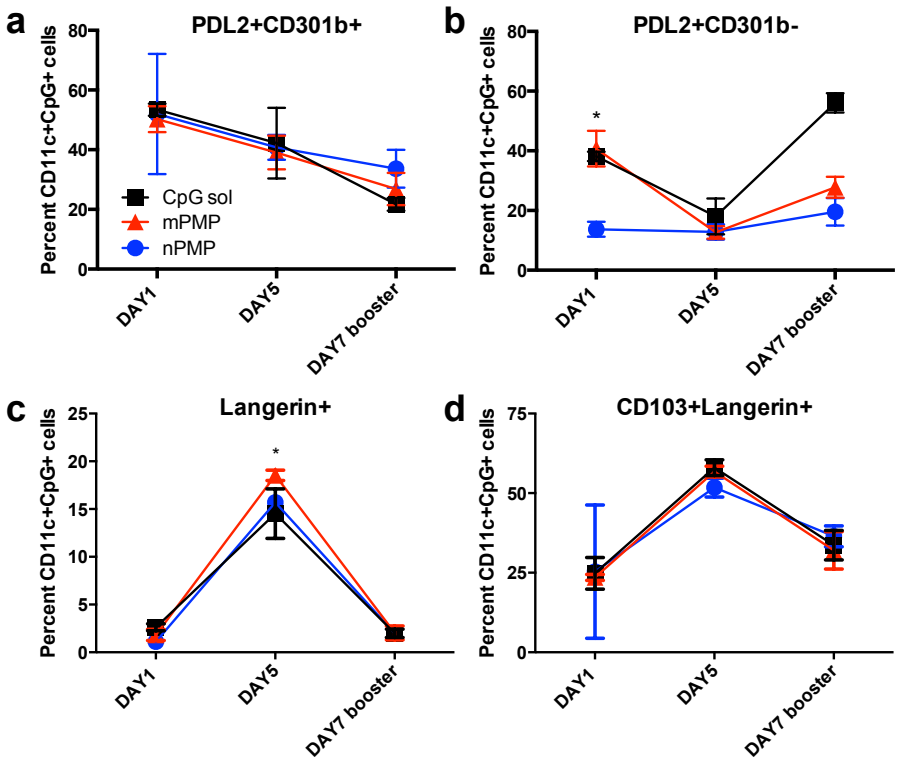

Figure 33: Langerin+ DCs exhibit delayed migration kinetics. Similar to what has been described in literature previously, Langerin expressing DC (regardless of CD103 expression) migration is delayed in comparison to other DC subsets. Specifically, these cell populations peak in the draining lymph node 5 days following initial injection. The PDL2+ DC subset described in literature also expressed CD301b. We therefore split this population into CD301b+ and CD301b- populations and did show differing kinetics in each subpopulation.

4.2.3 Immunological response to micro- and nano-PLPs

Following activated DC migration (or activation of lymphoid resident DCs), these cells will interact with T cells by providing signals described previously. From there, T cells will mature, proliferate and perform effector functions. These include producing cytokine, interacting with B cells to promote antibody class switching and secretion, killing infected cells and/or regulating immune activity. Therefore, these functions are analyzed as outputs of an immunological response and can be correlated with vaccine efficacy. For these studies, we vaccinated mice with a model protein antigen (OVA) alongside CpG. Mice were given an initial injection followed by 2 boosters at 2 week intervals. Lymphoid organs (i.e. spleen and inguinal lymph nodes) and serum were isolated one week following the final injection.

4.2.3.1 Lymph node – DC activation

We first analyzed whether any of the vaccine formulations caused proliferation of lymph node resident DC populations. Specifically, we looked at total DCs (CD11c+ cells), as well as CD8α+ DCs and CD4+ DCs, which are known to activate T cells that share their surface markers (CD8 and CD4, respectively)[17,49,181]. We observed no significant difference in total DCs nor CD8+ DCs. However, there was a small increase in the presence of CD4+ DCs after vaccination with micro-PLPs (Figure 34).

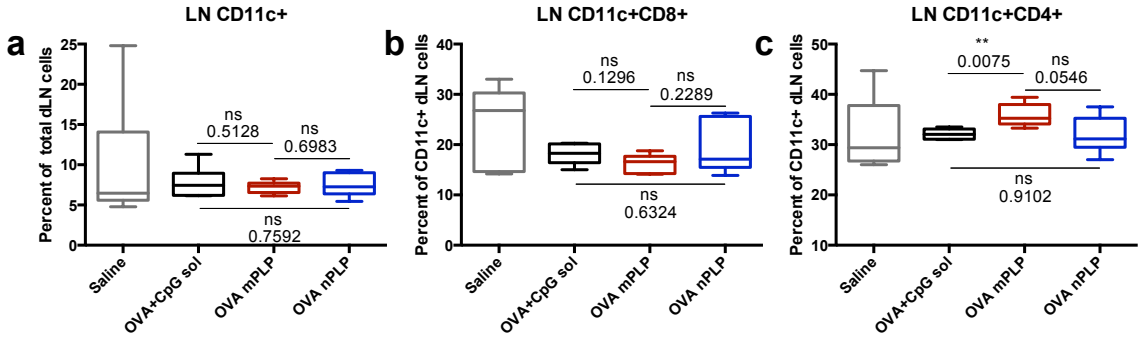

Figure 34: Only CD4+ DCs were enhanced by PLP vaccination, specifically with micro-PLPs.

4.2.3.2 Lymph node - T cell response

The first critical observation was that the PLP vaccines induce a CD4+ helper T cell dominated response in draining lymph nodes. Inversely, the soluble vaccine increased the percentage of CD8+ T cells over PLP vaccines (Figure 35).

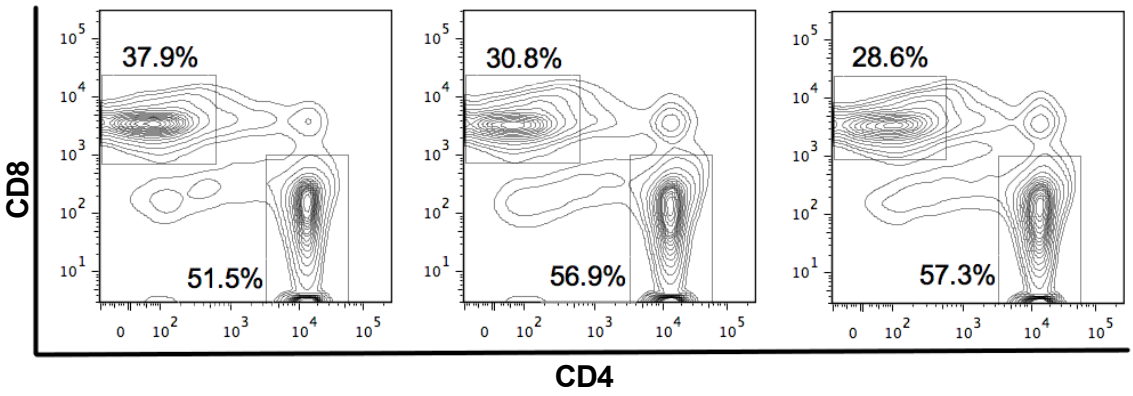

Figure 35: PLPs induce CD4 T cell dominated immunity. In mice treated with either PLP formulation, CD4+ T cells were dominant in draining lymph nodes. However, this shift was reversed in mice treated with soluble CpG, in which there was a significant increase in the CD8:CD4 ratio.

Interestingly, when the CD8+ population was further subtyped for antigen-specificity, mice treated with PLP vaccines had significantly larger populations of antigen-specific cytotoxic T cells (Figure 36). This population was most enhanced in mice treated with nano-PLPs, where the antigen-specific populations were nearly twice as large as those in micro-PLP treated mice. This is consistent with an anti-viral response and potentially driven by the early increase in pDC migration. This finding was confirmed by MHC-I-SIINKFEKL staining of DCs within the draining lymph nodes (Figure 37). Surprisingly, nano-PLPs also promoted the increase of regulatory T cell populations, both in the splenic and draining lymph node compartments (Figure 38).

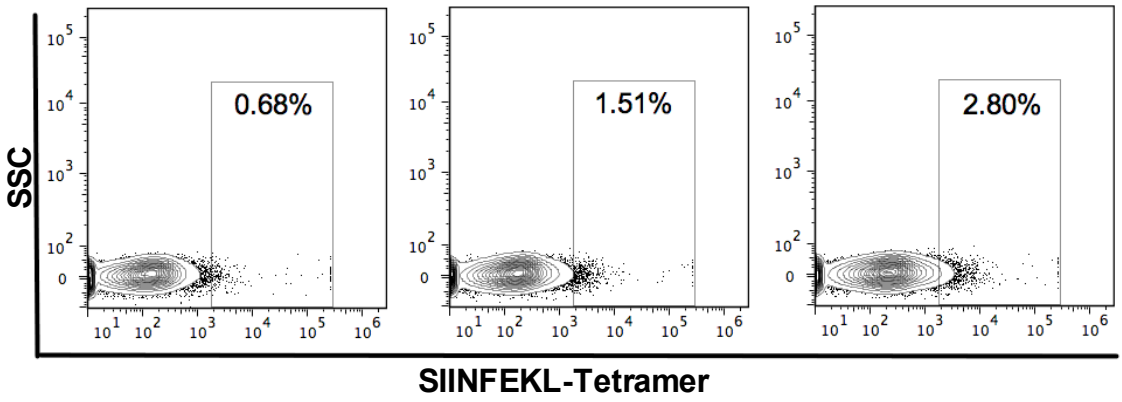

Figure 36: PLP vacciation results in more antigen-specific CD8+ T cells. In draining lymph nodes, there is a greater percentage of antigen-specific CD8+ T cells after vaccination with PLP formulations, espsecially nano-PLPs.

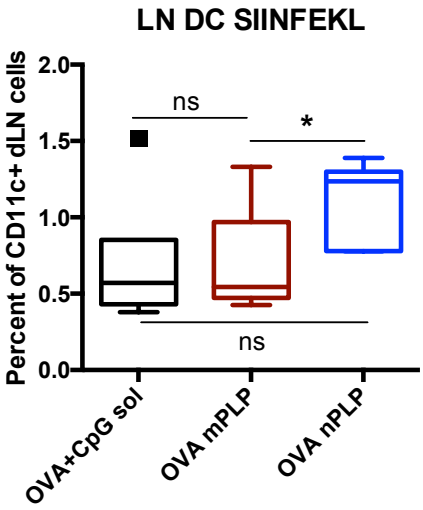

Figure 37: DCs in dLNs express MHCI-SIINFEKL after treatment with nano-PLPs.

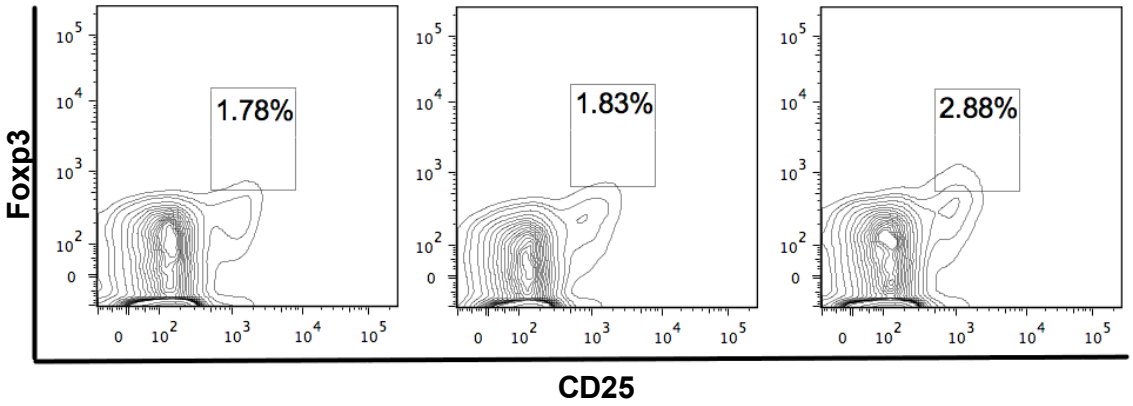

Figure 38: Nano-PLP vacciantion induces the upregulation of regulatory T cell populations in draining lymph nodes.

4.2.3.3 Spleen – DC Activation

Spleen DC populations were examined to determine whether there was a significant immunological response derived there. We observed no significant differences in DC populations between any treatment groups tested (Figure 39).

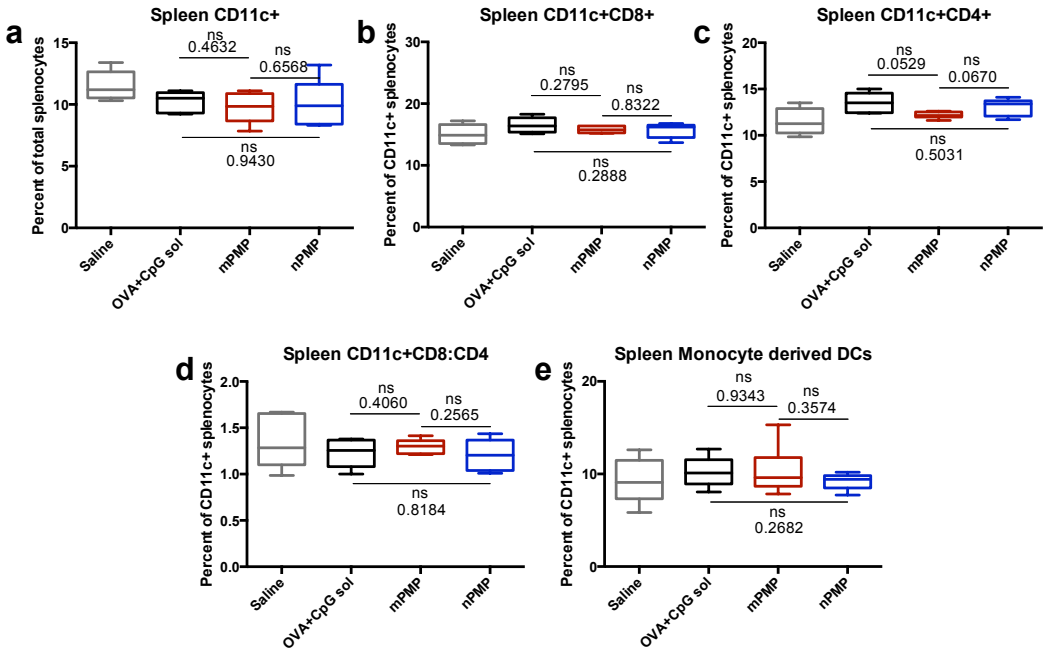

Figure 39: There was no detectable difference in DC subsets in vaccinated spleens.

4.2.3.4 Spleen – T cell response

We also did not see any significant differences between total, CD8+ or CD4+ populations of T cells in any treatment groups. This is likely due to the relatively low antigen dose used for this vaccination scheme (Figure 40).

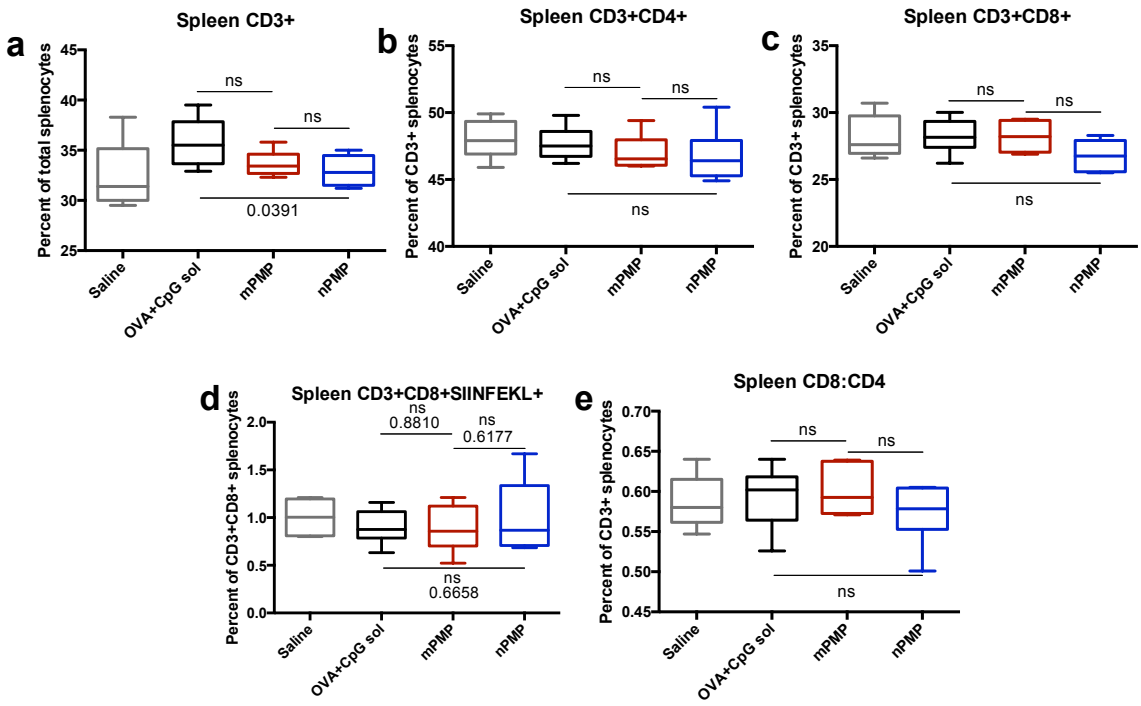

Figure 40: Splenic effector T cell populations did not vary for any treamtment groups.

Despite there being no effect of treatment on effector populations, splenic regulatory T cell populations were enhanced in both mice vaccinated with soluble formulations or nano-PLPs (Figure 41). This correlates with the regulatory response observed in the lymph nodes, as well as with in vitro data indicating that nano-PLPs promote Treg differentiation.

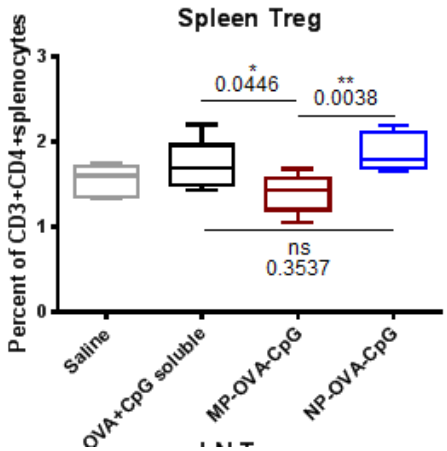

Figure 41: Splenic regulatory T cell activity is induced by nano-PLPs and soluble vaccinations.

4.2.3.5 Spleen – Natural killer cell and NK-T cell response

Natural killer cells and natural killer-T cells are two other cytotoxic cell types that aid in the removal of infectious cells[182–185]. Natural killer cell populations were increased after vaccination with PLPs and natural killer-T cell populations were enhanced in micro-PLP treated mice (Figure 42).

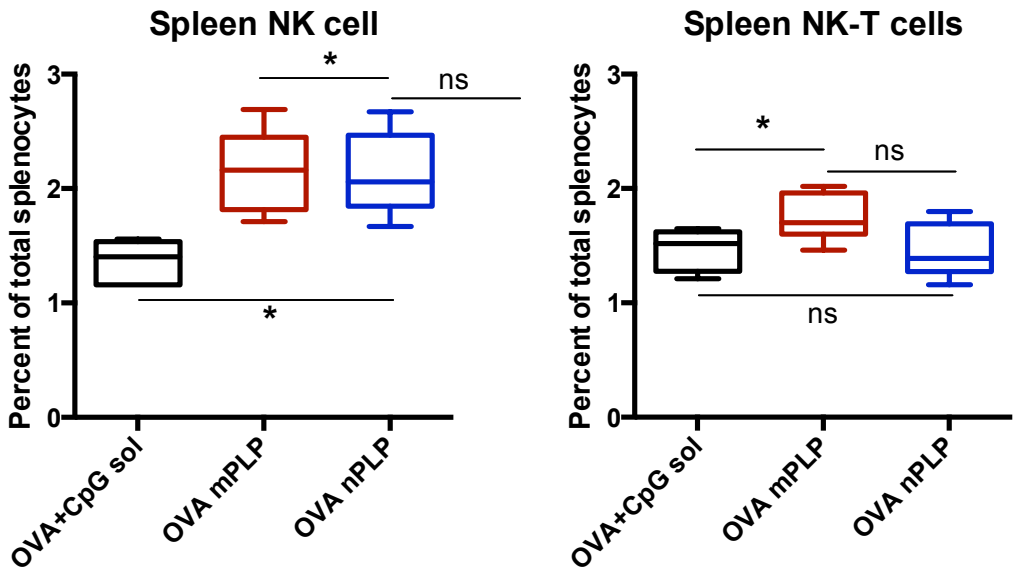

Figure 42: NK and NK-Tcell responses are enhanced by PLP vaccination. The presence of NK cells in the spleen are promoted by PLP vaccination. Additionally, micro-PLP vaccination also induced a small increase in NK-T cells.

4.2.3.6 Spleen – T cell Cytokine Secretome

To further characterize the T cell response, we restimulated splenocytes from vaccinated mice with whole ovalbumin antigen to evaluate their secretome. While there was no significant difference in the amount of IFN-γ produced by splenocytes from mice vaccinated with either PLP formulation, we observed a striking increase in the production of type 2 and anti-inflammatory cytokines, including IL4, IL5 and IL10 only in mice treated with nano-PLPs (Figure 43). Additionally, PLP formulations promoted greater production of IL2, indicating greater overall activation of T cell populations in PLP-treated mice. According to these findings, PLPs generally promote greater T cell activity and offer size-dependent tunability of T cell phenotype.

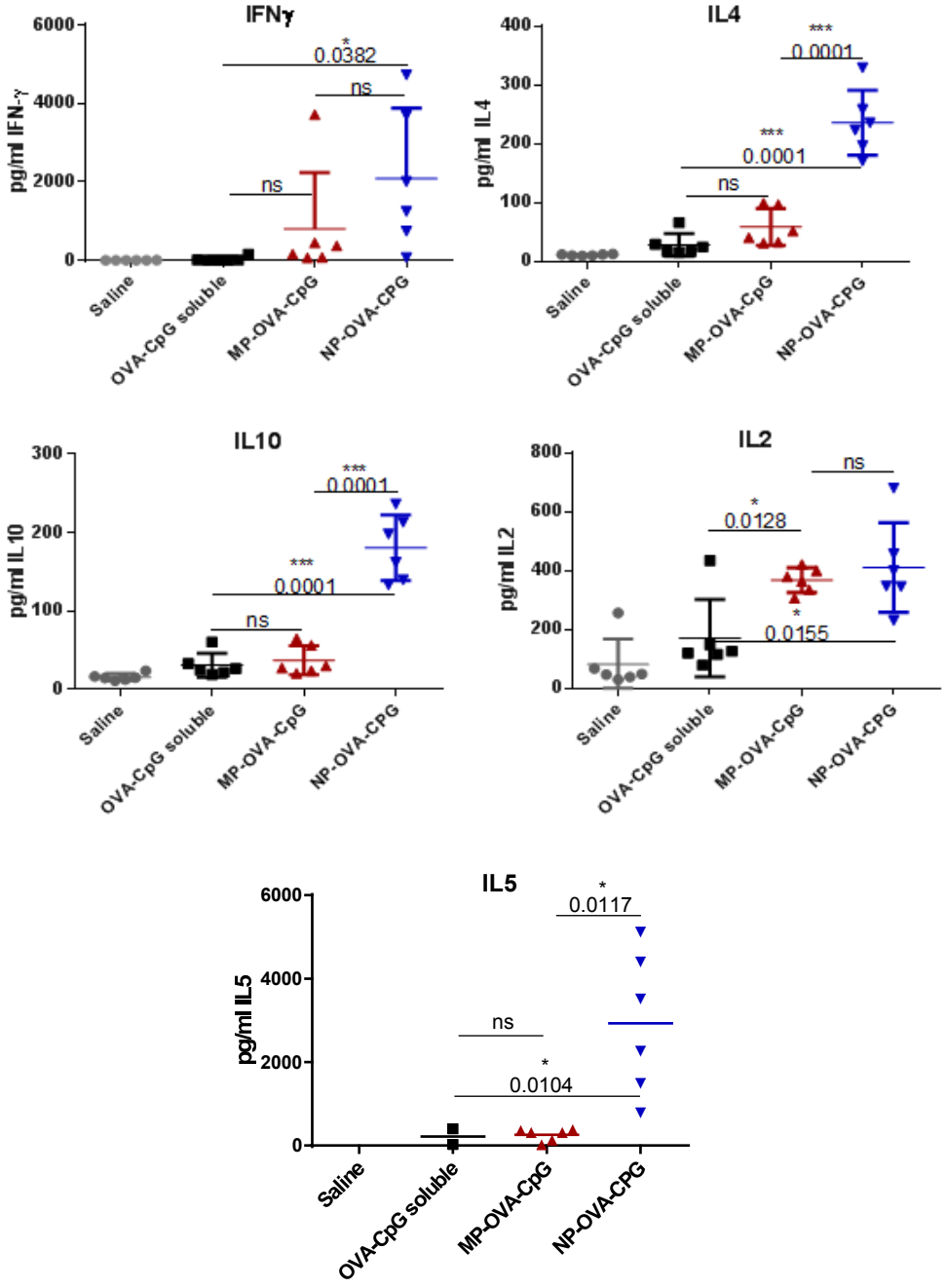

Figure 43: Secretome of splenic T cells from each treatment group indicates differential T cell polarization.

4.2.3.7 Lymph node – Germinal center formation

One of the primary roles of helper T cells is to provide signals to lymphoid resident B cells to promote class switching of secreted antibodies. This occurs in the germinal centers of lymphoid organs. We were able to identify germinal center formation in all treated lymph nodes. However, staining for IgG revealed that only mice treated with PLPs had highly functioning, IgG antibody-secreting B cells present in their lymph nodes (Figure 44) This was confirmed by flow cytometry analysis, where only PLP-treated mice had significant populations of activated germinal center B cells (Figure 45).

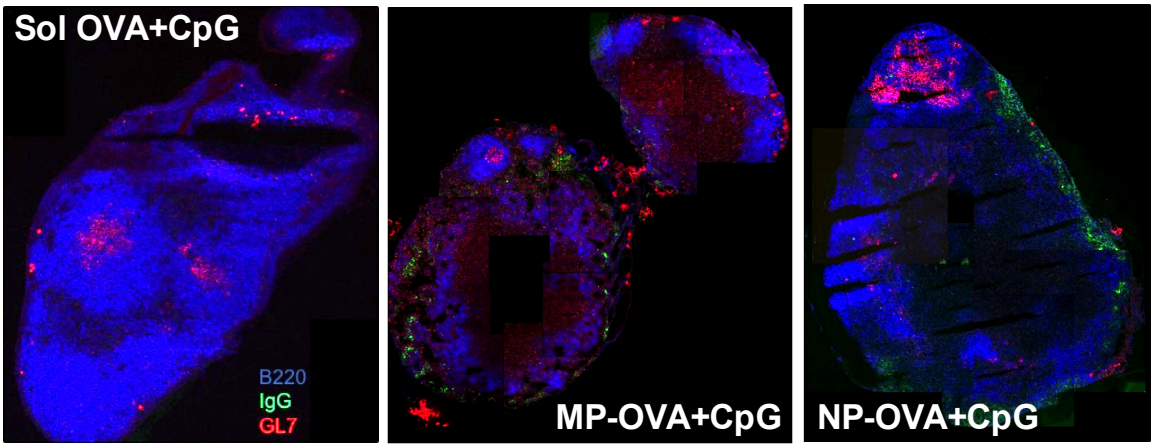

Figure 44: Only PLP vaccines induce IgG producing, germinal center B cells. All treatment groups induced the formation of germinal centers in lymph nodes. However, only lymph nodes taken from mice vaccinated with PLPs stained for IgG, indicating B cells are producing class-switched B cell receptors and antibodies.

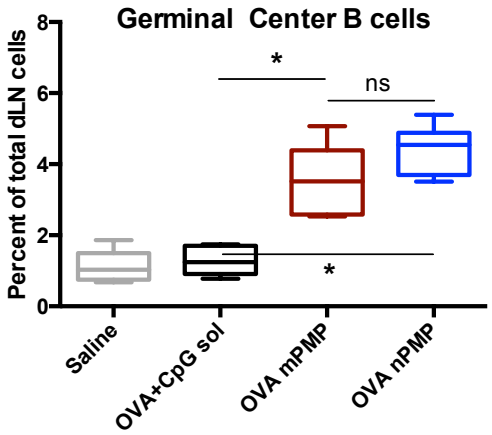

Figure 45: PLP vaccination produces activated, germinal center B cells.

4.2.3.8 Lymph node – Serum antibody titers

To further investigate the functionality of these activated B cells, we measured antibody levels in the serum of vaccinated mice. Both PLP vaccines increased the production of IgG1 over soluble vaccines (Figure 46). Strikingly, only mice that were treated with micro-PLP vaccines had high levels of IgG2c, which is associated with a type 1 cytotoxic response (Figure 47) and anti-bacterial immunity. Furthermore, we observed that serum cytokine content was indistinguishable from control mice treated only with saline (Figure 48). This demonstrates that robust immunity was achieved without undesirable systemic effects.

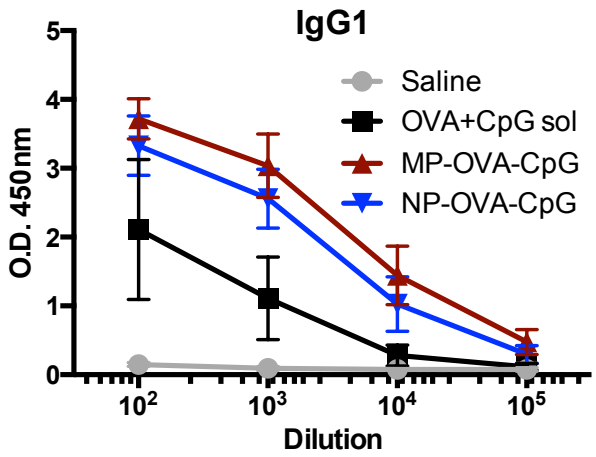

Figure 46: PLP vaccination induces higher IgG1 titers than a soluble vaccine.

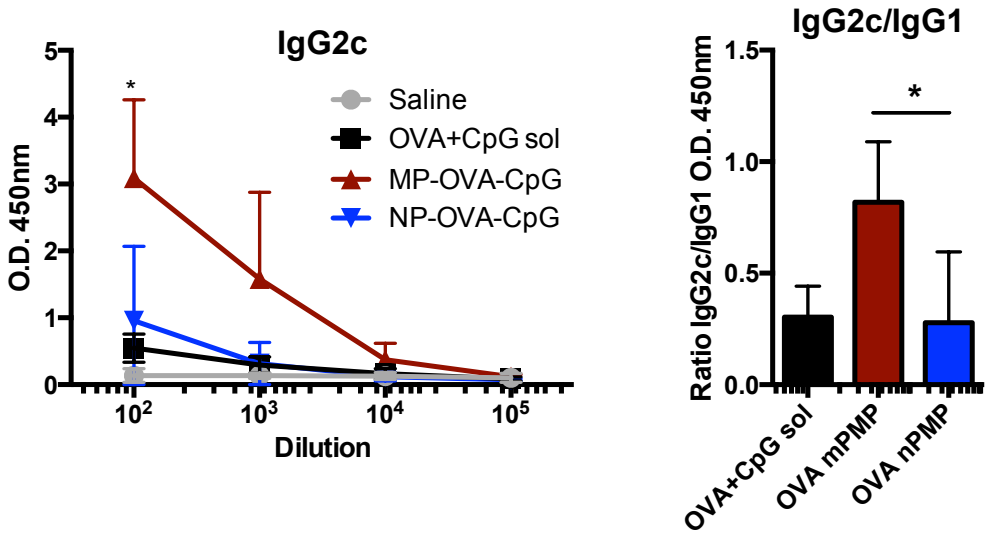

Figure 47: Only micro-PLPs promote class-switched IgG2c antibody.

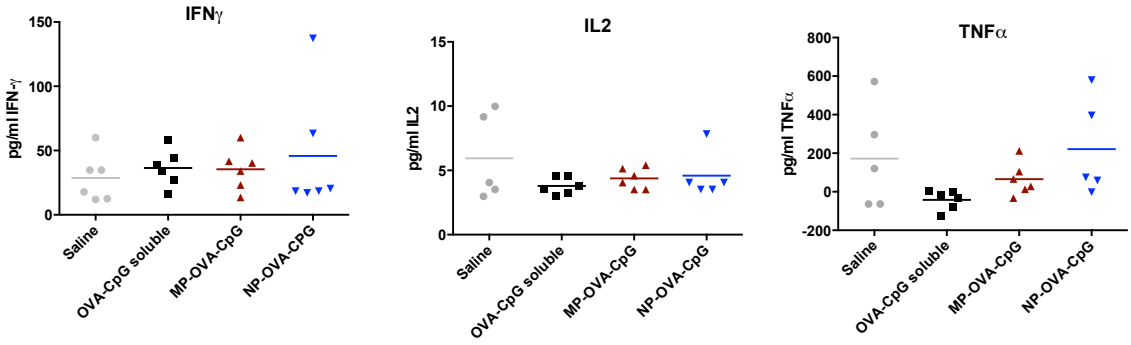

Figure 48: Serum cytokine levels are indistinguishable from saline control mice, indicating no undesired systemic effects.

4.2.4 Therapeutic value of micro- or nano-PLPs against tumor challenge

To determine whether the immunological response we observed previously has any therapeutic value, we challenged mice with an engineered melanoma cancer line (OVA-B16 melanoma). Mice were inoculated with melanoma, followed by 3 injections of either soluble antigen (OVA) alone, micro-PLPs carrying OVA+CpG or nano-PLPs carrying OVA+CpG. 29 days after inoculation, lymphoid organs and serum was collected for immunological analysis and the remaining mice were sacrificed according to tumor progression. Similar to our previous observations, we found that while PLPs did promote greater activation of germinal center B cells (Figure 49) and improve antibody production overall. Further, we again observed Th1 associated class-switching to IgG2b and IgG2c only in mice that were treated with micro-PLPs, indicating that this immunological modulation was potent enough to remain persistent despite tumor challenge (Figure 50).

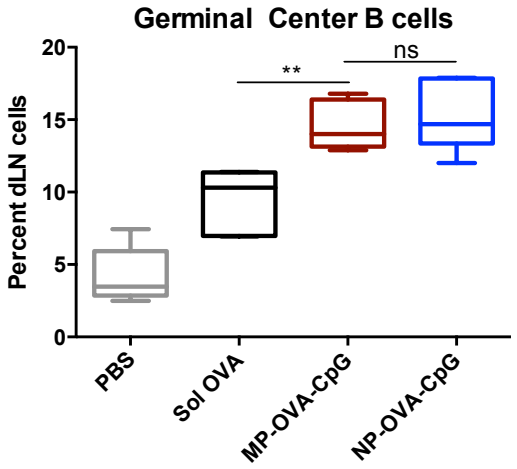

Figure 49: PLPs promote efficienct germinal center B cell activation, despite tumor challenge.

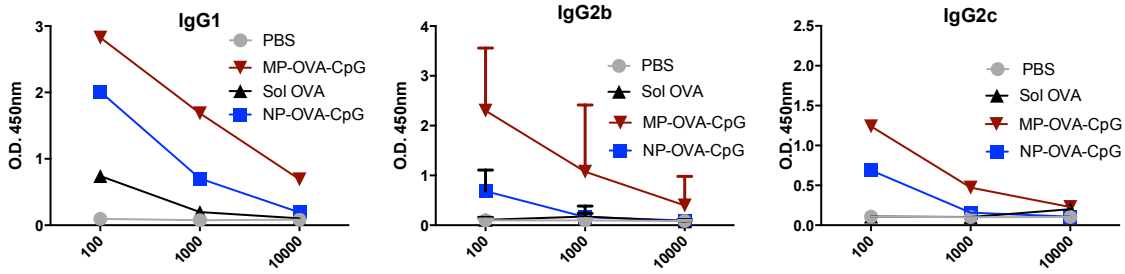

Figure 50: PLP promote antibody secretion, but only micro-PLPs induce Th1-associated class switching of antibodies.

We then investigated how these differences in immunological response translated to therapeutic value by tracking tumor growth and survival in challenged mice. Interestingly, we observed that both PLP treatments prolonged survival by delaying tumor growth significantly compared to controls. However, mice eventually succumbed to their tumor burdens in both groups with very similar kinetics (Figure 51).

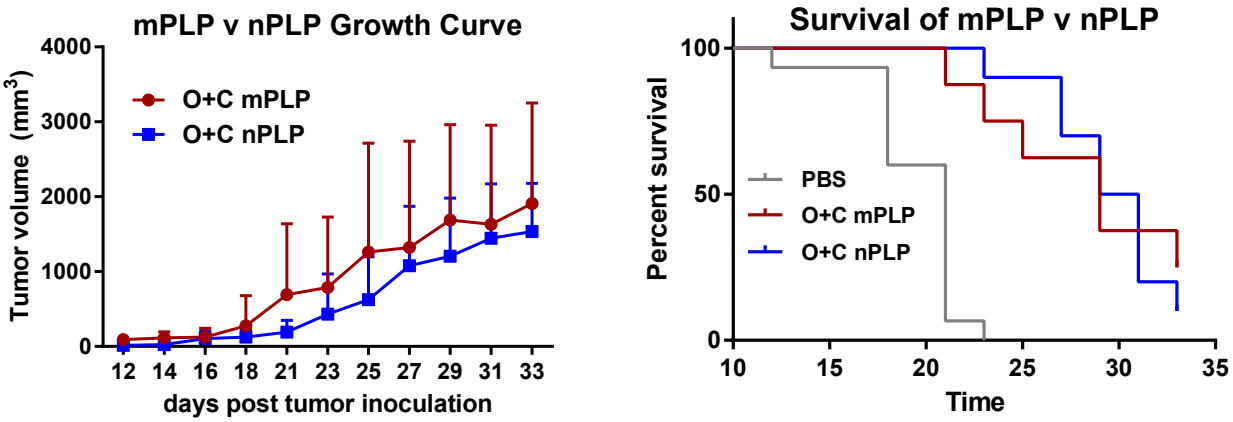

Figure 51: (left) Tumors of mice treated with either PLP formulations grew at a similar rate. (right) Likewise, while tumors growth was delayed after PLP treatment, mice in both treatment groups eventually sustained lethal tumors.

This finding has interesting implications for cancer immunotherapy design. While it is frequently hypothesized that a type 1 T cells response (and subsequent robust CTL activity) is necessary for efficient tumor elimination, here we show that there are perhaps multiple immunological mechanisms by which tumors may succumb to. Therefore, it may be most advantageous, in the end, to employ multiple therapeutic strategies simultaneously, to inundate the tumor's defense systems and promote elimination.

4.3 DISCUSSION

T cell maturation and proliferation are hallmarks of an effective immune response and are critical for both killing of infected and cancerous cells as well as building a humoral response [186]. It has been appreciated for decades now that dendritic cells play an essential role in initiation of an immune response by presenting antigens and stimulatory signals to dictate subsequent T cell responses [187]. Recent literature has expanded on the breadth of DC mediated responses, including functional characterization of many subsets [188]. These studies highlight the importance of studying how vaccine components interact with each of these subsets differently and what consequences this has for downstream immunity.

Here we make an argument for the importance of the role of peripheral DC induction of T cell immunity. We have shown that not only are particles taken up by different peripheral DC subsets in a size dependent manner but their migration to draining lymph nodes and T cell engagement also varies with size. We have also observed that particle size can initiate different DC activation programs within the same subset, directly affecting T cell maturation.

We suspect that the PDL2+ migratory DC subset may in fact include multiple subpopulations on its own and likely overlaps with other subsets that were screened in original trafficking assays. Therefore, the increase in PDL2+ DCs in the lymph node of mice treated with micro-PLPs may be indicative of a general preference for micro-sized carriers for many effector DCs in peripheral tissue. That in combination with the micro-PLP's ability to promote the production of a NFκB-mediated, pro-inflammatory DC cytokine profile could explain the Th1 skewing we observe. Additionally, micro-PLPs are able to induce a Th1 program, evident in T cell secretome and antibody class-switching observations. This response is in line with expected results of a CpG oligonulceotide supplemented vaccine and our lab has previously shown the therapeutic value of micro-PLP delivered CpG in the context of a lymphoma vaccine [158].

Nano-PLPs, on the other hand, skew the immune response towards a Th2 biased response, as well as a more defined regulatory response. . It has been shown previously that PLGA nanoparticles (400nm) can trigger the production of retinoic acid in dendritic cells isolated from cervical draining lymph nodes in vitro, leading to an increased induction of regulatory T cell proliferation [189]. However, there are likely many other mechanisms by which this can happen, one of which we will describe in Aim 3.

Interestingly, an increased occurrence of antigen-specific CD8+ T cells was also evident in nano-PMP treated mice. While this could be correlated with a number of events that are unknown to us in vivo, based on our data it's possible that the increase migration of CpG-carrying plasmacytoid DCs may contribute to this increase in cytotoxic T cell proliferation. Traditionally, activated pDCs produce interferon-α, promoting a cytotoxic response. Interestingly, there is also evidence that peripheral pDCs that have become matured previously will subsequently become tolerogenic, inducing regulatory T cell proliferation [178]. Further studies need to be performed to determine whether this is one cause of the increased regulatory response observed in mice treated with nano-PLPs.

Overall, these observations provide evidence that vaccine carrier size can have a distinct effect on the immune response outcome and may play a synergistic or antagonistic role with molecular pattern induced signaling. This has significant implications in vaccine design for anti-tumor, infectious disease or autoimmune applications.

4.4 ABBREVIATIONS

APC	Antigen presenting cell
DC	Dendritic cell
OVA	Ovalbumin
ELISA	Enzyme-linked immunosorbent assay
dLN	Draining lymph node
mPLP	Micro-pathogen-like particle
nPLP	Nano-pathogen-like-particle
pDC	Plasmacytoid dendritic cell
iDC	Inflammatory dendritic cell
NK	Natural killer
NKT	Natural killer- T cell
Treg	Regulatory T cell
GC	Germinal center

CHAPTER 5 AIM 3

INVESTIGATE MECHANISMS BEHIND SIZE-DEPENDENT DC PROGRAMMING

Molecular signaling has been studied and established for many toll-like receptor (TLR) activation dependent pathways. As described previously, unmethylated CpG, found in bacterial and viral DNA sequences, is an agonist for TLR9. Signaling propagation is illustrated in Figure 52[93]. Signaling associated with activated TLR9 proceeds by recruitment of MyD88, followed by phosphorylation of the IRAK complex (including IRAK4). Following recruitment of TRAF6, signaling can split to promote either NFκB mediated transcription of inflammatory cytokines and costimulatory molecules or IRF7 dependent production of type I interferons[99,190,191].

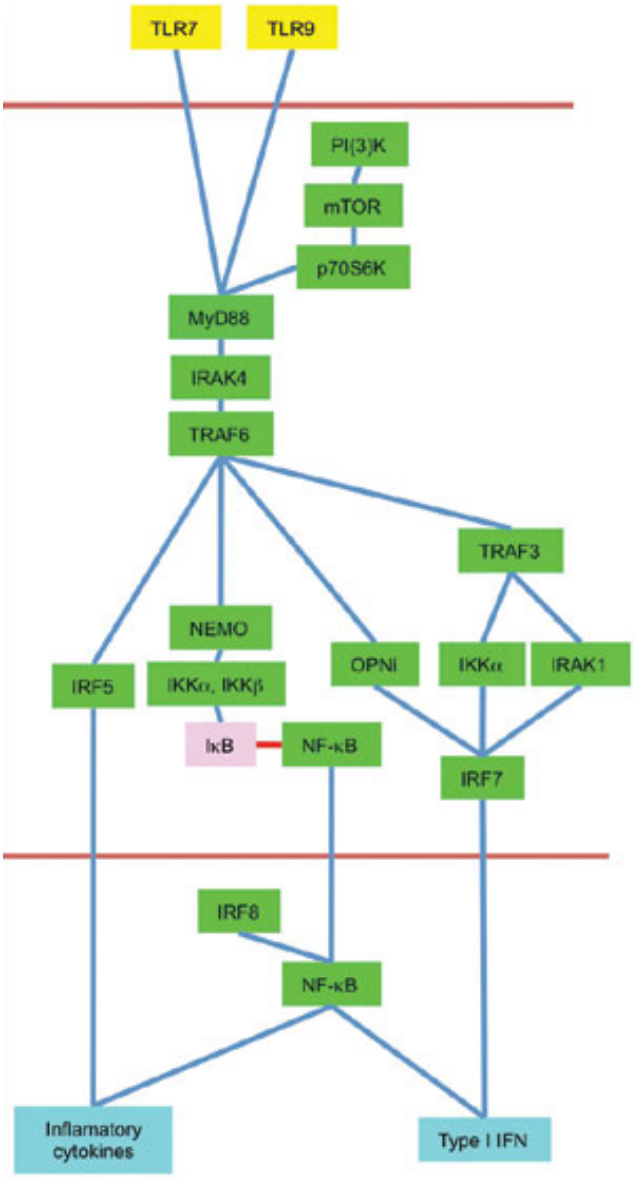

Figure 52: Activated TLR9 can signal through MyD88 to promote either NFkB dependent transcription of inflammatory cytokines or IRF7 dependent type I IFN production. * Modified from reference [93] with permission from publisher

In this aim, we hypothesized that there are four points in the signaling propagation that could be influenced by particle parameters when delivering CpG (Figure 53). Due to the lack of IFNα/β produced by PLP-treated DCs (Aim 1), we decided to focus on NFκB-mediated events. Specifically, we evaluated whether uptake kinetics varied between the two PLP formulations, TLR9-CpG ligation and signaling occurred rapidly after uptake, downstream NFκB-associated transcription events could be detected shortly thereafter and finally, whether we could detect major inhibitory signals that may block pro-inflammatory events.

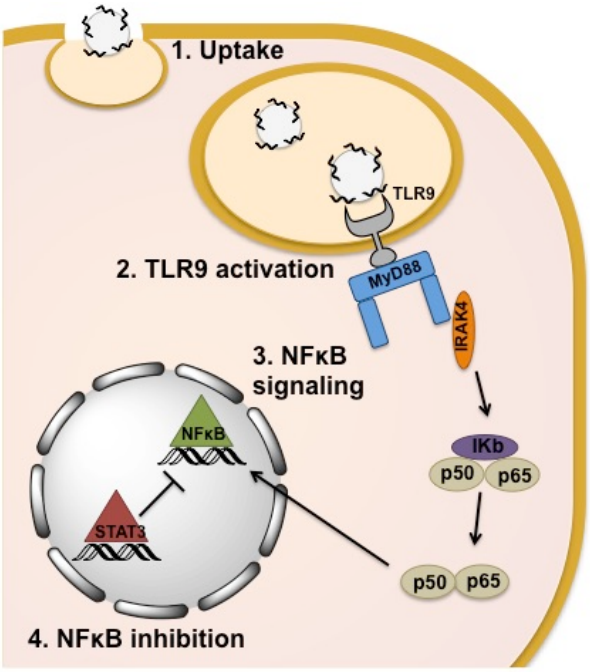

Figure 53: TLR9 signaling could be affected by the size of the CpG carrier at multiple points in the signaling axis.

5.1 METHODS

5.1.1 Materials

Fluorescent CpG was custom made by Integrated DNA Technologies (Coralville, IA). Duolink Proximity Ligation Assay (PLA) kits and reagents were all purchased from Sigma (St. Louis, MO). Primary antibodies for PLA assays were purchased from Lifespan Biosciences (Seattle, WA). Raw-Blue NFκB reporter cells were purchased from Invivogen (San Diego, CA) and cultured according to manufacturer's instructions. Anti-phospho-STAT3 was purchased from BD Biosciences (Franklin Lakes, NJ). Antibodies against IRF4 and IRF8 were purchased from Ebioscience (San Diego, CA) and antibodies against IRF5 and IRF7 are from Life Technologies (Carlsbad, CA).

5.1.2 Analysis of uptake preference by flow cytometry

Uptake preference of isolated dendritic cell subsets was analyzed using flow cytometry. For flow cytometry experiments, PDL2+ or sorted pDCs were incubated with soluble or PEI-PLGA particle loaded APC-CpG for 24 hours. CpG dosage was kept constant at 5ug/10^6 cells. Following incubation, cells were collected, washed, blocked for nonspecific Fc interactions using anti-mouse CD16/CD32 and stained with anti-mouse CD11c-PE-Cy7 and anti-mouse PDL2-PE antibodies according to previously published methods[158]. Cells were washed and resuspended in FACS buffer (PBS with 0.5% FBS) for analysis using a BD LSR II flow cytometer. Gates were applied to only include live, CD11c+ cells and both percent expression and mean fluorescent intensity were analyzed.

5.1.3 TLR9-IRAK4 Proximity Ligation Assay

BMDCs were sorted using a Pan DC Isolation kit (Miltenyi) to ensure purity. Cells were plated onto glass coverships and PLP formulations were added for 1 or 4 hours. Cells

were immediately fixed, blocked and stained with primary anti-TLR9 and anti-IRAK4 overnight. The following day, cells were stained using the Duolink PLA system instructions. Coverslips were mounted onto glass slides using Prolong mounting medium and imaged using a spinning disc confocal microscopy. Quantification of punctae was performed using Volocity image analysis software.

5.1.4 NFkB Activation Kinetics

The RAW-Blue reporter cell line was used to determine NFkB activation kinetics. Cells were cultured according to manufacturer's instructions and treated with particles for 1, 4, 6, 24 or 48 hours. Supernatant was then collected and added to the QUANTI-BLUE detection medium per the manufacturer's instructions.

5.1.5 Phospho-STAT3 Kinetics

Magnetic bead sorted (Pan DC Isolation Kit, Miltenyi) BMDCs were fixed, permeabilized and stained with anti-phopsho STAT3 (PY705). Cells were then analyzed using an Accuri C6 flow cytometer (BD).

5.1.6 IRF 4/5/7/8 regulation

Magnetic bead sorted BMDCs were fixed, permeabilized and stained with anti-IRF 4/5/7/8 according to the manufacturer's instructions. Cells were then analyzed using an Accuri C6 flow cytometer. Alternatively, cells were adhered to a glass slide before staining and analyzed using a Zeiss 700 Confocal microscope.

5.1.7 Statistical Analysis

Student's t-test was used to perform statistical analysis between two groups, where $p<0.05$ was considered significant. In vitro experiments were conducted with n=6 to ensure reproducibility.

5.2 RESULTS

5.2.1 Micro- and nano-PLPs are taken up with similar kinetics

While we have determined previously that various DC subsets exhibit preference towards a particular PLP formulation, we wanted to evaluate whether cells that did take up PLPs took up similar amounts of CpG and whether the kinetics of uptake were similar. This was done simply by quantifying fluorescence per cell (mean fluorescence intensity) of CpG+ cells in culture at multiple time points (1, 2, 4, 24 hours). We found that while soluble CpG was taken up more efficiently (faster and higher quantity), both PLP formulations were taken up at a similar rate. Additionally, cells that were CpG+ internalized equivalent amounts of CpG, regardless of carrier size (Figure 54). Therefore, it is unlikely that differences in uptake cause major signaling differences in DCs.

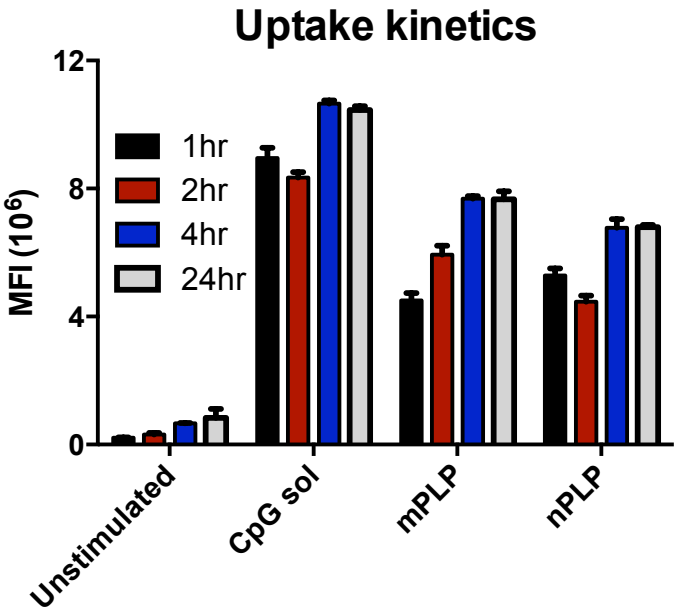

Figure 54: PLP uptake (magnitude or rate) did not vary in a size-dependent manner.

5.2.2 TLR9 signalig is delayed in nano-PLP treated BMDCs

The next step in the signaling pathway is ligation of CpG and TLR9, resulting in activation of TLR9 and subsequent recruitment of MyD88 and other adaptor proteins, including IRAK4[192,193]. MyD88 must be sufficiently activated before adaptor proteins like IRAK4 are recruited; therefore, it is possible to indirectly test TLR9 activation by quantifying its proximity to IRAK4. We did this using the well-established proximity ligation assay[194–196]. Briefly, primary antibodies (anti-TLR9 and anti-IRAK4) are applied to cells, followed by secondary antibodies functionalized with DNA oligos that are then hydridized, ligated and amplified increase fluorescence. Hybridization is only possible when secondary antibodies are within 30-40nm, indicating that IRAK4 must be recruited to the TLR9 activation complex for a fluorescent signal to occur.

We looked at TLR9 activation using this technique at early time points, specifically, 1 and 6 hours post-PLP treatment. We observed that cells treated with micro-PLPs initiated TLR9 signaling as early as 1 hour after treatment and this signaling was no longer active 6 hours after treatment. Inversely, signaling of TLR9 in cells treated with nano-PLPs was not evident until 6 hours post-treatment, indicating a significant delay in TLR9 activation (**Figure 55**).

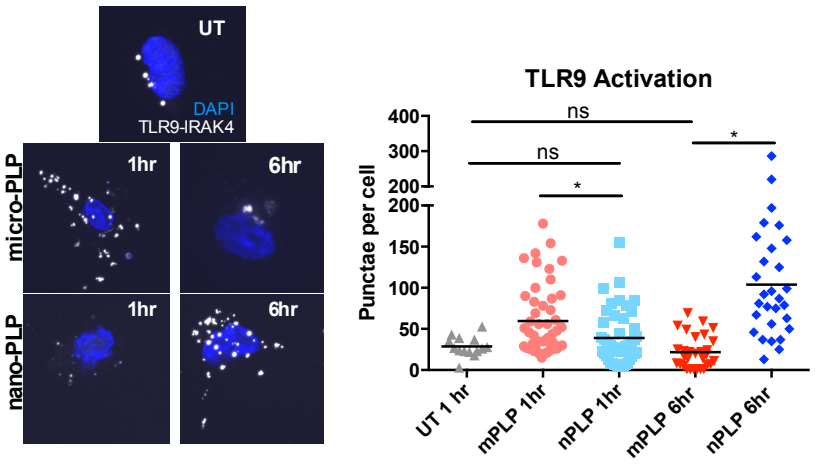

Figure 55: TLR9 activation is delayed in nano-PLP treated BMDCs but not in those treated with micro-PLPs.

5.2.2.1 NFκB-mediated transcription is delayed in nano-PLP treated BMDCs

NFκB is the transcription factor that has been identified as the key promoter of pro-inflammatory cytokine and co-stimulatory molecule production[197–199]. Because we have previously demonstrated a difference in cytokine production by cells given different PLP formulations (Aim 1), we wanted to investigate whether this was due to a difference NFκB activation kinetics. We quantified NFκB transcription using the Raw-Blue reporter cell line, which has a chromosomal incorporation of an NFκB-inducible secreted embryonic alkaline phosphatase (SEAP) reporter construct. We treated these cells with our PLP formulations (or soluble CpG) and quantified NFκB transcription over time. We observed that cells treated with both soluble or micro-PLPs have significant levels of NFκB-mediated transcription after 24 hours of treatment with PLPs. However, this was not observed for cells treated with nano-PLPs until 48 hours following treatment (Figure 56). This delay is likely linked to the delay in TLR9 activation we observed previously and also explains the decreased production of pro-inflammatory cytokines (e.g. IL12p70) in cells treated with nano-PLPs.

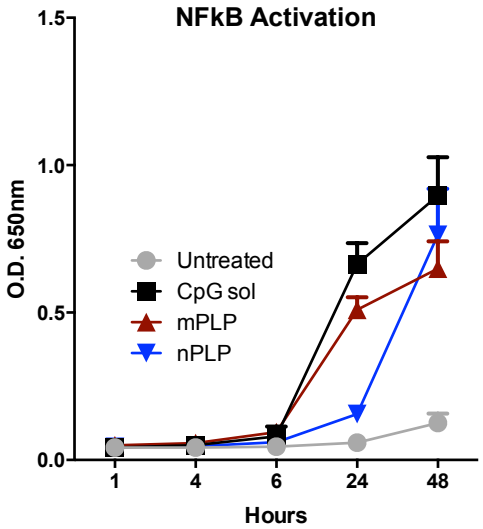

Figure 56: Activation of NFκB is delayed in cells treated with nano-PLPs.

5.2.3 Nano-PLPs induce rapid phosphorylation of STAT3

STAT3 is implicated in negative regulatory processes in DCs, specifically initiation of pro-inflammatory signals[200]. Additionally, it is thought that the STAT3 transcription factor is responsible for controlling IL10 gene expression[201,202]. We, therefore, were interested in assaying whether the delay in NFκB activation or the IL10 secretion we observed in nano-PLP groups was caused by STAT3 activation. Our observations validated our hypothesis that STAT3 was phosphorylated rapidly and preferentially in cells treated with nano-PLPs. Specifically, STAT3 was activated within one hour in cells given nano-PLPs, while STAT3 in other groups was not activated to the same level until 24 hours following treatment (Figure 57). In combination with the slower kinetics of NFκB activation, this is likely at least a partial explanation for the difference in polarization observed when DCs are treated with micro- vs nano-PLPs.

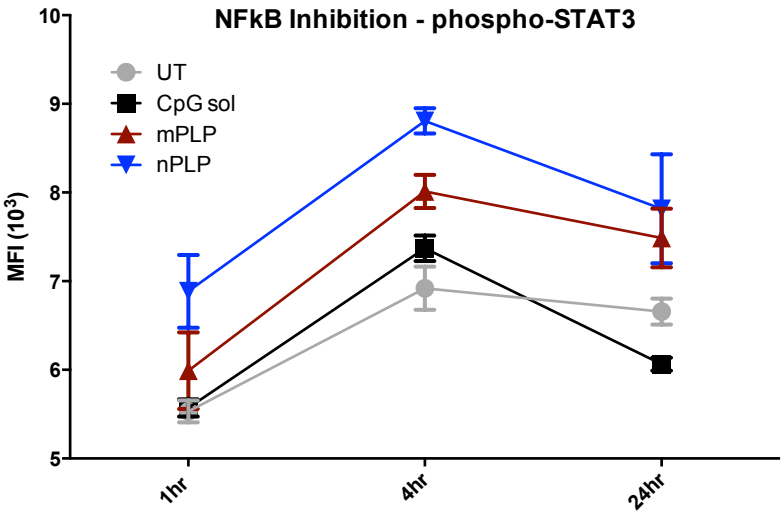

Figure 57: Nano-PLPs promote rapid and persistent STAT3 phosphorylation.

5.2.4 CpG-density play a critical role in modulating DC programming

When working with biomaterial carriers, there are many parameters that may or may not prove important for immune modulation that are hard to decouple. For example, in order to provide consistent dosing of both CpG and PLGA in our experiments, we are required to allow the density of CpG on micro- vs. nano-PLPs remain variable. Specifically, the density of CpG loaded onto micro-PLPs is approximately four times the density on nano-PLPs if they are loaded at the same w/w% (Table 5). Likewise, the amount of CpG loaded on the surface of PLPs directly affects their charge, thereby changing how they interact with cells[132]. Therefore, we evaluated how the size-dependent immunomodulation of PLPs on DCs is affected by ligand (i.e. CpG) density. We did this by loading the maximum amount of CpG onto nano-PLPs (Max nano-PLPs), providing us with a formulation with similar density to micro-PLPs. Using this system, we reassessed the kinetic profile of NFκB transcription and compared it with previously tested micro-PLP and nano-PLP formulations. We observed that when cells were treated with nano-PLPs that were density matched to micro-PLPs (Max-nano-PLPs) they no longer exhibited delayed NFκB transcription (Figure 58).

Table 5: Density Measurements

	Zeta	CpG Loading	% Max Density	Max Density
mPLP	-24.2±8.7 mV	13±1ug/mg	100%	1.83mg CpG/m^2
nPLP	4.65±4.12 mV	13±.0.1 ug/mg	26.8%	0.4mg CpG/m^2
Max-nPLP	(theoretical) -25mV	48±5 ug/mg	100%	1.49mg CpG/m^2

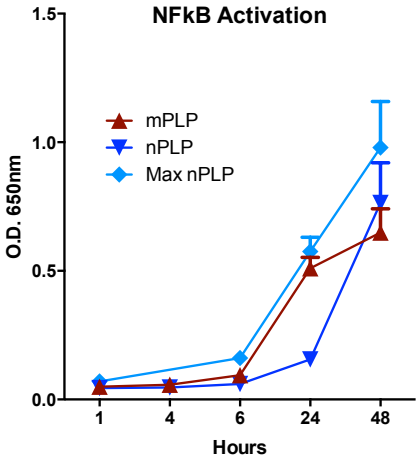

Figure 58: Density matched PLPs (micro- and Max-nano) promoted the same NFκB transcription profiles.

We went on to investigate whether STAT3 phosphorylation still occurred at the rapid rate observed with nano-PLP treated cells if they were instead treated with density matched nano-PLPs. Corroborating NFκB data, STAT3 phosphorylation was also decreased in cells treated with the Max-nano-PLP formulation compared to those treated with regular nano-PLPs. Interestingly, STAT3 phosphorylation in cells given Max-nano-PLPs never rose to the level that both nano-PLP and micro-PLP treated cells achieved, even at later time points (Figure 59). This indicates that there is still likely a size effect at play but we have demonstrated that ligand density plays an equally significant role in immune modulation.

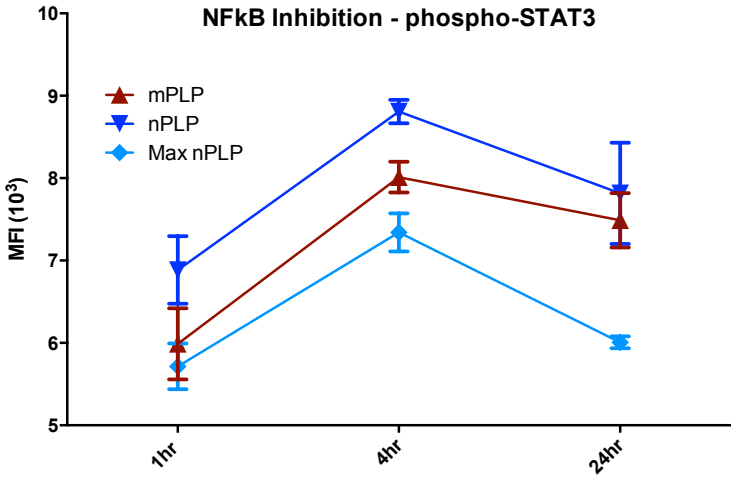

Figure 59: STAT3 phosphorylation kinetics vary in a size- and ligand density-dependent manner.

5.2.5 IRF4 may play a role in PLP mediated DC programming

The interferon regulatory factor (IRF) family plays many roles in both the regulation of DC phenotypic development, as well as maturation[203–206]. In the context of TLR signaling, each IRF protein has a distinct role. IRF7 signaling diverges from the NFκB signaling pathway, promoting the production of Type 1 interferons (**Figure 60**, left)[204]. IRF5 and IRF8 both play roles in the NFκB pathway by complementing previously discussed adaptor proteins (**Figure 60**, middle)[204]. Lastly, IRF4 shares a binding domain on MyD88 with IRF5 and therefore serves as an regulatory factor by competitively inhibiting IRF5 activation (**Figure 60**, right)[204].

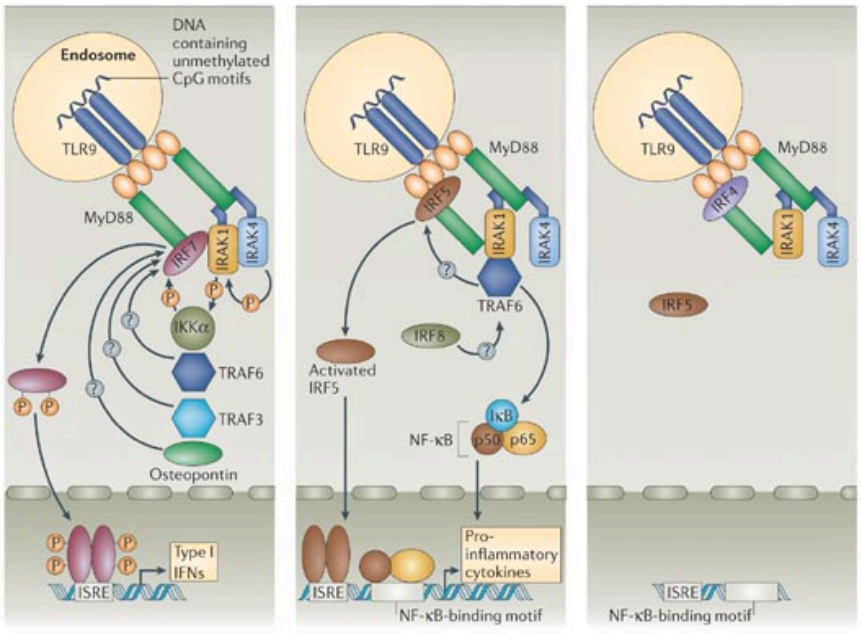

Figure 60: IRF5/7/8 are mediators of various inflammatory responses while IRF4 provides regulatory signals. *Figure from reference [204] with permission from publisher

We therefore analyzed the kinetics of expression of each of these regulatory factors. First we analyzed the expression of IRF8 at 24 hours. We did not suspect that IRF8 would play a large regulatory role in these cells, since it has been established previously that BMDCs cultured with GMCSF+IL4 are regulated primarily via IRF4, not IRF8[75]. Our hypothesis was correct, as we did not observe any difference in IRF8 expression at 24 hours (Figure 61).

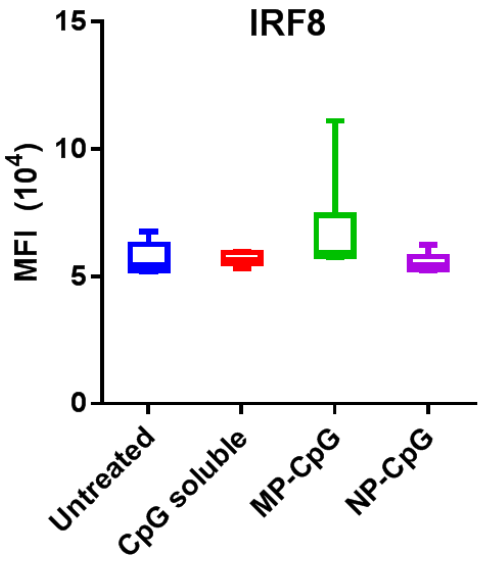

Figure 61: IRF8 expression does not vary in a formulation dependent manner at 24 hours.

We also suspected that IRF7 did not play a large role in the DC program we've observed due to the lack of Type 1 interferon present in our DC cultures. Our hypothesis proved to be correct, as we did not see an appreciable difference in IRF7 expression between cells treated with different PLP formulations at any time point between 1-24 hours (Figure 62).

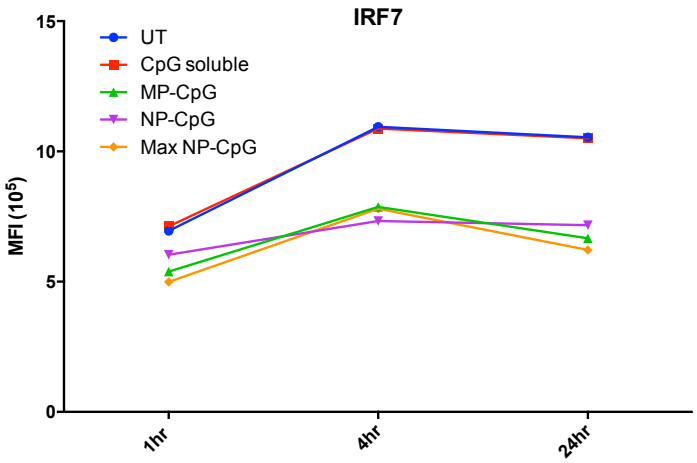

Figure 62: IRF7 expression does not vary in a formualtion dependent manner over a 24 hour period.

Given these findings, we hypothesized that the counterbalance between IRF4 and IRF5 binding to MyD88 play a significant role in the eventual activation of downstream transcription factors and subsequent production of DC signals. We did find IRF5 expression varies with treatment and that it is present in smaller amounts in cells treated with nano-PLPs (not density matched) (Figure 63).

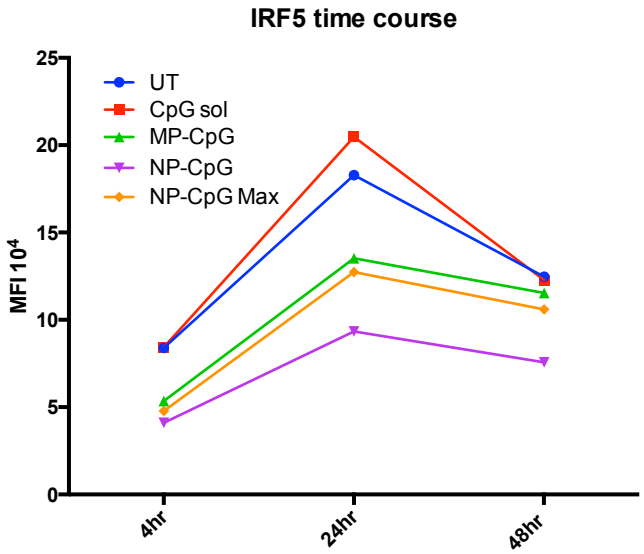

Figure 63: IRF5 expression varies in response to different formulations and over time. Nano-PLPs (not density matched) have the lowest exprsesion of IRF5 over all time points. However, all three PLP formulations induce a decrease in IRF5 expression relative to untreated cells.

IRF4 expression followed a very similar expression pattern, with the lowest expression exhibited by cells treated with nano-PLPs (Figure 64).

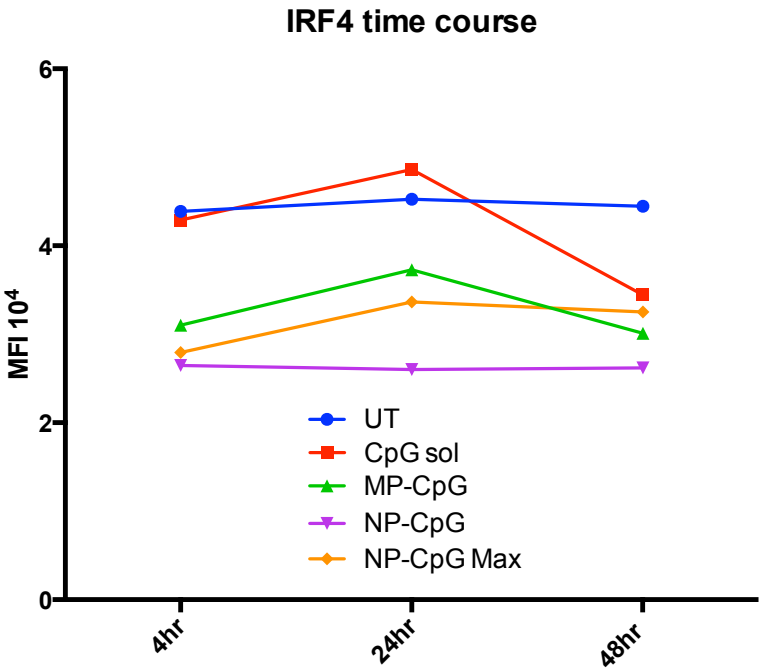

Figure 64: IRF4 expression over time is influenced by formulation treatment. PLPs, especially nano-PLPs induce a significant reduction of IRF4 expression over all time points relative to untreated cells.

It is also known that activated IRF4 and IRF5 translocate from the cytoplasm, where it interacts with MyD88, to the nucleus, where it can act as a cofactor or regulator of transcription. We therefore utilized confocal microscopy to determine where IRF4 and IRF5 were located within the cells (Figure 65). According to these preliminary results, there is a significant amount of both IRF4 and IRF5 in the nuclei of cells regardless of treatment. However, IRF4 expression does seem to decrease over time in most groups, which corroborates our flow analysis. However, this data does not provide us grounds for any further conclusions.

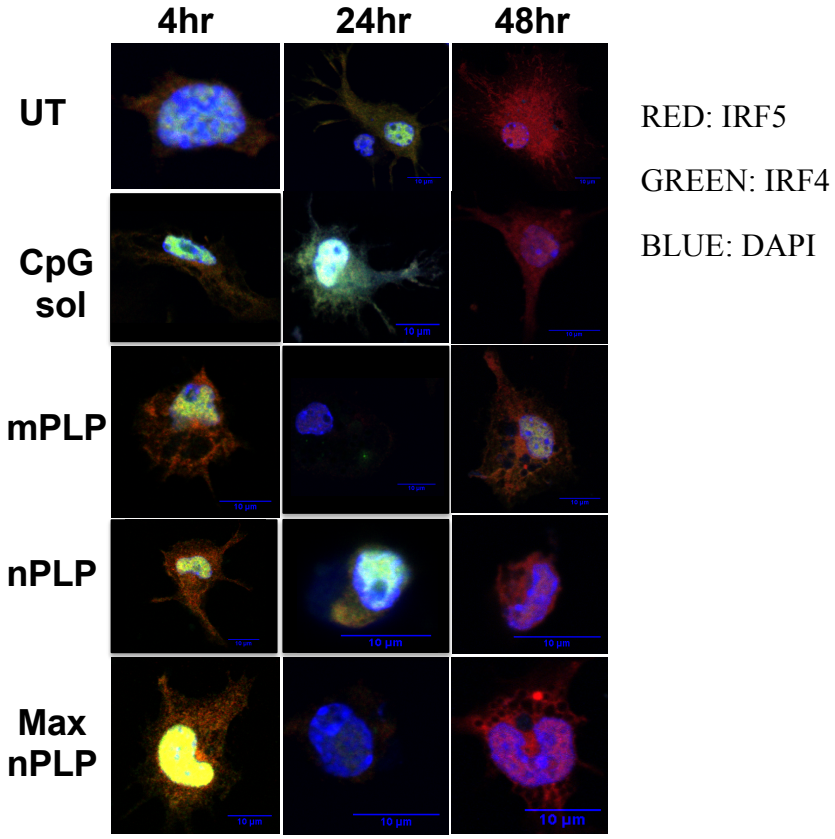

Figure 65: Microscopic evaluation of IRF4 and IRF5 localization. (red: IRF5, green:IRF4, blue: DAPI)

5.3 DISCUSSION

To gain greater insight into size-driven DC programming, we investigated multiple points in the TLR9 - NFκB axis, including PLP uptake, TLR9 signaling through MyD88 to IRAK4, transcription events of NFκB activation and NFκB inhibition through STAT3 phosphorylation (Figure 53). While uptake did not vary significantly between the two carriers over time we did observe a kinetic variation in TLR9 signaling. TLR9 activation occurred within one hour in cells treated with micro-PLPs but was delayed in cells treated with nano-PLPs, remaining equivalent to untreated cells at 1 hour, but signaling strongly by 6 hours post-treatment .

This led us to investigate whether the observed delay in signaling resulted in slower NFκB transcription, where we observed an equivalent delay in cells treated with nano-PLPs. This informs the observations made earlier than nano-PLP treated cells not only expressed less CD86 but also produced significantly less IL12p70 after 24 hours of PLP treatment. It is known that CpG induces a regulatory response in parallel with pro-inflammatory signals, hallmarked by production of IL10, to keep the immune response in check [207]. STAT3 plays a major role in the transcription of the IL10 gene and also inhibits NFκB activity. Furthermore, STAT3 inhibition has been linked to regulatory T cell ablation [208]. We therefore measured phosphorylation of STAT3 over time in PLP treated cells and observed that nano-PLP treatment did promote activation of STAT3. Taken together, the implication is that STAT3 dominates signaling in nano-PLP treated cells in early stages of DC programming, promoting a phenotype consistent with tolerogenic DCs and regulatory T cell phenotype development. IL10 in these cultures can also have an autocrine effect, promoting IL4 producing T cells [209].

Multiple modes of activation have been described for STAT3, one being through the IL10-receptor binding of extracellular IL10 [210]. However, based on the time scale of our observations, another mechanism must be dominant. We hypothesize that, in our system, STAT3 could be activated downstream of the PI3K pathway, which is independent of MyD88-IRAK4 activation and can be initiated very quickly after TLR activation [211,212]. Furthermore, it has been shown that activation of PI3K and downstream STAT3 both result in the enhancement of IL10 production and decrease in pro-inflammatory cytokine (i.e. IL12p70) production, similar to our observations [213]. Interestingly, it has also been demonstrated that type 1 interferons (e.g. IFNα) can induce activation of the IL10 promoter via STAT3, potentially linking the plasmacytoid and regulatory responses we observed in our in vivo studies [214].

Due to the greater surface to volume ratio of smaller spherical particles, ligand density is a variable that is linked to size. Specifically, at maximum loaded conditions, nano-PLPs were able to accommodate about 4 times more CpG than micro-PLPs. We discovered that the delay in NFκB transcription associated with nano-PLP treatment was completely recovered when the CpG density was matched to micro-PLPs. Interestingly, phosphorylation of STAT3 was also inhibited and remained ablated compared to micro or nano-PLP treated cells over the course of the experiment.

It has been described for other TLRs (TLR1/2) that clustering is required for robust signaling[215]. It has been suggested that clustering may also promote hyperactivation for other TLRs, including TLR9[216]. Furthermore, it has been described recently by Ohto et al. that TLR9 forms a homodimer following ligation with a stimulatory CpG molecule, preceding signal propagation[217]. This could be one explanation for the density-dependent

graded response we have observed. It also begs the question of how signaling kinetics influences eventual programming. For example, it is known that there is a significant amount of crosstalk between different signaling axes, including those of NFκB and STAT3[218–220]. Therefore, it is possible that ligand-receptor avidity and rate of signaling may provide sufficient stimulation for one pathway but not the other, allowing the first to dominate programming. Another hypothesis involves the finding that CpG that forms high-order structures provides more efficient signaling motifs[221]. Therefore, it is possible that CpG delivered at a higher density is perceived by TLR9 as a higher ordered structure, promoting stronger signaling. Overall, this finding encourages further study into these interactions and could provide a means of fine-tuning immunity using CpG density. In general, the findings in this aim are incredibly promising and indicate that carrier parameters play a significant role in immune modulation.

5.4 ABBREVIATIONS

TLR9	Toll-like receptor 9
IRAK	Interleukin-1 receptor-associated kinase
IRF	Interferon regulatory factor
NFκB	Nuclear factor kappa B
IFNα/β/γ	Interferon alpha/beta/gamma
FACS	Fluorescence-activated cell sorting
PLA	Proximity ligation assay
Phosphor-STAT3	Phosphorylated STAT3
MFI	Mean fluorescence intensity
SEAP	Secreted embryonic alkaline phosphate

CHAPTER 6 CONCLUSIONS AND FUTURE DIRECTIONS

6.1 CONCLUDING SUMMARY

Every year there are significant strides in medicine, yet there are diseases that plague huge portions of the population that remain unchecked. These range from infectious diseases (tuberculosis, malaria, HIV) to endogenous disease (cancer) to autoimmunity (diabetes, lupus, colitis). Dysregulation of the immune system is the link between all of these otherwise very different diseases. Immunotherapy provides an alternative to other medical approaches by teaching the body of the patient how to respond appropriately to its aberrant state. However, in order for an immunotherapeutic approach to be successful, it must be designed to simultaneously stimulate a robust response from the appropriate effector cells and overcome regulatory hurdles.

Polymer-based particulate delivery vehicles have emerged as one of the most promising strategies for a wide range of immunotherapeutic applications. Particulate systems provide a modular platform for delivering a large variety of synthetic or biologic drugs. Furthermore, the ease at which physical parameters can be modulated offers as many permutations of particulate immunotherapeutic systems as there are applications.

It has now been well established that there are many pathogen associated molecular patterns (PAMPs) that stimulate immune cells and promote robust, long-term responses. In addition to molecule signatures, pathogens come in a variety of shapes, sizes, charges and material compositions. However, there is still no conclusion whether these physical parameters contribute significantly to generation or alteration of the immune response. Likewise, this has also not been established for particle systems. In this work, we investigated whether a select couple of important physical parameters (i.e. size and ligand density) play a role in immunomodulation. We employed a pathogen-like microparticle (mPLP) system that our lab has extensively published on, in addition to a nano-scaled version of the same PLP system (nPLP).

We first examined whether our particles exhibited any ability to passively target particular subsets of phagocytes present at the site of injection. By injecting PLPs loaded with fluorescently labeled CpG, we were able to determine both when and where the particles were in the lymph nodes and identify which dendritic cell subsets were responsible for transport of the PLPs. Using this strategy, we were able to pinpoint two subsets that made the most meaningful contributions to transport; these were PDL2+ dermal DCs and plasmacytoid DCs. Both cell types have been described previously in literature and are thought to promote a Th2 or a Th1 response, respectively. PDL2+ DCs have been detected in the dermis of mice and have been shown to efficiently migrate to mesenteric or skin-draining lymph nodes. Additionally, these cells are less sensitive to TLR agonists and can be derived from bone marrow cultures using GMCSF and IL4 supplementation[75]. Plasmacytoid DCs, on the other hand, highly express TLRs that sense viral PAMPs and, upon activation, secrete large amounts of type 1 interferons, promoting cytotoxic T cell and type 1 helper responses. pDCs are found in both secondary lymphoid organs and in skin, especially during inflammation[23,55]. Therefore, by choosing these two subsets for PLP investigation allowed us to characterize PLP-DC interactions in two functionally distinct subsets.

We immediately observed that DC subsets exhibited distinct preferences towards particular PLPs and that each PLP promoted unique DC programs. PDL2+ DCs preferentially took up micro-PLPs and they were also activated more efficiently by mPLPs, indicated by increased co-stimulatory expression and pro-inflammation shifted cytokine production. On the other hand, pDCs were more efficiently activated by nPLPs. One could rationalize that pDCs are more efficiently activated by nPLPs due to their resemblance to large virsus, but PDL2+ DC's preference for mPLP was unexpected. Additionally, our finding that PDL2+ DC were capable of producing large amounts of pro-inflammatory cytokines following CpG stimulation countered previous literature, which indicated that PDL2+ BMDCs were not capable of this due to their spontaneously

matured nature. However, we argue that the previous characterization of PDL2+ as a marker identifying only Th2 programmed DCs is limited and PDL2+ may play a larger role in the activation state of DCs.

PLP-treatment also correlated with distinct T cell functionality. We've described a distinct PLP-size dependent dichotomy present in T cell polarization. In vivo, we determined that this dichotomy persisted and was characterized by an mPLP driven Th1 systemic response, hallmarked by high amounts of IgG2c, and an nPLP driven regulatory/ Th2 systemic response. These studies were performed at a constant antigen and adjuvant dose; therefore, size was the differentiating factor that drove these responses. One explanation for this lies in the mPLP preference of PDL2+ cells, which make up the majority of the migratory DCs in the skin draining lymph node. According to our in vitro studies, these cells also produce significant amounts of immunostimulatory cytokines, so likely are critical for robust immune response generation. Additionally, the increased regulatory response driven by nPLP treatment could play a role in skewing the T cell bias that may otherwise be more similar to that of mPLPs.

IRF4 has also been shown to be an important regulator of DC differentiation and maturation[203]. It's been implicated in many DC functions as well, including migration[222]. Based on our assessment of IRF4 expression after treatment with PLPs, it's possible than nano-PLPs modulate IRF4 expression in a way that prohibits migration of some cells to the skin-draining lymph nodes, thereby influencing the immune response.

To further characterize this response, we studied signaling along the well-characterized TLR9-NFκB axis to determine where it diverged between cells treated with mPLP or nPLP formulations. We've reported that TLR9 activation by nPLP delivered CpG is delayed significantly compared to mPLP delivery, resulting in subsequent inhibition of early NFκB controlled transcription. We have linked this inhibition to activation of STAT3, a known regulator of inflammation and promoter of IL10. Finally, for the first time, we have demonstrated that ligand density, a particle parameter that is inherently

linked to size, plays an essential role in signaling. By matching the density of CpG on the surface of mPLPs and nPLPs (Max-nPLP), we were able to shift DC programming from the original nPLP tropism.

We hypothesize that this phenomenon could be a function of receptor clustering. TLR2 has been shown to signal efficiency only after clustering[215]. Therefore, it's possible that other receptors in the same family (i.e. TLR9) may respond in a similar way. While more studies would need to be done to test this hypothesis, it is a rational explanation for the ability of ligand density to induce such drastic changes in TLR9-initiated signaling.

In conclusion, this work suggests that physical parameters of pathogens (e.g. size, ligand density, etc) play a influential role in the induction of signaling, whether by dictating receptor clustering or through another unknown mechanism. This can also be extrapolated to pathogen-like particle platforms, expanding the level of control we have over the immune response and significantly influencing immunotherapy design.

Future work will include further characterization of the immunomodulatory potential of ligand density and investigation of the impacts of IRF4 downregulation as a result of PLP treatment. A gradient of ligand densities should be tested to determine the resolution of immunomodulation that can be achieved. Additionally, it should be tested with other TLR agonists to determine if the phenomenon is specific to TLR9's interaction with CpG. In vitro migration studies can be conducted to validate whether IRF4 has an impact on DC mobility. Furthermore, in vivo migration studies using IRF4 knockout mice will provide conclusions about whether PLPs can induce a response without migration of skin-DCs.

6.2 FUTURE CONSIDERATIONS

We feel that our observations are transformative to the immunoengineering and immunity research communities and provide critical steps to furthering our understanding of how innate immune cells interact with vaccine carriers and potentially also pathogens. However, as with most biological research, there were simplifying assumptions made. Therefore, it is important to consider the broad meaning of our observations in the context of real pathogenic infection and biological relevance.

First, while we have broadly defined our two formulations as "virus like" (nano-PLPs) and "bacteria-like" (micro-PLP), it is know that the range of sizes associated with either pathogen is vast. For example, while the large majority of viruses are between 20 and 400 nm in diameter, some viruses, like paramyxovirus, can be up to 14 microns long[223]. However, larger viruses like the paramyxovirus are filamentous and are not modeled properly by our carrier platform in any way. This leaves viruses that are icosahedral in shape, which are closely mimicked by our spherical particles. These viruses generally do not exceed 300nm and this structure describes a large percentage of the viral families significant for human diseases (Table 41-1)[223]. Bacteria are thought to be around one tenth the size of eukaryotic cells, ranging in size from 500nm to around 5 microns[224,225]. Again, our spherical platform does not sufficiently mimic the shape of rod-like (bacillus), spiral or any other unique shapes, but does provide a satisfactory model for the coccus family. This could provide us with valuable information, as cocci and bacilli make up the large majority of infectious bacterial families.

In addition to the limiting factors of shape and size, it is also known that viral and bacterial pathogens carry many danger signals, including many of the pathogen associated molecular patterns (PAMPs) described in Chapter 2. Therefore, it is worth contemplating whether studying a single PAMP as an adjuvant is relevant when mimicking a pathogen. It is our opinion that infectious pathogens are incredibly complex and our understanding of how they trigger and simultaneously evade immune responses

is still not complete. Therefore, it is of the utmost importance that we use the investigation of simplified, individualized mechanisms in parallel with systems level characterization of pathogens themselves to teach the design of pathogen mimicking carriers. Furthermore, we believe that TLR9 agonist CpG is a particularly interesting molecule because it is found in both bacterial and viral DNA[226,227]. Interestingly, one investigator found that CpG motifs were relatively overrepresented in viruses with larger genomes (presumably making them physically larger) when compared to smaller viral genomes, perhaps indicating that our platform is even more qualified to represent larger viral pathogens[228]. Additionally, it has been shown that when CpG is deleted from viral vectors used for gene therapy, that the vectors become immune evasive, perhaps indicating that CpG provides one of the primary stimulatory signals associated many microbial pathogens[229,230]. We believe that all of this evidence motivates our studies, regardless of them being a simplified mimicry of natural pathogens. However, we also appreciate the utility of studying combinations of PAMPs to determine synergistic effects, and those studies are currently ongoing in our lab using the same particle platforms alongside mechanistic studies to investigate signaling associated with the synergy.

The final point that has been raised by others confronted with this research relates to how our system mimics chronic infection, like that of bacterial or viral infection. Because our particles degrade at a moderate speed (within 2-3 weeks of injection) they form a depot under the skin at the site of injection for that period of time. This gives resident innate immune cells sustained access to the particles carrying antigen and adjuvant, aptly imitating a site of injection where virus infected cells or bacteria would replicate over time. We argue that this provides a better model of injection than soluble injections, smaller particles or fast-degrading particles, as all of those are cleared from the site of injection quickly, limiting the modulatory potential of those platforms.

Overall, we feel that the conclusions drawn from the results in this work are not only important to the field of immunoengineering and vaccine design but also represent microbial infection sufficiently to provide relevant knowledge to that community as well.

APPENDIX

A.1. NANO-PLPs DECREASE INDUCED EXPRESSION OF PDL2

Programmed death ligand 2 (PDL2) was originally discovered in the context of immunoregulation, as a ligand for programmed death receptor-1 (PD-1) on T cells[231]. It has been shown to promote T cell anergy and apoptosis and originally thought to play a role in tolerance. Furthermore, cancer cells express PDL2 (and PDL1) to induce activation-induced cell death of cytotoxic T cells and, therefore, immune evasion[232]. Only recently, PDL2 has been used as a characteristic marker for a new subset of DCs (PDL2+CD301b+ dermal DCs) that are skin-resident, migratory and play a significant role in Th2-driven immunity[75,76]. It was also established in this work that PDL2+CD301b+ DCs are phenotypically regulated by IRF4.

In our studies, PDL2+ dermal DCs appear in the draining lymph nodes within 24 hours of injection with fluorescent PLPs and they make up one of the largest populations of migratory CpG carrying DCs. We, therefore, chose this subset as one to study in vitro to characterize interactions between our PLPs and relevant migratory DC subsets. We confirmed that BMDC cultures supplemented with GMCSF and IL4 do indeed have a significant population of PDL2+ cells and that this populations remains intact after treatment with soluble CpG. We also observed that a large portion of these PDL2+ DCs were "induced" PDL2+ cells, that upregulated the expression of PDL2 after mechanical disruption (i.e. replating). These are different from the "spontaneously matured" population described by Gao et al., which express high levels of PDL2 in addition to other maturation markers (e.g. CD86, CD40)[75]. However, we observed that, in samples treated with micro- or nano-PLPs, the population expression of PDL2 was lower than in both untreated and soluble CpG treated cells. Since all samples were derived from the same original BMDC population, we made the assumption that the population of "spontaneously matured" cells. We therefore, deigned an experiment to verify this

assumption and determine the functional difference between spontaneously matured and induced PDL2+ DCs.

A.1.1. MATERIALS AND METHODS

A.1.1.1. Materials

Growth factors (GMCSF, IL4) were purchased from Peprotech (Rocky Hill, NJ). Antibodies against PDL2, CD11c, IL10 and TNFα were purchasesd from Ebioscience (San Diego, CA) and against IL12p70 was from BD Biosciences (Franklin Lakes, NJ).

A.1.1.2. Quantification of spontaneously matured vs induced PDL2+ cells

BMDCs were cultured for 6 days following the protocol described earlier. On Day 6, loosely adherent cells were isolated from original culture dishes and immediately stained with FITC-PDL2 to tag spontaneously matured cells. Cells were washed, replated at the appropriate density and treated with CpG formulations. After 24 hours, cells were collected and stained with PE-PDL2 to stain cells that expressed PDL2 between initial isolation and collection for analysis. Analysis was performed using an Accuri C6 flow cytometer. Double positive cells (FITC+PE+) were labeled spontaneously matured DCs and single positive (PE+) cells were labeled induced PDL2+ DCs.

A.1.1.3. Intracellular staining for immunomodulatory cytokines

Cells that were double stained for PDL2 were fixed and permeabilized using the protocol described previously. Cells were then stained for IL10, IL12p70 and TNFα to determine which subpopulation was responsible for cytokine production. Cells were analyzed using a Accuri C6 flow cytometer.

A.1.2. RESULTS

A.1.2.1. Quantification of spontaneously matured vs induced PDL2+ cells

Figure 66 depicts the strategy used to differentiate spontaneously matured (PDL2.1) and induced (PDL2.2) PDL2+ DCs. Briefly, cells were stained with anti-PDL2-FITC immediately following isolation from original culture plates on Day 6. After washing, cells were replated and treated with CpG formulations. Following a 24 hour incubation period, cells were collected and stained with anti-PDL2-PE to differentiate cells that previously expressed PDL2 from those that gained expression following mechanical disruption (replating).

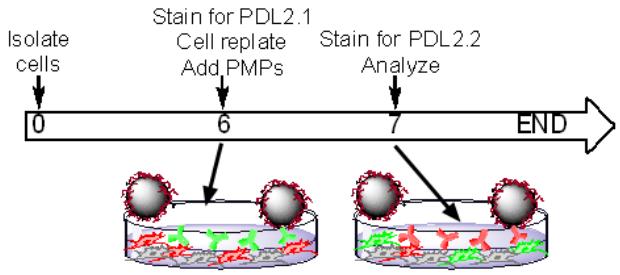

Figure 66: Schematic of spontanously matured (PDL2.1) and induced (PDL2.2) PDL2+ DC analysis strategy.

We found that cells that were untreated responded as previously described, where a large population of cells were induced by mechanical disruption to express PDL2. However, we observed that treatment with PLPs reduced this population, almost completely ablating it after treatment with nano-PLPs (Figure 67).

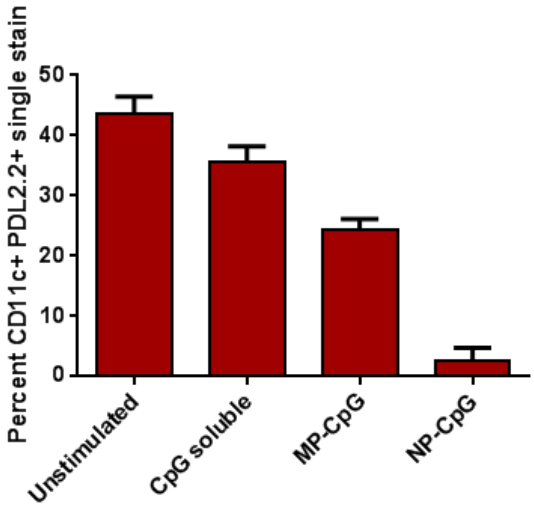

Figure 67: Induced PDL2 expression (PDL2.2+PDL2.1-) was almost completely abrogated in cells that were treated with nano-PLPs.

A.1.2.2. Intracellular staining for immunomodulatory cytokines

Earlier, we established that PDL2+ cells were responsible for production of the majority of immunomodualtory cytokines in these BMDC cultures. We were therefore interested in identifying whether spontaneously matured (PDL2.1) or induced (PDL2.2) cells contributed to this response. We found that spontaneously matured cells, despite previous observations made by Gao et al., were the primary producers of all three immunodulatory cytokines studied (Figure 68).

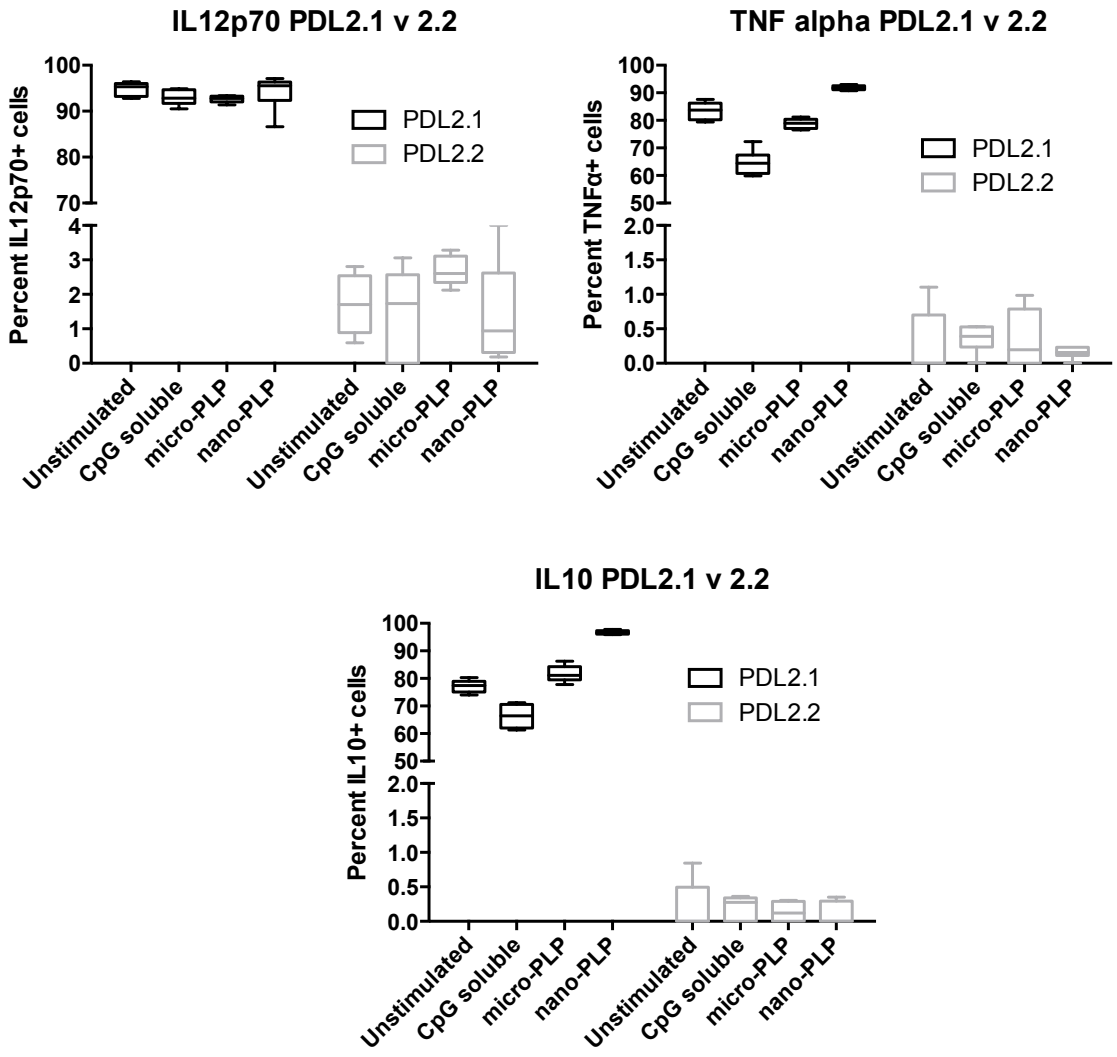

Figure 68: Spontaneously matured PDL2+ DCs (PDL2.1) cells are responsible for cytokine production.

A.1.3. DISCUSSION

The finding that mechanical disruption induced expression of PDL2 in nano-PLP treated samples is a novel finding with interesting implications. Other data we've collected up to this point also may result in an interesting regulatory mechanism. For example, we've already established that cells treated with nano-PLPs do not produce IFNγ, which is known to enhance the expression of PDL2[233]. Additionally, we have also shown that, while IRF4 expression is high in untreated cells in PDL2+ cultures (as described by Gao et al.) that nano-PLP treatment leads to significant downregulation of IRF4 protein content within the cells. This could lead to a variety of functional changes. Bajana et al. demonstrated that IRF4 positively regulates migration of skin-resident DCs[222]. Therefore, it is possible that the downregulation of IRF4 we observe in PDL2+ DCs cultured with nano-PLPs indicates that these cells also migrate less efficiently. This may explain the significant decrease in cells carrying nano-PLPs to the draining lymph node. We hypothesize that this is all linked to the expression of PDL2, however, more experiments need to be conducted to reach any definite conclusions. These include controlled in vitro and in vivo migratory studies as well as PDL2 knock down studies to pinpoint PDL2's role in the above processes.

REFERENCES

1. Naik, S. H. *et al.* Development of plasmacytoid and conventional dendritic cell subtypes from single precursor cells derived in vitro and in vivo. *Nat. Immunol.* **8,** 1217–1226 (2007).

2. Cruz, L. J. *et al.* in *Methods in Enzymology* **509,** 143–163 (Elsevier, 2012).

3. Masihi, K. . Immunomodulatory agents for prophylaxis and therapy of infections. *Int. J. Antimicrob. Agents* **14,** 181–191 (2000).

4. Hilleman, M. R. Vaccines in historic evolution and perspective: a narrative of vaccine discoveries. *Vaccine* **18,** 1436–1447 (2000).

5. Murphy, K. M., Travers, P. & Walport, M. *Janeway's Immunobiology (Immunobiology: The Immune System*. (Garland Science, 2007).

6. Akira, S. Innate immunity and adjuvants. *Philos. Trans. R. Soc. B Biol. Sci.* **366,** 2748–2755 (2011).

7. Steinman, R. M. Decisions About Dendritic Cells: Past, Present, and Future. *Annu. Rev. Immunol.* **30,** 1–22 (2012).

8. Knight, S. C. & Stagg, A. J. Antigen-presenting cell types. *Curr. Opin. Immunol.* **5,** 374–382 (1993).

9. Medzhitov, R. & Janeway, C. A., Jr. Innate immunity: impact on the adaptive immune response. *Curr. Opin. Immunol.* **9,** 4–9 (1997).

10. Alberts, B. *et al. Molecular Biology of the Cell*. (Garland Science, 2002).

11. Berg, J., Tymoczko, J. & Stryer, L. in *Biochemistry* (W H Freeman, 2002).

12. Andrian, U. H. von & Mackay, C. R. T-cell function and migration. Two sides of the same coin. *N. Engl. J. Med.* **343,** 1020–1034 (2000).

13. Zhu, J. & Paul, W. E. CD4 T cells: fates, functions, and faults. *Blood* **112,** 1557–1569 (2008).

14. Chu, V. T., Beller, A., Nguyen, T. T. N., Steinhauser, G. & Berek, C. The Long-Term Survival of Plasma Cells. *Scand. J. Immunol.* **73,** 508–511 (2011).

15. Plotkin, S. A. Correlates of Protection Induced by Vaccination. *Clin. Vaccine Immunol.* **17,** 1055–1065 (2010).

16. Amanna, I. J. & Slifka, M. K. Contributions of humoral and cellular immunity to vaccine-induced protection in humans. *Virology* **411,** 206–215 (2011).

17. Haan, J. M. M. den, Lehar, S. M. & Bevan, M. J. Cd8+ but Not Cd8- Dendritic Cells Cross-Prime Cytotoxic T Cells in Vivo. *J. Exp. Med.* **192,** 1685–1696 (2000).

18. Pooley, J. L., Heath, W. R. & Shortman, K. Cutting Edge: Intravenous Soluble Antigen Is Presented to CD4 T Cells by CD8- Dendritic Cells, but Cross-Presented to CD8 T Cells by CD8+ Dendritic Cells. *J. Immunol.* **166,** 5327–5330 (2001).

19. Belz, G. T. *et al.* The CD8 + Dendritic Cell Is Responsible for Inducing Peripheral Self-Tolerance to Tissue-associated Antigens. *J. Exp. Med.* **196,** 1099–1104 (2002).

20. Radtke, A. J. *et al.* Lymph-Node Resident CD8α+ Dendritic Cells Capture Antigens from Migratory Malaria Sporozoites and Induce CD8+ T Cell Responses. *PLOS Pathog.* **11,** e1004637 (2015).

21. Edwards, A. D. *et al.* Toll-like receptor expression in murine DC subsets: lack of TLR7 expression by CD8 alpha+ DC correlates with unresponsiveness to imidazoquinolines. *Eur. J. Immunol.* **33,** 827–833 (2003).

22. Maldonado-Lopez, R. *et al.* CD8 + and CD8 - Subclasses of Dendritic Cells Direct the Development of Distinct T Helper Cells In Vivo. *J. Exp. Med.* **189,** 587–592

(1999).

23. Cella, M., Facchetti, F., Lanzavecchia, A. & Colonna, M. Plasmacytoid dendritic cells activated by influenza virus and CD40L drive a potent TH1 polarization. *Nat. Immunol.* **1,** 305–310 (2000).

24. Lund, J., Sato, A., Akira, S., Medzhitov, R. & Iwasaki, A. Toll-like Receptor 9-mediated Recognition of Herpes Simplex Virus-2 by Plasmacytoid Dendritic Cells. *J. Exp. Med.* **198,** 513–520 (2003).

25. Collin, M., McGovern, N. & Haniffa, M. Human dendritic cell subsets. *Immunology* **140,** 22–30 (2013).

26. Gregorio, J. *et al.* Plasmacytoid dendritic cells sense skin injury and promote wound healing through type I interferons. *J. Exp. Med.* **207,** 2921–2930 (2010).

27. Valladeau, J. *et al.* Langerin, a novel C-type lectin specific to Langerhans cells, is an endocytic receptor that induces the formation of Birbeck granules. *Immunity* **12,** 71–81 (2000).

28. Heath, W. R. & Carbone, F. R. Dendritic cell subsets in primary and secondary T cell responses at body surfaces. *Nat. Immunol.* **10,** 1237–1244 (2009).

29. Igyártó, B. Z. *et al.* Skin-resident murine dendritic cell subsets promote distinct and opposing antigen-specific T helper cell responses. *Immunity* **35,** 260–272 (2011).

30. Nizza, S. T. & Campbell, J. J. CD11b+ migratory dendritic cells mediate CD8 T cell cross-priming and cutaneous imprinting after topical immunization. *PloS One* **9,** e91054 (2014).

31. Henri, S. *et al.* CD207+ CD103+ dermal dendritic cells cross-present keratinocyte-derived antigens irrespective of the presence of Langerhans cells. *J. Exp. Med.* **207,** 189–206 (2010).

32. del Rio, M.-L., Rodriguez-Barbosa, J.-I., Kremmer, E. & Förster, R. CD103- and CD103+ bronchial lymph node dendritic cells are specialized in presenting and cross-presenting innocuous antigen to CD4+ and CD8+ T cells. *J. Immunol. Baltim. Md 1950* **178,** 6861–6866 (2007).

33. Furio, L., Briotet, I., Journeaux, A., Billard, H. & Péguet-Navarro, J. Human langerhans cells are more efficient than CD14(-)CD1c(+) dermal dendritic cells at priming naive CD4(+) T cells. *J. Invest. Dermatol.* **130,** 1345–1354 (2010).

34. Plantinga, M. *et al.* Conventional and monocyte-derived CD11b(+) dendritic cells initiate and maintain T helper 2 cell-mediated immunity to house dust mite allergen.

Immunity **38,** 322–335 (2013).

35. Guilliams, M. *et al.* Skin-draining lymph nodes contain dermis-derived CD103(-) dendritic cells that constitutively produce retinoic acid and induce Foxp3(+) regulatory T cells. *Blood* **115,** 1958–1968 (2010).

36. Fehres, C. M. *et al.* In situ Delivery of Antigen to DC-SIGN(+)CD14(+) Dermal Dendritic Cells Results in Enhanced CD8(+) T-Cell Responses. *J. Invest. Dermatol.* (2015). doi:10.1038/jid.2015.152

37. Santegoets, S. J. A. M. *et al.* Transcriptional profiling of human skin-resident Langerhans cells and CD1a+ dermal dendritic cells: differential activation states suggest distinct functions. *J. Leukoc. Biol.* **84,** 143–151 (2008).

38. Klechevsky, E. *et al.* Cross-priming CD8+ T cells by targeting antigens to human dendritic cells through DCIR. *Blood* **116,** 1685–1697 (2010).

39. Caux, C. *et al.* CD34+ hematopoietic progenitors from human cord blood differentiate along two independent dendritic cell pathways in response to granulocyte-macrophage colony-stimulating factor plus tumor necrosis factor alpha: II. Functional analysis. *Blood* **90,** 1458–1470 (1997).

40. Stoitzner, P. *et al.* Human skin dendritic cells can be targeted in situ by intradermal injection of antibodies against lectin receptors. *Exp. Dermatol.* **23,** 909–915 (2014).

41. Haniffa, M. *et al.* Human tissues contain CD141hi cross-presenting dendritic cells with functional homology to mouse CD103+ nonlymphoid dendritic cells. *Immunity* **37,** 60–73 (2012).

42. Steinman, R. M. IDENTIFICATION OF A NOVEL CELL TYPE IN PERIPHERAL LYMPHOID ORGANS OF MICE: I. MORPHOLOGY, QUANTITATION, TISSUE DISTRIBUTION. *J. Exp. Med.* **137,** 1142–1162 (1973).

43. Bachem, A. *et al.* Superior antigen cross-presentation and XCR1 expression define human CD11c+CD141+ cells as homologues of mouse CD8+ dendritic cells. *J. Exp. Med.* **207,** 1273–1281 (2010).

44. Segura, E., Durand, M. & Amigorena, S. Similar antigen cross-presentation capacity and phagocytic functions in all freshly isolated human lymphoid organ-resident dendritic cells. *J. Exp. Med.* **210,** 1035–1047 (2013).

45. Allan, R. S. *et al.* Migratory Dendritic Cells Transfer Antigen to a Lymph Node-Resident Dendritic Cell Population for Efficient CTL Priming. *Immunity* **25,** 153–162 (2006).

46. Petersen, T. R., Sika-Paotonu, D., Knight, D. A., Simkins, H. M. A. & Hermans, I. F. Exploiting the Role of Endogenous Lymphoid-Resident Dendritic Cells in the Priming of NKT Cells and CD8+ T Cells to Dendritic Cell-Based Vaccines. *PLoS ONE* **6,** e17657 (2011).

47. Yamazaki, S. *et al.* CD8+CD205+ Splenic Dendritic Cells Are Specialized to Induce Foxp3+ Regulatory T Cells. *J. Immunol.* **181,** 6923–6933 (2008).

48. Iwasaki, A. & Kelsall, B. L. Unique Functions of CD11b+, CD8 +, and Double-Negative Peyer's Patch Dendritic Cells. *J. Immunol.* **166,** 4884–4890 (2001).

49. MacDonald, A. S., Straw, A. D., Bauman, B. & Pearce, E. J. CD8- Dendritic Cell Activation Status Plays an Integral Role in Influencing Th2 Response Development. *J. Immunol.* **167,** 1982–1988 (2001).

50. Gerner, M. Y., Torabi-Parizi, P. & Germain, R. N. Strategically Localized Dendritic Cells Promote Rapid T Cell Responses to Lymph-Borne Particulate Antigens. *Immunity* **42,** 172–185 (2015).

51. Doxsee, C. L. *et al.* The Immune Response Modifier and Toll-Like Receptor 7 Agonist S-27609 Selectively Induces IL-12 and TNF- Production in CD11c+CD11b+CD8- Dendritic Cells. *J. Immunol.* **171,** 1156–1163 (2003).

52. Nakano, H. CD11c+B220+Gr-1+ Cells in Mouse Lymph Nodes and Spleen Display Characteristics of Plasmacytoid Dendritic Cells. *J. Exp. Med.* **194,** 1171–1178 (2001).

53. Wollenberg, A. *et al.* Plasmacytoid Dendritic Cells: A New Cutaneous Dendritic Cell Subset with Distinct Role in Inflammatory Skin Diseases. *J. Invest. Dermatol.* **119,** 1096–1102 (2002).

54. Kadowaki, N. *et al.* Subsets of human dendritic cell precursors express different toll-like receptors and respond to different microbial antigens. *J. Exp. Med.* **194,** 863–869 (2001).

55. Asselin-Paturel, C. Type I interferon dependence of plasmacytoid dendritic cell activation and migration. *J. Exp. Med.* **201,** 1157–1167 (2005).

56. Hornung, V. *et al.* Sequence-specific potent induction of IFN-α by short interfering RNA in plasmacytoid dendritic cells through TLR7. *Nat. Med.* **11,** 263–270 (2005).

57. Gilliet, M., Cao, W. & Liu, Y.-J. Plasmacytoid dendritic cells: sensing nucleic acids in viral infection and autoimmune diseases. *Nat. Rev. Immunol.* **8,** 594–606 (2008).

58. Farkas, L., Beiske, K., Lund-Johansen, F., Brandtzaeg, P. & Jahnsen, F. L. Plasmacytoid Dendritic Cells (Natural Interferon- α/β-Producing Cells) Accumulate

in Cutaneous Lupus Erythematosus Lesions. *Am. J. Pathol.* **159,** 237–243 (2001).

59. L�vgren, T., Eloranta, M.-L., B�ve, U., Alm, G. V. & R�nnblom, L. Induction of interferon-? production in plasmacytoid dendritic cells by immune complexes containing nucleic acid released by necrotic or late apoptotic cells and lupus IgG. *Arthritis Rheum.* **50,** 1861–1872 (2004).

60. Lande, R. *et al.* Neutrophils Activate Plasmacytoid Dendritic Cells by Releasing Self-DNA-Peptide Complexes in Systemic Lupus Erythematosus. *Sci. Transl. Med.* **3,** 73ra19–73ra19 (2011).

61. Gilliet, M. Generation of Human CD8 T Regulatory Cells by CD40 Ligand-activated Plasmacytoid Dendritic Cells. *J. Exp. Med.* **195,** 695–704 (2002).

62. Jego, G. *et al.* Plasmacytoid Dendritic Cells Induce Plasma Cell Differentiation through Type I Interferon and Interleukin 6. *Immunity* **19,** 225–234 (2003).

63. de Heer, H. J. Essential Role of Lung Plasmacytoid Dendritic Cells in Preventing Asthmatic Reactions to Harmless Inhaled Antigen. *J. Exp. Med.* **200,** 89–98 (2004).

64. Moseman, E. A. *et al.* Human Plasmacytoid Dendritic Cells Activated by CpG Oligodeoxynucleotides Induce the Generation of CD4+CD25+ Regulatory T Cells.

J. Immunol. **173,** 4433–4442 (2004).

65. Ito, T. *et al.* Plasmacytoid dendritic cells prime IL-10-producing T regulatory cells by inducible costimulator ligand. *J. Exp. Med.* **204,** 105–115 (2007).

66. Valladeau, J. *et al.* Identification of mouse langerin/CD207 in Langerhans cells and some dendritic cells of lymphoid tissues. *J. Immunol. Baltim. Md 1950* **168,** 782–792 (2002).

67. Merad, M., Sathe, P., Helft, J., Miller, J. & Mortha, A. The dendritic cell lineage: ontogeny and function of dendritic cells and their subsets in the steady state and the inflamed setting. *Annu. Rev. Immunol.* **31,** 563–604 (2013).

68. Chorro, L. *et al.* Langerhans cell (LC) proliferation mediates neonatal development, homeostasis, and inflammation-associated expansion of the epidermal LC network. *J. Exp. Med.* **206,** 3089–3100 (2009).

69. Kaplan, D. H. In vivo function of Langerhans cells and dermal dendritic cells. *Trends Immunol.* **31,** 446–451 (2010).

70. Guilliams, M. *et al.* From skin dendritic cells to a simplified classification of human and mouse dendritic cell subsets. *Eur. J. Immunol.* **40,** 2089–2094 (2010).

71. Broggi, A., Zanoni, I. & Granucci, F. Migratory conventional dendritic cells in the induction of peripheral T cell tolerance. *J. Leukoc. Biol.* **94,** 903–911 (2013).

72. Sung, S.-S. J. *et al.* A Major Lung CD103 (αE)-β7 Integrin-Positive Epithelial Dendritic Cell Population Expressing Langerin and Tight Junction Proteins. *J. Immunol.* **176,** 2161–2172 (2006).

73. King, I. L., Kroenke, M. A. & Segal, B. M. GM-CSF-dependent, CD103+ dermal dendritic cells play a critical role in Th effector cell differentiation after subcutaneous immunization. *J. Exp. Med.* **207,** 953–961 (2010).

74. Malissen, B., Tamoutounour, S. & Henri, S. The origins and functions of dendritic cells and macrophages in the skin. *Nat. Rev. Immunol.* **14,** 417–428 (2014).

75. Gao, Y. *et al.* Control of T Helper 2 Responses by Transcription Factor IRF4-Dependent Dendritic Cells. *Immunity* **39,** 722–732 (2013).

76. Kumamoto, Y. *et al.* CD301b+ Dermal Dendritic Cells Drive T Helper 2 Cell-Mediated Immunity. *Immunity* **39,** 733–743 (2013).

77. Idoyaga, J. *et al.* Specialized role of migratory dendritic cells in peripheral tolerance induction. *J. Clin. Invest.* **123,** 844–854 (2013).

78. Keijzer, C. *et al.* PLGA nanoparticles enhance the expression of retinaldehyde dehydrogenase enzymes in dendritic cells and induce FoxP3(+) T-cells in vitro. *J. Control. Release Off. J. Control. Release Soc.* **168,** 35–40 (2013).

79. Van Gool, S. W., Vandenberghe, P., Boer, M. de & Ceuppens, J. L. CD80, CD86 and CD40 Provide Accessory Signals in a Multiple-Step T-Cell Activation Model. *Immunol. Rev.* **153,** 47–83 (1996).

80. Jaffar, Z. H. *et al.* Essential Role for Both CD80 and CD86 Costimulation, But Not CD40 Interactions, in Allergen-Induced Th2 Cytokine Production from Asthmatic Bronchial Tissue: Role for αβ, But Not γδ, T Cells. *J. Immunol.* **163,** 6283–6291 (1999).

81. Kuklina, E. M. Molecular mechanisms of T-cell anergy. *Biochem. Mosc.* **78,** 144–156 (2013).

82. Hopp, A.-K., Rupp, A. & Lukacs-Kornek, V. Self-Antigen Presentation by Dendritic Cells in Autoimmunity. *Front. Immunol.* **5,** (2014).

83. Gunn, M. D. *et al.* Mice Lacking Expression of Secondary Lymphoid Organ Chemokine Have Defects in Lymphocyte Homing and Dendritic Cell Localization. *J. Exp. Med.* **189,** 451–460 (1999).

84. MartIn-Fontecha, A. *et al.* Regulation of dendritic cell migration to the draining lymph node: impact on T lymphocyte traffic and priming. *J. Exp. Med.* **198,** 615–621 (2003).

85. Yoshida, M. & Babensee, J. E. Poly(lactic-co-glycolic acid) enhances maturation of human monocyte-derived dendritic cells. *J. Biomed. Mater. Res. A* **71,** 45–54 (2004).

86. Patel, D. D. *et al.* Chemokines Have Diverse Abilities to Form Solid Phase Gradients. *Clin. Immunol.* **99,** 43–52 (2001).

87. Swartz, M. A., Hubbell, J. A. & Reddy, S. T. Lymphatic drainage function and its immunological implications: from dendritic cell homing to vaccine design. *Semin. Immunol.* **20,** 147–156 (2008).

88. Baratin, M. *et al.* Homeostatic NF-κB Signaling in Steady-State Migratory Dendritic Cells Regulates Immune Homeostasis and Tolerance. *Immunity* **42,** 627–639 (2015).

89. Singh, M. & O'Hagan, D. Advances in vaccine adjuvants. *Nat. Biotechnol.* **17,** 1075–1081 (1999).

90. Akira, S., Takeda, K. & Kaisho, T. Toll-like receptors: critical proteins linking innate and acquired immunity. *Nat. Immunol.* **2,** 675–680 (2001).

91. Medzhitov, R. TOLL-LIKE RECEPTORS AND INNATE IMMUNITY. *Nat. Rev. Immunol.* **1,** 135–145 (2001).

92. Takeda, K. Toll-like receptors in innate immunity. *Int. Immunol.* **17,** 1–14 (2004).

93. Kawai, T. & Akira, S. The role of pattern-recognition receptors in innate immunity: update on Toll-like receptors. *Nat. Immunol.* **11,** 373–384 (2010).

94. Pietrocola, G. *et al.* Toll-like receptors (TLRs) in innate immune defense against Staphylococcus aureus. *Int. J. Artif. Organs* **34,** 799–810 (2011).

95. Sethi, S. & Chakraborty, T. Role of TLR- / NLR-signaling and the associated cytokines involved in recruitment of neutrophils in murine models of Staphylococcus aureus infection. *Virulence* **2,** 316–328 (2011).

96. Burns, K. *et al.* MyD88, an adapter protein involved in interleukin-1 signaling. *J. Biol. Chem.* **273,** 12203–12209 (1998).

97. Takeuchi, O. & Akira, S. Toll-like receptors; their physiological role and signal transduction system. *Int. Immunopharmacol.* **1,** 625–635 (2001).

98. Ghosh, S., May, M. J. & Kopp, E. B. NF-kappa B and Rel proteins: evolutionarily conserved mediators of immune responses. *Annu. Rev. Immunol.* **16,** 225–260 (1998).

99. Honda, K. Role of a transductional-transcriptional processor complex involving MyD88 and IRF-7 in Toll-like receptor signaling. *Proc. Natl. Acad. Sci.* **101,** 15416–15421 (2004).

100. Kawai, T. & Akira, S. Signaling to NF-κB by Toll-like receptors. *Trends Mol. Med.* **13,** 460–469 (2007).

101. Yamamoto, M. *et al.* Role of Adaptor TRIF in the MyD88-Independent Toll-Like Receptor Signaling Pathway. *Science* **301,** 640–643 (2003).

102. Dunne, A., Marshall, N. A. & Mills, K. H. TLR based therapeutics. *Curr. Opin. Pharmacol.* **11,** 404–411 (2011).

103. Higgins, S. C. & Mills, K. H. G. TLR, NLR Agonists, and Other Immune Modulators as Infectious Disease Vaccine Adjuvants. *Curr. Infect. Dis. Rep.* **12,** 4–

12 (2010).

104. Martinon, F. & Tschopp, J. NLRs join TLRs as innate sensors of pathogens. *Trends Immunol.* **26,** 447–454 (2005).

105. Kabelitz, D. & Medzhitov, R. Innate immunity — cross-talk with adaptive immunity through pattern recognition receptors and cytokines. *Curr. Opin. Immunol.* **19,** 1–3 (2007).

106. Osorio, F. & Reis e Sousa, C. Myeloid C-type Lectin Receptors in Pathogen Recognition and Host Defense. *Immunity* **34,** 651–664 (2011).

107. Napolitani, G., Rinaldi, A., Bertoni, F., Sallusto, F. & Lanzavecchia, A. Selected Toll-like receptor agonist combinations synergistically trigger a T helper type 1–polarizing program in dendritic cells. *Nat. Immunol.* **6,** 769–776 (2005).

108. Ghosh, T. K. *et al.* TLR–TLR cross talk in human PBMC resulting in synergistic and antagonistic regulation of type-1 and 2 interferons, IL-12 and TNF-α. *Int. Immunopharmacol.* **7,** 1111–1121 (2007).

109. O'Hagan, D. T. & Singh, M. Microparticles as vaccine adjuvants and delivery systems. *Expert Rev. Vaccines* **2,** 269–283 (2003).

110. Jones, K. S. Biomaterials as vaccine adjuvants. *Biotechnol. Prog.* **24,** 807–814 (2008).

111. De Temmerman, M.-L. *et al.* Particulate vaccines: on the quest for optimal delivery and immune response. *Drug Discov. Today* **16,** 569–582 (2011).

112. O'Hagan, D. T., Palin, K., Davis, S. S., Artursson, P. & Sjöholm, I. Microparticles as potentially orally active immunological adjuvants. *Vaccine* **7,** 421–424 (1989).

113. Tacken, P. J. *et al.* Targeted delivery of TLR ligands to human and mouse dendritic cells strongly enhances adjuvanticity. *Blood* **118,** 6836–6844 (2011).

114. Liu, H. *et al.* Structure-based programming of lymph-node targeting in molecular vaccines. *Nature* **507,** 519–522 (2014).

115. Hanson, M. C. *et al.* Nanoparticulate STING agonists are potent lymph node–targeted vaccine adjuvants. *J. Clin. Invest.* **125,** 2532–2546 (2015).

116. Mui, B., Raney, S. G., Semple, S. C. & Hope, M. J. Immune stimulation by a CpG-containing oligodeoxynucleotide is enhanced when encapsulated and delivered in lipid particles. *J. Pharmacol. Exp. Ther.* **298,** 1185–1192 (2001).

117. Hubbell, J. A., Thomas, S. N. & Swartz, M. A. Materials engineering for immunomodulation. *Nature* **462,** 449–460 (2009).

118. Lin, M.-L., Zhan, Y., Villadangos, J. A. & Lew, A. M. The cell biology of cross-presentation and the role of dendritic cell subsets. *Immunol. Cell Biol.* **86,** 353–362 (2008).

119. Shedlock, D. J. & Weiner, D. B. DNA vaccination: antigen presentation and the induction of immunity. *J. Leukoc. Biol.* **68,** 793–806 (2000).

120. Chiellini, F., Piras, A. M., Errico, C. & Chiellini, E. Micro/nanostructured polymeric systems for biomedical and pharmaceutical applications. *Nanomed.* **3,** 367–393 (2008).

121. Cui, Z., Oyewumi, M. O. & Kumar, A. Nano-microparticles as immune adjuvants: correlating particle sizes and the resultant immune responses. *Expert Rev. Vaccines* **9,** 1095–1107 (2010).

122. Chadwick, S., Kriegel, C. & Amiji, M. Nanotechnology solutions for mucosal immunization. *Adv. Drug Deliv. Rev.* **62,** 394–407 (2010).

123. Samuelsen, M., Nygaard, U. C. & Løvik, M. Particle Size Determines Activation of the Innate Immune System in the Lung. *Scand. J. Immunol.* **69,** 421–428 (2009).

124. Mottram, P. L. *et al.* Type 1 and 2 immunity following vaccination is influenced by nanoparticle size: formulation of a model vaccine for respiratory syncytial virus. *Mol. Pharm.* **4,** 73–84 (2007).

125. Xiang, S. D. *et al.* Pathogen recognition and development of particulate vaccines: does size matter? *Methods San Diego Calif* **40,** 1–9 (2006).

126. Gutierro, I., Hernández, R. ., Igartua, M., Gascón, A. . & Pedraz, J. . Size dependent immune response after subcutaneous, oral and intranasal administration of BSA loaded nanospheres. *Vaccine* **21,** 67–77 (2002).

127. Desai, M. P., Labhasetwar, V., Amidon, G. L. & Levy, R. J. Gastrointestinal uptake of biodegradable microparticles: effect of particle size. *Pharm. Res.* **13,** 1838–1845 (1996).

128. Reddy, S. T., Rehor, A., Schmoekel, H. G., Hubbell, J. A. & Swartz, M. A. In vivo targeting of dendritic cells in lymph nodes with poly(propylene sulfide) nanoparticles. *J. Controlled Release* **112,** 26–34 (2006).

129. Cruz, L. J. *et al.* Targeted PLGA nano- but not microparticles specifically deliver antigen to human dendritic cells via DC-SIGN in vitro. *J. Controlled Release* **144,** 118–126 (2010).

130. Katare, Y. K., Muthukumaran, T. & Panda, A. K. Influence of particle size, antigen load, dose and additional adjuvant on the immune response from antigen loaded PLA microparticles. *Int. J. Pharm.* **301,** 149–160 (2005).

131. Kohli, A. K. & Alpar, H. O. Potential use of nanoparticles for transcutaneous vaccine delivery: effect of particle size and charge. *Int. J. Pharm.* **275,** 13–17 (2004).

132. Foged, C., Brodin, B., Frokjaer, S. & Sundblad, A. Particle size and surface charge affect particle uptake by human dendritic cells in an in vitro model. *Int. J. Pharm.* **298,** 315–322 (2005).

133. Champion, J. A., Walker, A. & Mitragotri, S. Role of Particle Size in Phagocytosis of Polymeric Microspheres. *Pharm. Res.* **25,** 1815–1821 (2008).

134. Reddy, S. T. *et al.* Exploiting lymphatic transport and complement activation in nanoparticle vaccines. *Nat. Biotechnol.* **25,** 1159–1164 (2007).

135. Lagrange, P. H. INFLUENCE OF DOSE AND ROUTE OF ANTIGEN INJECTION ON THE IMMUNOLOGICAL INDUCTION OF T CELLS. *J. Exp. Med.* **139,** 528–542 (1974).

136. Hosken, N. A. The effect of antigen dose on CD4+ T helper cell phenotype development in a T cell receptor-alpha beta-transgenic model. *J. Exp. Med.* **182,** 1579–1584 (1995).

137. Iezzi, G., Karjalainen, K. & Lanzavecchia, A. The Duration of Antigenic Stimulation Determines the Fate of Naive and Effector T Cells. *Immunity* **8,** 89–95 (1998).

138. Rees, W. *et al.* An inverse relationship between T cell receptor affinity and antigen dose during CD4+ T cell responses in vivo and in vitro. *Proc. Natl. Acad. Sci.* **96,** 9781–9786 (1999).

139. Babensee, J. E. & Paranjpe, A. Differential levels of dendritic cell maturation on different biomaterials used in combination products. *J. Biomed. Mater. Res. A* **74,** 503–510 (2005).

140. Bandyopadhyay, A., Fine, R. L., Demento, S., Bockenstedt, L. K. & Fahmy, T. M. The impact of nanoparticle ligand density on dendritic-cell targeted vaccines.

Biomaterials **32,** 3094–3105 (2011).

141. Iwasaki, A. & Medzhitov, R. Toll-like receptor control of the adaptive immune responses. *Nat. Immunol.* **5,** 987–995 (2004).

142. Platanias, L. C. Mechanisms of type-I- and type-II-interferon-mediated signalling. *Nat. Rev. Immunol.* **5,** 375–386 (2005).

143. Kawai, T. & Akira, S. Innate immune recognition of viral infection. *Nat. Immunol.* **7,** 131–137 (2006).

144. Iwasaki, A. & Medzhitov, R. Regulation of Adaptive Immunity by the Innate Immune System. *Science* **327,** 291–295 (2010).

145. Leleux, J. & Roy, K. Micro and Nanoparticle-Based Delivery Systems for Vaccine Immunotherapy: An Immunological and Materials Perspective. *Adv. Healthc. Mater.* **2,** 72–94 (2013).

146. Lewis, J. S., Roy, K. & Keselowsky, B. G. Materials that harness and modulate the immune system. *MRS Bull.* **39,** 25–34 (2014).

147. Purwada, A., Roy, K. & Singh, A. Engineering vaccines and niches for immune modulation. *Acta Biomater.* **10,** 1728–1740 (2014).

148. Inaba, K. *et al.* Generation of large numbers of dendritic cells from mouse bone marrow cultures supplemented with granulocyte/macrophage colony-stimulating factor. *J. Exp. Med.* **176,** 1693–1702 (1992).

149. Hochrein, H. *et al.* Interleukin (IL)-4 is a major regulatory cytokine governing bioactive IL-12 production by mouse and human dendritic cells. *J. Exp. Med.* **192,** 823–833 (2000).

150. Yin, S.-Y., Wang, C.-Y. & Yang, N.-S. Interleukin-4 enhances trafficking and functional activities of GM-CSF-stimulated mouse myeloid-derived dendritic cells at late differentiation stage. *Exp. Cell Res.* **317,** 2210–2221 (2011).

151. Helft, J. *et al.* GM-CSF Mouse Bone Marrow Cultures Comprise a Heterogeneous Population of CD11c+MHCII+ Macrophages and Dendritic Cells. *Immunity* **42,** 1197–1211 (2015).

152. Ito, T., Wang, Y.-H. & Liu, Y.-J. Plasmacytoid dendritic cell precursors/type I interferon-producing cells sense viral infection by Toll-like receptor (TLR) 7 and TLR9. *Springer Semin. Immunopathol.* **26,** 221–229 (2004).

153. Bjorck, P. Isolation and characterization of plasmacytoid dendritic cells from Flt3 ligand and granulocyte-macrophage colony-stimulating factor-treated mice. *Blood* **98,** 3520–3526 (2001).

154. Brasel, K., De Smedt, T., Smith, J. L. & Maliszewski, C. R. Generation of murine dendritic cells from flt3-ligand-supplemented bone marrow cultures. *Blood* **96,** 3029–3039 (2000).

155. Gilliet, M. *et al.* The development of murine plasmacytoid dendritic cell precursors is differentially regulated by FLT3-ligand and granulocyte/macrophage colony-stimulating factor. *J. Exp. Med.* **195,** 953–958 (2002).

156. Kasturi, S. P., Sachaphibulkij, K. & Roy, K. Covalent conjugation of polyethyleneimine on biodegradable microparticles for delivery of plasmid DNA vaccines. *Biomaterials* **26,** 6375–6385 (2005).

157. Singh, A. *et al.* Efficient modulation of T-cell response by dual-mode, single-carrier delivery of cytokine-targeted siRNA and DNA vaccine to antigen-presenting cells. *Mol. Ther. J. Am. Soc. Gene Ther.* **16,** 2011–2021 (2008).

158. Pradhan, P. *et al.* The effect of combined IL10 siRNA and CpG ODN as pathogen-mimicking microparticles on Th1/Th2 cytokine balance in dendritic cells and

protective immunity against B cell lymphoma. *Biomaterials* **35,** 5491–5504 (2014).

159. Jiang, A. *et al.* Disruption of E-cadherin-mediated adhesion induces a functionally distinct pathway of dendritic cell maturation. *Immunity* **27,** 610–624 (2007).

160. Thompson, A. G. & Thomas, R. Induction of immune tolerance by dendritic cells: Implications for preventative and therapeutic immunotherapy of autoimmune disease. *Immunol. Cell Biol.* **80,** 509–519 (2002).

161. Perona-Wright, G. *et al.* Distinct sources and targets of IL-10 during dendritic cell-driven Th1 and Th2 responsesin vivo. *Eur. J. Immunol.* **36,** 2367–2375 (2006).

162. Huang, H. *et al.* Regulatory dendritic cell expression of MHCII and IL-10 are jointly requisite for induction of tolerance in a murine model of OVA-asthma. *Allergy* **68,** 1126–1135 (2013).

163. Lanzavecchia, A. & Sallusto, F. The instructive role of dendritic cells on T cell responses: lineages, plasticity and kinetics. *Curr. Opin. Immunol.* **13,** 291–298 (2001).

164. Krummen, M. *et al.* Release of IL-12 by dendritic cells activated by TLR ligation is dependent on MyD88 signaling, whereas TRIF signaling is indispensable for TLR

synergy. *J. Leukoc. Biol.* **88,** 189–199 (2010).

165. Duramad, O. IL-10 regulates plasmacytoid dendritic cell response to CpG-containing immunostimulatory sequences. *Blood* **102,** 4487–4492 (2003).

166. Boonstra, A. *et al.* Macrophages and Myeloid Dendritic Cells, but Not Plasmacytoid Dendritic Cells, Produce IL-10 in Response to MyD88- and TRIF-Dependent TLR Signals, and TLR-Independent Signals. *J. Immunol.* **177,** 7551–7558 (2006).

167. Hervas-Stubbs, S. *et al.* Direct Effects of Type I Interferons on Cells of the Immune System. *Clin. Cancer Res.* **17,** 2619–2627 (2011).

168. Pan, J. *et al.* Interferon-gamma is an autocrine mediator for dendritic cell maturation. *Immunol. Lett.* **94,** 141–151 (2004).

169. Snapper, C. & Paul, W. Interferon-gamma and B cell stimulatory factor-1 reciprocally regulate Ig isotype production. *Science* **236,** 944–947 (1987).

170. Eisenthal, A., Cameron, R. B. & Rosenberg, S. A. Induction of antibody-dependent cellular cytotoxicity in vivo by IFN-alpha and its antitumor efficacy against established B16 melanoma liver metastases when combined with specific anti-B16 monoclonal antibody. *J. Immunol. Baltim. Md 1950* **144,** 4463–4471 (1990).

171. Severinson, E. *et al.* Interleukin 4 (IgG1 induction factor): a multifunctional lymphokine acting also on T cells. *Eur. J. Immunol.* **17,** 67–72 (1987).

172. Boyman, O. & Sprent, J. The role of interleukin-2 during homeostasis and activation of the immune system. *Nat. Rev. Immunol.* (2012). doi:10.1038/nri3156

173. Maldonado, R. A. & Andrian, U. H. von. in *Advances in Immunology* **108,** 111–165 (Elsevier, 2010).

174. Pai Kasturi, S. *et al.* Prophylactic anti-tumor effects in a B cell lymphoma model with DNA vaccines delivered on polyethylenimine (PEI) functionalized PLGA microparticles. *J. Controlled Release* **113,** 261–270 (2006).

175. Singh, A., Suri, S. & Roy, K. In-situ crosslinking hydrogels for combinatorial delivery of chemokines and siRNA–DNA carrying microparticles to dendritic cells. *Biomaterials* **30,** 5187–5200 (2009).

176. Oyewumi, M. O., Kumar, A. & Cui, Z. Nano-microparticles as immune adjuvants: correlating particle sizes and the resultant immune responses. *Expert Rev. Vaccines* **9,** 1095–1107 (2010).

177. Bachmann, M. F. & Jennings, G. T. Vaccine delivery: a matter of size, geometry, kinetics and molecular patterns. *Nat. Rev. Immunol.* **10,** 787–796 (2010).

178. Bjorck, P., Leong, H. X. & Engleman, E. G. Plasmacytoid Dendritic Cell Dichotomy: Identification of IFN- Producing Cells as a Phenotypically and Functionally Distinct Subset. *J. Immunol.* **186,** 1477–1485 (2011).

179. Platt, A. M. & Randolph, G. J. in *Advances in Immunology* **120,** 51–68 (Elsevier, 2013).

180. Tomura, M. *et al.* Tracking and quantification of dendritic cell migration and antigen trafficking between the skin and lymph nodes. *Sci. Rep.* **4,** 6030 (2014).

181. Jiao, Z. *et al.* The Closely Related CD103+ Dendritic Cells (DCs) and Lymphoid-Resident CD8+ DCs Differ in Their Inflammatory Functions. *PLoS ONE* **9,** e91126 (2014).

182. Biron, C. A., Nguyen, K. B., Pien, G. C., Cousens, L. P. & Salazar-Mather, T. P. NATURAL KILLER CELLS IN ANTIVIRAL DEFENSE: Function and Regulation by Innate Cytokines. *Annu. Rev. Immunol.* **17,** 189–220 (1999).

183. Topham, N. J. & Hewitt, E. W. Natural killer cell cytotoxicity: how do they pull the trigger? *Immunology* **128,** 7–15 (2009).

184. Singh, A. K. Natural Killer T Cell Activation Protects Mice Against Experimental Autoimmune Encephalomyelitis. *J. Exp. Med.* **194,** 1801–1811 (2001).

185. Kitamura, H. *et al.* The Natural Killer T (NKT) Cell Ligand -Galactosylceramide Demonstrates Its Immunopotentiating Effect by Inducing Interleukin (IL)-12 Production by Dendritic Cells and IL-12 Receptor Expression on NKT Cells. *J. Exp. Med.* **189,** 1121–1128 (1999).

186. Jung, S. *et al.* In Vivo Depletion of CD11c+ Dendritic Cells Abrogates Priming of CD8+ T Cells by Exogenous Cell-Associated Antigens. *Immunity* **17,** 211–220 (2002).

187. Kapsenberg, M. L. Dendritic-cell control of pathogen-driven T-cell polarization. *Nat. Rev. Immunol.* **3,** 984–993 (2003).

188. Guilliams, M. *et al.* From skin dendritic cells to a simplified classification of human and mouse dendritic cell subsets. *Eur. J. Immunol.* **40,** 2089–2094 (2010).

189. Keijzer, C. *et al.* PLGA nanoparticles enhance the expression of retinaldehyde dehydrogenase enzymes in dendritic cells and induce FoxP3(+) T-cells in vitro. *J.*

Control. Release Off. J. Control. Release Soc. **168,** 35–40 (2013).

190. Kawai, T. *et al.* Interferon-α induction through Toll-like receptors involves a direct interaction of IRF7 with MyD88 and TRAF6. *Nat. Immunol.* **5,** 1061–1068 (2004).

191. Honda, K. *et al.* IRF-7 is the master regulator of type-I interferon-dependent immune responses. *Nature* **434,** 772–777 (2005).

192. Kaisho, T. & Akira, S. Dendritic-cell function in Toll-like receptor- and MyD88-knockout mice. *Trends Immunol.* **22,** 78–83 (2001).

193. Hemmi, H., Kaisho, T., Takeda, K. & Akira, S. The Roles of Toll-Like Receptor 9, MyD88, and DNA-Dependent Protein Kinase Catalytic Subunit in the Effects of Two Distinct CpG DNAs on Dendritic Cell Subsets. *J. Immunol.* **170,** 3059–3064 (2003).

194. Fredriksson, S. *et al.* Protein detection using proximity-dependent DNA ligation assays. *Nat. Biotechnol.* **20,** 473–477 (2002).

195. Söderberg, O. *et al.* Characterizing proteins and their interactions in cells and tissues using the in situ proximity ligation assay. *Methods* **45,** 227–232 (2008).

196. Weibrecht, I. *et al.* Proximity ligation assays: a recent addition to the proteomics toolbox. *Expert Rev. Proteomics* **7,** 401–409 (2010).

197. Alexopoulou, L., Holt, A. C., Medzhitov, R. & Flavell, R. A. Recognition of double-stranded RNA and activation of NF-kappaB by Toll-like receptor 3. *Nature* **413,** 732–738 (2001).

198. Yoshimura, S. Effective antigen presentation by dendritic cells is NF-kappaB dependent: coordinate regulation of MHC, co-stimulatory molecules and cytokines. *Int. Immunol.* **13,** 675–683 (2001).

199. Tak, P. P. & Firestein, G. S. NF-κB: a key role in inflammatory diseases. *J. Clin. Invest.* **107,** 7–11 (2001).

200. Melillo, J. A. *et al.* Dendritic Cell (DC)-Specific Targeting Reveals Stat3 as a Negative Regulator of DC Function. *J. Immunol.* **184,** 2638–2645 (2010).

201. Benkhart, E. M., Siedlar, M., Wedel, A., Werner, T. & Ziegler-Heitbrock, H. W. L. Role of Stat3 in Lipopolysaccharide-Induced IL-10 Gene Expression. *J. Immunol.* **165,** 1612–1617 (2000).

202. Murray, P. Understanding and exploiting the endogenous interleukin-10/STAT3-mediated anti-inflammatory response. *Curr. Opin. Pharmacol.* **6,** 379–386 (2006).

203. Tamura, T. *et al.* IFN regulatory factor-4 and -8 govern dendritic cell subset development and their functional diversity. *J. Immunol. Baltim. Md 1950* **174,** 2573–2581 (2005).

204. Honda, K. & Taniguchi, T. IRFs: master regulators of signalling by Toll-like receptors and cytosolic pattern-recognition receptors. *Nat. Rev. Immunol.* **6,** 644–658 (2006).

205. Williams, J. W. *et al.* Transcription factor IRF4 drives dendritic cells to promote Th2 differentiation. *Nat. Commun.* **4,** (2013).

206. Vander Lugt, B. *et al.* Transcriptional programming of dendritic cells for enhanced MHC class II antigen presentation. *Nat. Immunol.* **15,** 161–167 (2013).

207. Samarasinghe, R. *et al.* Induction of an anti-inflammatory cytokine, IL-10, in dendritic cells after toll-like receptor signaling. *J. Interferon Cytokine Res. Off. J. Int. Soc. Interferon Cytokine Res.* **26,** 893–900 (2006).

208. Pallandre, J.-R. *et al.* Role of STAT3 in CD4+CD25+FOXP3+ regulatory lymphocyte generation: implications in graft-versus-host disease and antitumor

immunity. *J. Immunol. Baltim. Md 1950* **179,** 7593–7604 (2007).

209. Liu, L. Induction of Th2 cell differentiation in the primary immune response: dendritic cells isolated from adherent cell culture treated with IL-10 prime naive CD4+ T cells to secrete IL-4. *Int. Immunol.* **10,** 1017–1026 (1998).

210. Saraiva, M. & O'Garra, A. The regulation of IL-10 production by immune cells. *Nat. Rev. Immunol.* **10,** 170–181 (2010).

211. Brown, J., Wang, H., Hajishengallis, G. N. & Martin, M. TLR-signaling Networks: An Integration of Adaptor Molecules, Kinases, and Cross-talk. *J. Dent. Res.* **90,** 417–427 (2011).

212. Gunzl, P. *et al.* Anti-inflammatory properties of the PI3K pathway are mediated by IL-10/DUSP regulation. *J. Leukoc. Biol.* **88,** 1259–1269 (2010).

213. Vogt, P. K. & Hart, J. R. PI3K and STAT3: A New Alliance. *Cancer Discov.* **1,** 481–486 (2011).

214. Ziegler-Heitbrock, L. *et al.* IFN- Induces the Human IL-10 Gene by Recruiting Both IFN Regulatory Factor 1 and Stat3. *J. Immunol.* **171,** 285–290 (2003).

215. Inoue, M. & Shinohara, M. L. Clustering of Pattern Recognition Receptors for Fungal Detection. *PLoS Pathog.* **10,** e1003873 (2014).

216. Wagner, H. New vistas on TLR9 activation. *Eur. J. Immunol.* **41,** 2814–2816 (2011).

217. Ohto, U. *et al.* Structural basis of CpG and inhibitory DNA recognition by Toll-like receptor 9. *Nature* **520,** 702–705 (2015).

218. Hoentjen, F. STAT3 regulates NF- B recruitment to the IL-12p40 promoter in dendritic cells. *Blood* **105,** 689–696 (2005).

219. Grivennikov, S. I. & Karin, M. Dangerous liaisons: STAT3 and NF-κB collaboration and crosstalk in cancer. *Cytokine Growth Factor Rev.* **21,** 11–19 (2010).

220. Oeckinghaus, A., Hayden, M. S. & Ghosh, S. Crosstalk in NF-κB signaling pathways. *Nat. Immunol.* **12,** 695–708 (2011).

221. Hanagata, N. Structure-dependent immunostimulatory effect of CpG oligodeoxynucleotides and their delivery system. *Int. J. Nanomedicine* 2181 (2012). doi:10.2147/IJN.S30197

222. Bajaña, S., Roach, K., Turner, S., Paul, J. & Kovats, S. IRF4 promotes cutaneous dendritic cell migration to lymph nodes during homeostasis and inflammation. *J. Immunol. Baltim. Md 1950* **189,** 3368–3377 (2012).

223. Gelderblom, H. R. in *Medical Microbiology* (ed. Baron, S.) (University of Texas Medical Branch at Galveston, 1996). at <http://www.ncbi.nlm.nih.gov/books/NBK8174/>

224. Portillo, M. C., Leff, J. W., Lauber, C. L. & Fierer, N. Cell Size Distributions of Soil Bacterial and Archaeal Taxa. *Appl. Environ. Microbiol.* **79,** 7610–7617 (2013).

225. Schulz, H. N. & Jorgensen, B. B. Big bacteria. *Annu. Rev. Microbiol.* **55,** 105–137 (2001).

226. Klinman, D. M., Yi, A. K., Beaucage, S. L., Conover, J. & Krieg, A. M. CpG motifs present in bacteria DNA rapidly induce lymphocytes to secrete interleukin 6, interleukin 12, and interferon gamma. *Proc. Natl. Acad. Sci. U. S. A.* **93,** 2879–2883 (1996).

227. Hoelzer, K., Shackelton, L. A. & Parrish, C. R. Presence and role of cytosine methylation in DNA viruses of animals. *Nucleic Acids Res.* **36,** 2825–2837 (2008).

228. Karlin, S., Doerfler, W. & Cardon, L. R. Why is CpG suppressed in the genomes of virtually all small eukaryotic viruses but not in those of large eukaryotic viruses? *J. Virol.* **68,** 2889–2897 (1994).

229. Zhu, J., Huang, X. & Yang, Y. The TLR9-MyD88 pathway is critical for adaptive immune responses to adeno-associated virus gene therapy vectors in mice. *J. Clin. Invest.* **119,** 2388–2398 (2009).

230. Faust, S. M. *et al.* CpG-depleted adeno-associated virus vectors evade immune detection. *J. Clin. Invest.* **123,** 2994–3001 (2013).

231. Nishimura, H. & Honjo, T. PD-1: an inhibitory immunoreceptor involved in peripheral tolerance. *Trends Immunol.* **22,** 265–268 (2001).

232. Liu, X. *et al.* B7DC/PDL2 Promotes Tumor Immunity by a PD-1-independent Mechanism. *J. Exp. Med.* **197,** 1721–1730 (2003).

233. Yamazaki, T. *et al.* Expression of programmed death 1 ligands by murine T cells and APC. *J. Immunol. Baltim. Md 1950* **169,** 5538–5545 (2002).